Charles University in Prague

Faculty of Science

Ph.D. study program: Molecular and Cellular Biology, Genetics and Virology

Ph.D. Dissertation

Tanmoy Bhattacharyya M.Sc

Genetics and genomics of hybrid sterility

Supervisor: Prof. Jiri Forejt, MUDr, DrSc.

Prague 2013

Univerzita Karlova v Praze, Přírodovědecká fakulta

Charles University in Prague, Faculty of Science

Doktorský studijní program: Molekulární a Buněčná biologie, Genetika a Virologie

Ph.D. study program: Molecular and Cellular Biology, Genetics and Virology

Disertační práce

Ph.D. Dissertation

Tanmoy Bhattacharyya M.Sc

Genetika a genomika hybridní sterility

Genetics and genomics of hybrid sterility

Školitel/ Supervisor: Prof. Jiri Forejt, MUDr, DrSc.

Praha 2013

Declaration

This dissertation has been submitted in fulfillment of requirements for the degree of Doctor of Philosophy at the Faculty of Science, Charles University in Prague. I hereby declare this PhD thesis has been compiled by me under the supervision of Prof.Jiri Forejt.

This thesis has not been previously submitted for the award of any degree, diploma, associateship, fellowship or its equivalent to any other University or Institution.

Prague, Signed

Tanmoy Bhattacharyya

Prohlášení

Prohlašuji, že jsem závěrečnou práci zpracoval samostatně a že jsem uvedl všechny použitéi nformační zdroje a literaturu.Tato práce ani její podstatná část nebyla předložena k získání jiného nebo stejného akademického titulu.

V Praze, Podpis

Tanmoy Bhattacharyya

This work was accomplished at the Department of Mouse Molecular Genetics of the Institute of Molecular Genetics v.v.i, Academy of Sciences of the Czech Republic, under the supervision of Prof. Jiri Forejt.

Acknowledgements

This dissertation was completed with the effort of several people and I am grateful to their contribution and help. First of all, I would like to thank my supervisor Prof. Jiri Forejt for giving me an opportunity to carry out my dissertation research under his supervision. During my tenure in his lab, Prof. Forejt provided me with excellent guidance on the design, execution and completion of my experiments. He provided me with stimulating and interactive research environment along with encouragement for creativity and independent thinking. Importantly, his mentoring extended beyond primary research issues and I benefited greatly from his insightful advice and support. I am thankful to him for corridor discussions and advice on the best ways to achieve my academic and professional goals. It was a privilege to be his student.

I would like to thank Institute of Molecular Genetics, ASCR and Faculty of Science of Charles University for allowing me to carry out my dissertation work and for their financial support. I am thankful to Dr. Sona Gregorova for providing excellent training in mouse genetics and for help in breeding experiments. Dr. Petr Jansa offered a unique perspective and was instrumental in introducing me to male reproductive biology. Dr. Zdenek Trachtulec provided valuable feedback on speciation and mapping experiments. I am thankful for Dr. Petr Simecek for helping me with bioinformatics analysis. I am fortunate to have had the opportunity to do research with and learn from Dr.Ondrej Mihola and Dr. David Homolka. A great deal of my intellectual development can be attributed to the excellent academic environment provided by the Department Mouse Molecular Genetics at Institute of Molecular Genetics. I am eternally grateful for the friendship and scientific collaborations of Dr. James Turner, Dr. Brett Payseur, Dr.AtillaToth, Dr.Martin Anger, Dr. Paul Denny, Dr. Jaroslav Pialek and Dr. Martin Mistrik. Several past and present graduate students played an important role in my success. In particular, I would like to thank Petr Flachs, Maria Dzur-Gejdosova and Dr. Radka Reifová. I would like to thank Jana Perlova and Irena Chvatalova for their help and kind cooperation. I am indebted to Dr. K Thangaraj, Dr. K.R.Sridhar and Dr.M Krishnamurthy for giving me insight into molecular biology and genetics. Finally, I would like to thank Dr. Chitra Thakur and Dr. Soumen Roy for their unwavering love, support and unconditional friendship, for which I am grateful. I would like to thank Dr. Šarka Takáčová for helping me with Czech translations.

Dedication

I would like to dedicate my thesis to my parents and my wife, for their continuous love and support.

"Nothing in biology makes sense except in the light of evolution"

Theodosius Dobzhansky, 1973

Contents

Abstract

Male-limited hybrid sterility restricts gene flow between the related species, an important pre-requisite of speciation. The F1 hybrid males of PWD/Ph female (M*us m. musculus* subspecies) and C57BL/6J or B6 male (*Mus m. domesticus*) are azoospermic and sterile (PB6F1), while the hybrids from the reciprocal (B6PF1) cross are semi fertile. A disproportionately large effect of the X chromosome (Chr) on hybrid male sterility is a widespread phenomenon accompanying the origin of new species. In the present study, we mapped two phenotypically distinct hybrid sterility loci *Hstx1* and *Hstx2* to a common 4.7 Mb region on Chr. X. Analysis of meiotic prophase I of PB6F1 sterile males revealed meiotic block at mid-late pachynema and the TUNEL assay showed apoptosis of arrested spermatocytes. In sterile males over 95% of pachytene spermatocytes showed one or more unsynapsed autosomes visualized by anti SYCP1, HORMAD2 and SYCP3 antibodies. The phosphorylated form of H2AFX histone, normally restricted only to XY chromosome containing sex body decorated unsynapsed autosomes while abnormal sex body engulfed one or two univalents in 90% of the mid-late pachynemas. The unsynapsed chromosomes were additionally decorated by ATR and RAD51/DMC1 indicating the persistence of unrepaired DNA double-strand breaks (DSBs).The analysis of expression of X-linked genes in individual cells by RNA FISH and genome-wide expression profiling by Affymetrix GeneChips revealed the failure of MSCI in mid-pachynema of PB6F1 sterile hybrids. We have also demonstrated that the above mentioned phenotypes are strongly linked to 4.7 Mb $Hstx2^{PWD}$ locus on Chr X. Oocytes of F1 hybrid females showed the same kind of synaptic problems but with the incidence reduced to half. Most of the oocytes with pachytene asynapsis were eliminated before birth. In contrast to the hybrid males of the same genotype, the incidence of oocytes with asynapsis was not changed by the *Prdm9* or *Hstx2* genotype. We also found that F1 hybrid females carrying homozygous $Hstx2^{PWD}$ allele are fertile contradicting Muller's dominance theory that attempts to explain Haldane's rule. To analyze the possible cause of meiotic asynapsis we compared genome-wide meiotic recombination rate by counting MLH1 nodules in the parental strains, a set of partially overlapping B6.PWD-Chr X. # sub-consomics and their sterile and fertile hybrids. Strikingly, we found the recombination rate-controlling locus in the same 4.7Mb interval as the *Hstx1/2* hybrid sterility gene. Overall, we dissected the genetic and mechanistic basis of F1 hybrid sterility and its possible interconnection with genetics of meiotic recombination.

Abstrakt

Samčí hybridní sterilita je překážkou v přenosu genů mezi příbuznými druhy, což je významným předpokladem pro vznik nových druhů. F1 hybridní samci vzniklí křížením samice PWD/Ph (poddruhu *Mus m. musculus*) a samce C57BL/6J nebo B6 (*Mus m. domesticus*) mají azoospermii a jsou sterilní (PB6F1), zatímco hybridi z recipročního (B6PF1) křížení jsou částečně fertilní. Nadměrně převládající vliv chromosomu (Chr) X na sterilitu samčích hybridů představuje jev, který je při vzniku nových druhů široce zastoupen. V této studii jsme mapovali dva fenotypově odlišné lokusy pro hybridní sterilitu *Hstx1* a *Hstx2* do společné oblasti o délce 4,7 Mb na Chr X. Analýza meiotické profáze I odhalila u sterilních samců PB6F1 meiotický blok ve střední fázi pozdního pachytenu a testem TUNEL byla prokázána apoptóza blokovaných spermatocytů. U sterilních samců byla v 95 % pachytenních spermatocytů vizualizací protilátkami anti SYCP1, HORMAD2 a SYCP3 zjistěna asynapse jednoho či více autosomů. Fosforylovaná forma histonu H2AFX, normálně pozorovaná pouze v pohlavním tělísku obsahujícím chromosomy XY, barvila nespárované autosomy, zatímco abnormální pohlavní tělísko v 90 % chromosomů střední fáze pozdního pachytenu absorbovalo jeden či dva univalenty. Nespárované pachytenní chromosomy byly navíc obarveny ATR a RAD51/DMC1, což poukazuje na přetrvání neopravených dvouvláknových zlomů DNA (DSB). Analýza exprese X-vázaných genů v jednotlivých buňkách pomocí RNA FISH a celogenomového expresního profilování na Affymetrix GeneChips prokázala u sterilních hybridů PB6F1 poruchu meiotické inaktivace sex chromozomů (MSCI) ve středním pachytenu. Prokázali jsme také silnou souvislost výše uvedených fenotypů s lokusem 4.7 Mb $Hstx2^{PWD}$ na Chr X. U oocytů F1 hybridních samic se vyskytoval stejný typ problémů párování chromosomů, avšak s poloviční frekvencí výskytu. Většina oocytů s pachytenní asynapsí byla před porodem eliminována. Na rozdíl od hybridních samců téhož genotypu, genotyp *Prdm9* či *Hstx2* frekvenci výskytu oocytů s asynapsí nezměnil. Zjistili jsme také, že F1 hybridní samice s homozygotní alelou $Hstx2^{PWD}$ jsou fertilní, což je v rozporu s Mullerovou teorií dominance, která by měla představovat vysvětlení Haldanova pravidla. S cílem analyzovat možnou příčinu meiotické asynapse jsme porovnali výskyt rekombinace v celém genomu kvantifikací MLH1 nodulů v parentálních kmenech, v souboru částečně se překrývajících subkonsomických kmenů B6.PWD-Chr X.# a v jejich sterilních a fertilních hybridech. Překvapivě jsme zjistili, že lokus kontrolující frekvenci rekombinace se nachází ve stejném 4,7Mb intervalu jako gen pro hybridní sterilitu

Hstx1/2. Souhrnně lze říci, že jsme odhalili celkové genetické a mechanistické základy sterility F1 hybridů a její možné souvislosti s genetikou meiotické rekombinace.

Introduction

1. Speciation: Understanding the concept of reproductive isolation.

The diversity in the living world demonstrates a key evolutionary process called speciation. The concept is under investigation since mid-19th century, when many evolutionary biologist including Charles Darwin and Alfred R Wallace, found that species begin to diverge in due course of evolution giving rise to new species. As per accepted definitions, the formation of new and independent species from common ancestor under the influence of evolutionary pressure is viewed as speciation. The evolved species cannot merge and phenotypic differences such as physical differences, ecological adaptation, viability and sterility are distinguishable. The genetic loci that influence reduction in hybrid fitness are called "speciation genes". These genes help the diverged species to become separate organisms.

The genetics involved in these phenotypic differences are largely unknown. The answer to speciation related questions might be explained by dissecting genetic basis of reduced fitness in hybrids between the two species. The main influence on theory of speciation came from the concept of reproductive isolation. According to Mayr (Mayr, 1963) , species are "groups of interbreeding natural populations that are reproductively isolated from other such groups". As per Wu and Ting (Wu and Ting, 2004) "Reproductive isolation is defined as the non-exchange of genes between two species that are in contact with each other. The cessation of gene flow is the result of the genetic properties of the two species in question, and not the result of extrinsic barriers that prevent the contact".

The reproductive isolation is divided into two categories namely pre-mating and post-mating isolations. In Pre-mating isolation, interspecific hybrids are absent between two species due to ecological or behavioural factors. In Post-mating isolation, hybrids between two species are inviable, sterile or lack ecological adaptation. Reproductive isolation leads to evolution of distinct genetic organism under independent selective pressure. Dobzhansky and Muller explained the problem that how evolution as a gradual process, leads to the formation of discrete morphologically and genetically incompatible species (Dobzhansky, 1937; Muller, 1940). Dobzhansky-Muller model of speciation underline the epistasis between genetic loci and its contribution in development of reproductive isolation mechanism (explained later). After remaining dormant for four decades in 1980's evolutionary biologist found new interest in genetic basis of reproductive isolation especially with focus on hybrid sterility and inviability.

Using newly available genetic techniques and *Drosophila* as model organism, the most comprehensive data on genetic architecture of reproductive isolation was discovered (Orr and Coyne, 1989; Coyne, 1989; 1992). *Drosophila* as a model organism has lots of advantage like short generation time, knowledge of its genetic map and the existence of large number of closely related species which could be used for breeding experiments. The most extensive studies on reproductive isolation such as hybrid sterility and inviability was studied using hybrids between *D. simulans* and *D. mauritiana* and *D. simulans* and *D. melanogaster* respectively (Sawamura et al., 1993b; Sawamura, 1996; Ting et al., 1998; Barbash et al., 2003; Brideau et al., 2006; Ferree and Barbash, 2009; Presgraves et al., 2003; Sun et al., 2004b; Bayes and Malik, 2009; Phadnis and Orr, 2009; Tang and Presgraves, 2009). In recent two decades there were significant breakthroughs in speciation studies. With the emergence of new molecular methods, high throughput sequencing technology and free available whole genome sequencing data of many organisms; it is possible to identify the individual genes involved in reproductive isolation and possible to dissect the Dobzhansky-Muller interactions involved with it (Orr and Presgraves, 2000). In the last decade numbers of genes involved in reproductive isolation were discovered in fish, *Drosophila* and mouse. The *Xmrk-2* gene involved in melanoma formation in Xiphophorus species hybrids (Wittbrodt et al., 1989), *OdsH, Ovd* and *JYAlpha* genes are involved in hybrid male sterility in *Drosophila* species (Ting et al., 1998; Masly et al., 2006; Phadnis and Orr, 2009), *Hmr* and *Nup96* are involved in hybrid inviability in *Drosophila* species (Barbash and Ashburner, 2003; Barbash et al., 2003; Presgraves et al., 2003) and *desat-2* is determining ecological/behavioural characters in *Drosophila melanogaster* (Dallerac et al., 2000; Takahashi et al., 2001). Recently the first mammalian hybrid sterility gene *Prdm9* was mapped in mouse (Mihola et al., 2009). With the advancement of molecular and genetics tools new questions arise on horizon. With significant leap in speciation studies in recent years identification of full genetic architecture of reproductive isolation is far from reality. Answers to questions like "what are the causes of genetic incompatibilities? What types of genes are involved in such incompatibilities? How many of them are involved? What mechanisms have led to the divergence of these genes? What is the role of non-coding genome in such incompatibilities? What is the role of epigenetics in reproductive isolation mechanism? " are still unknown. The answer to these questions will give us a better understanding of the quest for the "*origin of species*".

2. Introduction to hybrid sterility.

The concept of speciation is under scientific discussion from the times of Charles Darwin. While its concepts were well discussed in his book "*The origin of species*" but actual breakthroughs were very recent. Understanding of genetic basis of speciation is scarce and very few studies were done to get an insight of this phenomenon. The major problem in understanding the genetic basis of speciation has been the studying of exact patterns occurring in nature under laboratory conditions. The phenotype such as sexual isolation or behavioral pattern which occurs in nature is hard to emulate in laboratory. Moreover, some speciation genetics experiment conducted in laboratory is absent in nature (Barbash et al., 2003; Brideau et al., 2006; Presgraves et al., 2003; Masly and Presgraves, 2007).Though the above studies increase our understanding the genetics of speciation, the actual relevance to natural phenomena is hard to establish (Harrison, 1990; Orr and Presgraves, 2000).

Reproductive isolation is a population genetics term that refers to non-exchange of genes between two species due to their genetic properties and not because of extrinsic barriers (Wu and Ting, 2004). The major contribution in understanding the genetics of speciation came from reproductive isolating barriers of different species like *Drosophila* and mouse (Tucker et al., 1992; Dod et al., 1993; Coyne et al., 2002; Payseur et al., 2004; Macholan et al., 2007). Importantly these species were reproductively isolated in nature and form hybrids which are sterile and can be emulated in laboratory. The post zygotic reproductive isolation in hybrids between different species is a contributing factor to speciation and termed as "Hybrid sterility". It is defined as a condition where two fertile parental forms produce hybrids which are sterile and can't breed (Dobzhansky, 1951; Maheshwari et al., 2008). Hybrid sterility is studied in both animal and plant kingdom. Though it was studied for the last 90 years; the genetics and underline molecular mechanism still remain vague. Genetic element that can contribute to reproductive isolation can be broadly categorized as extra-chromosomal, chromosomal and genic. In recent times some breakthroughs were made with discovery of 3 hybrid sterility gene in *Drosophila* namely *OdsH, JYAlpha, Ovd* and one mouse speciation gene called *Prdm9* (Ting et al., 1998; Masly et al., 2006; Mihola et al., 2009; Phadnis and Orr, 2009). Knowledge of genetic and molecular mechanism's involved in hybrid sterility is limited due to its oligogenic complexity. The genetic studies involving mouse and *Drosophila* hybrid models showed post zygotic reproductive isolation restricts gene flow between different species (Coyne and Orr, 2004;

Moehring et al., 2006; Slotman et al., 2004). With the discovery of more speciation genes we might be able to understand the epistasis involved between the genes contributing to the reproductive isolation mechanism. It is far different from the knockout models as each epistasis involved in hybrid sterility is unique to its prerogative.

2.1 The Dobzhansky–Muller model.

The best explanation for hybrid sterility are the epistatic incompatibilities involving two or more genes between diverged species called the Dobzhansky–Muller incompatibilities (henceforth, D-M incompatibilities (Muller and Pontecorvo, 1942; Dobzhansky, 1951). The model explains when an ancestral population with genotype AA BB split into two, A allele mutated into a allele in one population and B allele mutated into b allele in other. The a and b allele are epistatically incompatible with each other. But in pure species a-b interaction never happens and the incompatibility continues to evolve. But the problem appears when these diversely evolved species mate to produce hybrids. In hybrids a-b incompatibility causes the manifestation of different reproductive isolation related phenotypes (Figure 2.1).

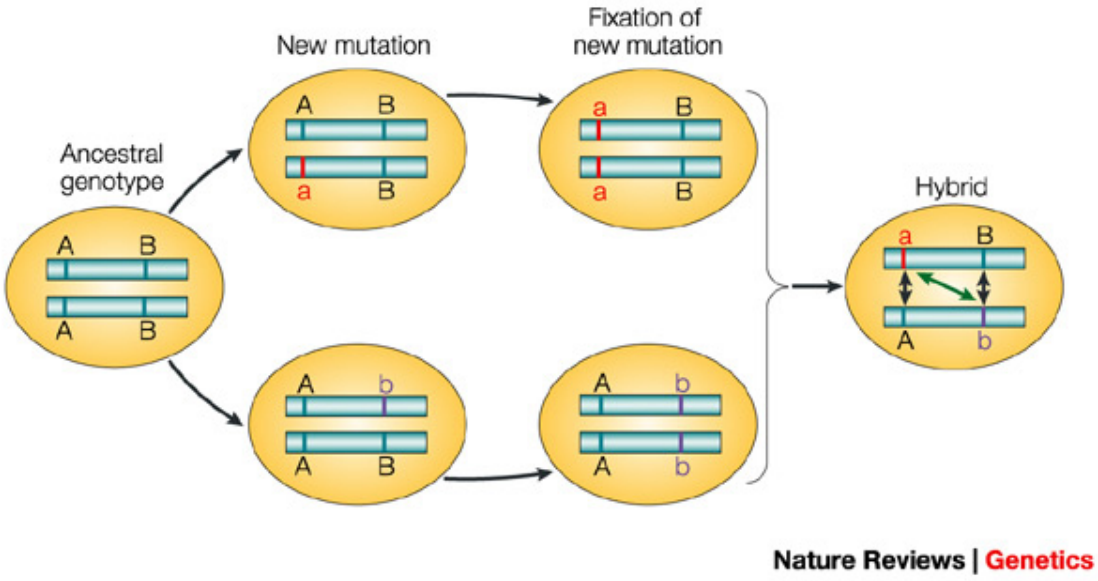

Figure 2.1: The Dobzhansky–Muller incompatibility model. From (Wu and Ting, 2004).

D-M incompatibilities can be of two types. In first type the diverged alleles are unable to have a functional interaction termed as “loss of function”. Alternatively, when one mutated allele starts a new interaction with another allele which is earlier absent in parental background leads to

condition called “gain of function” (Figure 2.2). In hybrids either or both of them can contribute to reproductive isolation mechanism.

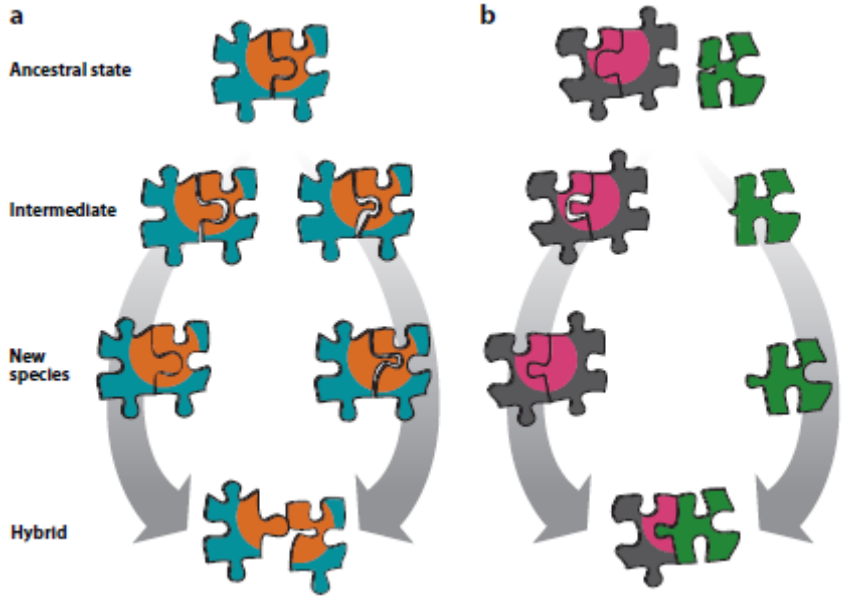

Figure 2.2: Model explaining the possible D-M incompatibilities. a) Model explaining the loss of function. b) Model the explaining gain of function. From (Maheshwari and Barbash, 2011).

2.2 The Haldane’s rule of hybrid sterility. The hybrid sterility in mouse and *Drosophila* is male limited, following Haldane’s rule which states “when in the F1 offspring of two different animal races one sex is absent, rare, or sterile; that sex is the heterozygous [heterogametic] sex” (Haldane, 1922). This rule is applicable to both XY heterogametic males found in mammals and *Drosophila* and ZW type heterogametic female in birds, *Lepidoptera* and dioecious plants like Silene. Different explanations have been given explaining Haldane’s rule. Some of the most prominent among them are discussed below.

2.3 The Muller’s dominance theory (Muller and Pontecorvo, 1942; Orr, 1987; Orr and Coyne, 1989) explains that the Haldane’s rule is applicable to homogametic hybrids when the new allele is recessive. Then the original dominant allele can compensate for it under hybrid genetic condition. In heterogametic sex; because of its hemizygous genetic status the recessive mutated allele can affect the phenotype in the absence of dominant allele. It is mainly linked to recessive X-linked D-M incompatibilities (Turelli and Orr, 1995; 2000; Muller and Pontecorvo, 1942). The

X-linked recessive mutations present in single copy in hemizygous genome can explain the male limited hybrid sterility.

2.4 Rapid evolution of male limited traits (Wu and Davis, 1993; Wu et al., 1996; Presgraves and Orr, 1998) or "faster male" effect states that the male genes evolved faster in sexual selection than female. So, male limited sterility is much more evident in heterogametic sex i.e. XY males. The major limitation of this hypothesis is that it does not explain the Haldane's rule in reproductive isolation of heterogametic female's i.e. ZW females.

2.5 Positive selection on X chromosome (Chr) (Charlesworth et al., 1987) were proposed as possible explanations contributing to male limited hybrid sterility. The hypothesis explains that the X-linked genes are evolving much faster than autosomes, causing a larger effect on reproductive isolation.

2.6 The large X effect.

Genetic studies on different hybrid models of post zygotic reproductive isolation from *Drosophila* and mouse showed the central role of Chr X in male limited hybrid sterility (Coyne and Orr, 2004; Moehring et al., 2006; Slotman et al., 2004). While, hybrid sterility is polygenic in nature, abundance of these genes are X-linked (Presgraves, 2008; Lu et al., 2010). The chromosome substitution experiments in *Drosophila* have shown that X chromosome introgression have higher effect on hybrid sterility compare to autosomes (Orr, 1987; Orr and Coyne, 1989; Masly and Presgraves, 2007). Genetic experiments involving consomics (chromosome substitution strains) showed that introgression of Chr X from *M. m. musculus* or *M. m. molossinus* subspecies on the *M. m. domesticus* genetic background causes sterility of males effecting post-meiotic process (Oka et al., 2007; Oka et al., 2004; Storchova et al., 2004). Alternative models studying F1 hybrid male sterility between *M. m. musculus* and *M. m. domesticus* also shows a strong role of Chr X in hybrid sterility between interspecific F1 hybrids (Good et al., 2008a; Good et al., 2008b; Dzur-Gejdosova et al., 2012; White et al., 2011). The X chromosome showed low level of gene flow in European hybrid zone compare to autosomes (Tucker et al., 1992; Dod et al., 1993; Besansky et al., 2003). The disproportionate contribution of Chr X on hybrid sterility was called "the large X effect" (Turelli and Orr, 1995; 2000).

3. Hybrid sterility in mouse: Brief overview

Mouse is the most successfully studied hybrid sterility model after *Drosophila*. The only known mammalian speciation gene *Prdm9* was discovered recently on mouse chromosome 17 (Mihola et al., 2009). The presence of considerable amount of genetic resources made it a preferred model for genetic research (Dietrich et al., 1996; Waterston et al., 2002; Shifman et al., 2006; Su et al., 2004). Three species of house mouse (*M. domesticus*, *M. musculus*, and *M. castaneus*) evolved from a shared common ancestor about 0.5 million years ago (She et al., 1990; Boursot et al., 1993). Hybrid sterility involving *M. m. musculus* and *M. m. domesticus* (hereafter, *Mmm* and *Mmd*) mouse species emerged as a preferred model for studying mammalian speciation. The two subspecies diverged from common ancestor around 0.3 to 0.5 million years ago (Boursot et al., 1996; Geraldes et al., 2008; She et al., 1990) and widely spread on both sides of hybrid zone across Europe (Dod et al., 1993; Macholan et al., 2007; Payseur et al., 2004; Tucker et al., 1992) (Figure 3.1). Wild trapped hybrids between these two subspecies from within hybrid zone showed significant genetic variation, but fail to provide high resolution genetic maps. Alternatively, representative strains of *Mmm* and *Mmd* were crossed in laboratory for high-resolution genetic dissection. Crossing experiments in laboratories between *Mmm* and *Mmd* showed they are reproductively isolated (Forejt and Ivanyi, 1974; Forejt et al., 1991; Forejt, 1996; Vyskocilova et al., 2005). In recent studies models involving *Mmm* and *Mmd* subspecies were widely used to get further insight into X-linked hybrid sterility. In first, *Mmm* (PWD or PWK/PhJ) Chr X was introgressed onto *Mmd* genomic background (B6 or LEWES/EiJ) (Storchova et al., 2004; Good et al., 2008a). The consomic males generated from these experiments were sterile with low testis weight, low sperm count and higher sperm abnormality. Multiple overlapping X-linked quantitative trait loci (QTL) contributing to hybrid sterility were mapped in these models) (Storchova et al., 2004; Good et al., 2008a). An introgression hybrid sterility model involving of *M. m. molossinus* (MSM) chromosome X into the B6 strain i.e. B6.MSM-ChrX males showed incomplete block of spermatogenesis and presence of some sperm.

Figure 3.1: The mouse hybrid zone in Europe. From (Macholan et al., 2008).

The authors showed the elimination of germ cells at pachytene stage and at first meiotic division. On the other hand introgression of *M. m. molossinus* (MSM) chromosome X into the wild derived *Mmd* PGN strain i.e. PGN.MSM-ChrX, the male meiosis was affected in pachytene and meiosis I (Oka et al., 2010).

The second model evaluated F1 hybrid sterility involving *Mmm* (PWD; CZECHII/EiJ or PWK/PhJ) and *Mmd* (B6; WSB/EiJ or LEWES/EiJ) (Forejt et al., 1991; Gregorova et al., 1996; Mihola et al., 2009; Trachtulec et al., 2008; Good et al., 2008a; Good et al., 2010; White et al., 2011). Crosses between the above mentioned *Mmm* and *Mmd* subspecies resulted in asymmetric F1 hybrid male sterility, linked to maternal strains of *Mmm* origin (White et al., 2011; Mihola et al., 2009; Good et al., 2010; Good et al., 2008b). Strong QTL's were mapped between PWD and WSB using F_2 cross in multiple autosome and X chromosome (White et al., 2011). Moreover, using F_2 hybrids between wild-derived inbred strains from *Mus musculus castaneus* and *M. m. domesticus* many autosomal and X-linked QTL associated with a range of hybrid male sterility phenotypes were identified (White et al., 2011). The pseudoautosomal region was found

to be associated with hybrid sterility between *Mus musculus castaneus* and *M. m. domesticus*. Three autosomal hybrid sterility linked QTLs were found to be common between *Mus musculus castaneus* and *M. m. domesticus* and *Mus musculus musculus* and *M. m. domesticus* mapping experiments (White et al., 2012). Recently using PWK (wild derived *Mmm*) and LEWES (wild derived *Mmd*) hybrid sterility model, the role of Y chromosome in hybrid sterility was reported. The authors found evidence for a negative interaction between the *M. m. domesticus* Y and an interval on the *M. m. musculus* X that resulted in abnormal sperm morphology (Campbell et al., 2012). New *M. m. musculus* inbred strains STUF and STUS producing only fertile and only sterile males with B10 mice, respectively were established. Using the (STUS × STUF) × B10 cross, the authors found that 90% of genetic variance between STUF and STUS is due to a QTL in the proximal part of chromosome 17 and 10% by another QTL in the central part of chromosome X (Pialek et al., 2008; Vyskocilova et al., 2009).

4. Introduction to the model.

The present study is focused on hybrid sterility model involving PWD/Ph and C57BL/6J (henceforth PWD and B6) inbred strains representing *Mmm* and *Mmd* subspecies respectively. The genetic and genomic tools available with this model are an advantage for studying genetic and molecular mechanisms associated with hybrid sterility. The full genomic sequence of B6 and 17 other strains comprising of *Mmm* and *Mmd* subspecies are freely available (Keane et al., 2011). A panel of 28 mouse intersubspecific consomic (chromosome substitution) strains with PWD chromosome in B6 background (Gregorova et al., 2008) can be used for high resolution mapping experiments to dissect oligogenic complexity. B6 is the model of choice for generating majority of mouse mutants for protein coding genes useful for functional analysis (Skarnes et al., 2011).

Earlier it has been published that F1 hybrids between PWD female and B6 male (hence forth PB6F1) were sterile with low testis weight and azoospermic whereas reciprocal F1 hybrids between B6 female and PWD male were fertile (Figure: 4.1) (Trachtulec et al., 2008). The first mammalian speciation gene *Prdm9/Hst1* was mapped in PB6F1 hybrid sterility model (Mihola et al., 2009). The hybrid sterility model involving PWD and B6 can be a great tool to do genetic and molecular dissection for understanding the complex nature of F1 male sterility. Even there are

overwhelming advantages with the model but the sort comings cannot be ignored. The model is after all a representative artificial model, perhaps not the most quintessential for the two subspecies.

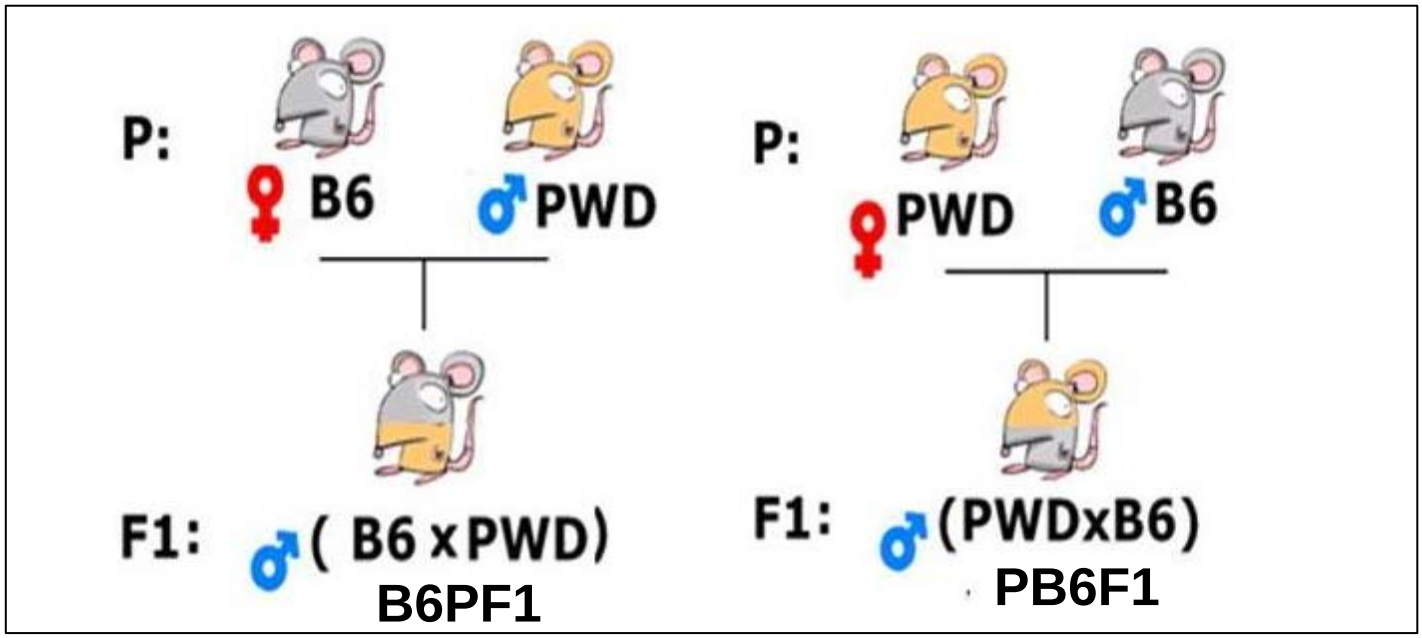

Figure 4: Cartoon explaining the hybrid sterility model involving PWD and B6.

4.1. Hybrid sterility 1 (*Hst1*) speciation gene in mouse.

While studying new H2 histocompatibility polymorphism, Ivanyi and co-workers first time described infertility of hybrids between wild and laboratory mice (Ivanyi et al., 1969). They reported that hybrid mice between wild trapped mice with different laboratory strains like B10 and A/Ph were sterile, while they were fertile with C3H/Di strain. They associated the phenotype to H2-histocompatibility linked locus and considered it as the effect of an incomplete *t*-haplotype. Later the phenomenon was recognized as interspecific hybrid sterility and the locus was mapped between *T* and *H2* markers on chromosome 17 (Forejt and Ivanyi, 1974). This locus was named Hybrid sterility 1 *(Hst1*) locus. Afterwards high resolution genetic mapping experiment was carried out using test crosses between wild trapped mice × (B10 × C3H) or PWD × ((B10 × C3H) × B10) (Forejt et al., 1981; Forejt, 1985; 1996). To further reduce the interval and to identify *Hst1* gene; haplotype associated mapping was carried out (Trachtulec et al., 2008). Three

haplotypes were found within 252 Kb region. Next the candidate genes were screened across the region in terms of sequence polymorphism, expression label, isoforms and tissue specific expression. Out of 7 candidate genes only *Prdm9* differed in the number of zinc finger repeats between B6 and C3H which also have germ cell specific expression (Hayashi et al., 2005). Using BAC transgenesis it was concluded that *Prdm9* is *Hst1* gene which encodes H3K4 methyltransferase (Mihola et al., 2009). The *Prdm9* gene also controls hotspot of meiotic recombination which is an important component of meiosis (Baudat et al., 2010; Parvanov et al., 2010). The dual role of *Prdm9* in hybrid sterility and control of the meiotic recombination also inspired us to look at the mechanistic basis of hybrid sterility in mice. Recent study on interallelic and intergenic incompatibilities of the *Prdm9* gene was published (Flachs et al., 2012). The authors showed upon removal of $Prdm9^{B6}$ allele (sterile allele) from PB6F1 male, the animals regain partial fertility. These results directs towards *Prdm9* independent incompatibility also contributes in PB6F1 hybrid sterility (Flachs et al., 2012). The research work concluded in the present dissertation thesis will further contribute to the knowledge regarding genetic and mechanistic aspects of hybrid sterility.

5. Brief introduction to the meiotic prophase I in mouse.

The formation of haploid cells from their pluripotent progenitors is conserved in most eukaryotic species; subsequently these haploid gametes fuse to form new zygote. The process of gamete formation goes through a distinct process called meiosis, which leads to two-fold reduction in chromosome number and help maintaining the ploidy from one generation to the other. The prophase I of meiosis ensures the correct segregation of chromosomes to each haploid gamete. This phase includes the pairing, synapsis and recombination of homologous chromosomes. The chromosomal abnormalities, such as translocations and inversions complicate these processes causing failure of synapsis process. Asynapsis of homologous chromosome activates the meiotic check points, which lead to cells cycle arrest and apoptosis. The sexual dimorphism of involved pathways leads to different reproductive outcomes between male and females. For example, spermatogeneic cells appear to be more vulnerable to pachytene checkpoint leading to infertility, but oocytes can bypass the checkpoint and thus affecting different stages of oogenesis. In this section we will discuss the prophase I in meiosis in both male and female which will be relevant for the different aspects of the thesis.

5.1 Initiation and regulation of meiotic program in mouse.

The entry to the meiotic process is sexually dimorphic during male and female gametogenesis. The decision to exit proliferative state and begin meiosis starts the differentiation of progenitor cells into gametes. In mammalian females this process initiates in the embryo while in males it starts only after birth. As in different developmental processes gamete formation requires unique transcriptional program. In yeast the genes activated in the first wave include *NDT80* and *IME2* (Kassir et al., 1988; Kassir et al., 2003; Handel and Schimenti, 2010). Mammals have no clear orthologs of either of these genes. The germ cell specific male-germ-cell-associated kinase (*Mak*) gene showed sequence homology to *IME2* but further experimentation found it non-essential for fertility in mouse (Shinkai et al., 2002). Though the transcriptome during male meiosis is well studied, the regulators of meiotic program are far from clear. A major discovery showed that beginning of meiosis is regulated by retinoic acid (RA) and mediated by the product of gene stimulated by retinoic acid 8 (*Stra8*) (Bowles et al., 2006; Bowles and Koopman, 2007; Koubova et al., 2006). The effect of RA and *Stra8* is sexually dimorphic. In fetal ovaries RA induces *Stra8* to enter meiosis, which can be detected by expression of meiotic markers such as disrupted

meiotic cDNA 1 homologue (*Dmc1*) and synaptonemal complex protein 3 (*Sycp3*). In fetal testis *Stra8* is not induced due to RA degrading enzyme CYP26B1 (a member of the cytochrome P450 family), expressed in Sertoli cells, so male germ cells don't enter meiosis during this time (Anderson et al., 2008). Another meiotic inhibitor gene *Nanos2* is specifically expressed in fetal male germ cells (Suzuki and Saga, 2008). The regulation of meiotic inception by RA is mediated by germ cell initiation factor such as deleted in azoospermia-like (*DAZL*) RNA-binding protein, which acts before *Stra8* in pathway of meiotic induction (Lin et al., 2008). It is still unclear whether meiotic entry failure underlies any case of human infertility. The questions associated with initiation and specifications of female's germ cells are still unresolved.

5.2 Chromosome dynamics associated with pairing and segregation of homologous chromosome.

Once the cells enter meiosis; the nuclear envelop (NE) plays a critical role in early event of mammalian meiosis. Meiotic processes like non-homologous centromere coupling, telomere bouquet formation, homolog alignment, pairing and initiation of synapsis and double strand breaks are facilitated by NE (Yanowitz, 2010). Knowledge about early events of pairing and synapsis is still unclear in mammals. The most frequent assumption is that the single strand overhangs at DSBs mediate the search of homologous chromosomes. This assumption may hold for final stages of homologous synapsis but unlikely to be affective for large compacted DNA. Alternatively, some suprachromosomal components might play a role of important facilitators in homology recognition process. There are two such components in mammalian germ cells, the clustering of telomeres and the assembly of chromosomal axis to form the synaptonemal complex (SC). These two processes are absolutely essential for mammalian fertility. The early meiotic events are highly conserved among various species. In early prophase the telomeres attach to the nuclear envelop and form a chromosomal bouquet (Scherthan, 2001; Alsheimer, 2009), which facilitates the homologous alignment of chromosomes axis. In mammals the suprachromosomal component of bouquet formation by telomeres clustering involves an inner nuclear membrane protein called SuN1 (also known as *UNC84A*). SuN1 acts as an anchoring protein in nuclear membrane. SuN1 protein also localizes at the telomeres of the spermatocytes. The knockout of the SuN1 gene in mouse causes sterility in both males and females by disruption of bouquet formation and homologous synapsis (Ding et al., 2007) (Figure 5.1). As there is differential

expression of reproductive genes and Piwi-interacting RNAs (piRNAs) in *SuN1* mutant mice, it was difficult to pinpoint the cause of phenotypic defects (Chi et al., 2009). Moreover, the telomeric sequences might have a role in meiotic recombination, as the rate of recombination is higher in subtelomeric sequences in the male germline (Paigen et al., 2008). In telomerase deficient mice; impaired homologous synapsis and decreased recombination's were observed (Liu et al., 2004). Therefore, structural and functional components of telomeres are required for initiation of meiosis in mammals.

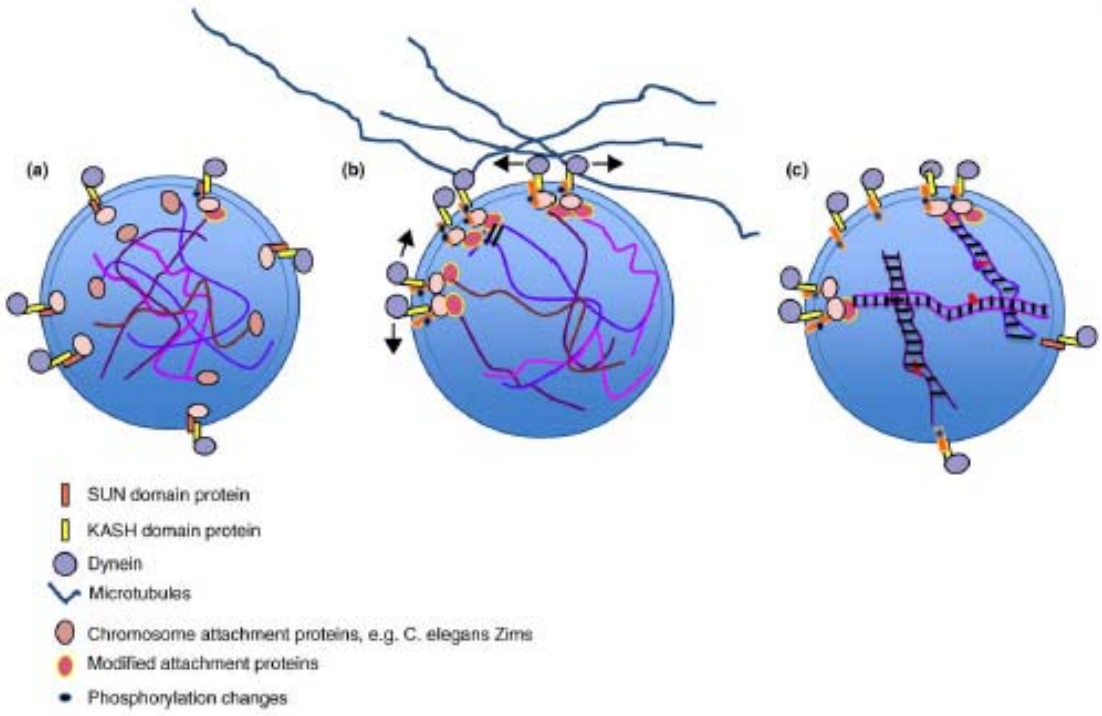

Figure 5.1: The process of chromosome pairing. (a) A SuN1 complex binds to nuclear envelop connected with dynein on cytoplasmic side. Chromosomes attached via telomeres or special pairing centers with the nuclear membrane (b) The SuN1 complex's binds together into large patches. In patches dynein mediated forces lead to detachment of non-homologous attachment followed by homologous synapsis. (c) The process of homologous synapsis synchronized with DSB repair and initiation of pachytene stage. From (Yanowitz, 2010).

5.3 Understanding the dynamics of meiotic prophase I in mouse.

After meiotic pairing the homologous chromosomes get synapsed by a unique meiotic scaffold called the synaptonemal complex (SC).The process of meiotic pairing and synapsis initiates are leptotene and zygotene stages respectively. The process of synapsis is completed by pachytene stage and desynapsis of SC's occurs at diplotene stage. These processes of synapsis and desynapsis are intricately linked with the process of meiotic recombination. In leptonema, the homologous chromosomes are aligned but not paired. The cohesin proteins such as REC8, STAG3 and SMC1β and SC proteins as SYCP3, HORMAD1, HORMAD2 and SYCP2 from a chromosomal scaffold around axial elements (AEs) (Revenkova et al., 2004; Xu et al., 2005; Prieto et al., 2001; Yuan et al., 2000; Yang et al., 2006; Shin et al., 2010; Fukuda et al., 2010; Wojtasz et al., 2012). At this stage initiation of recombination starts with formation of double strand breaks (DSB's) on chromatids catalyzed by SPO11 transesterase (Romanienko and Camerini-Otero, 2000) (Figure 5.2).

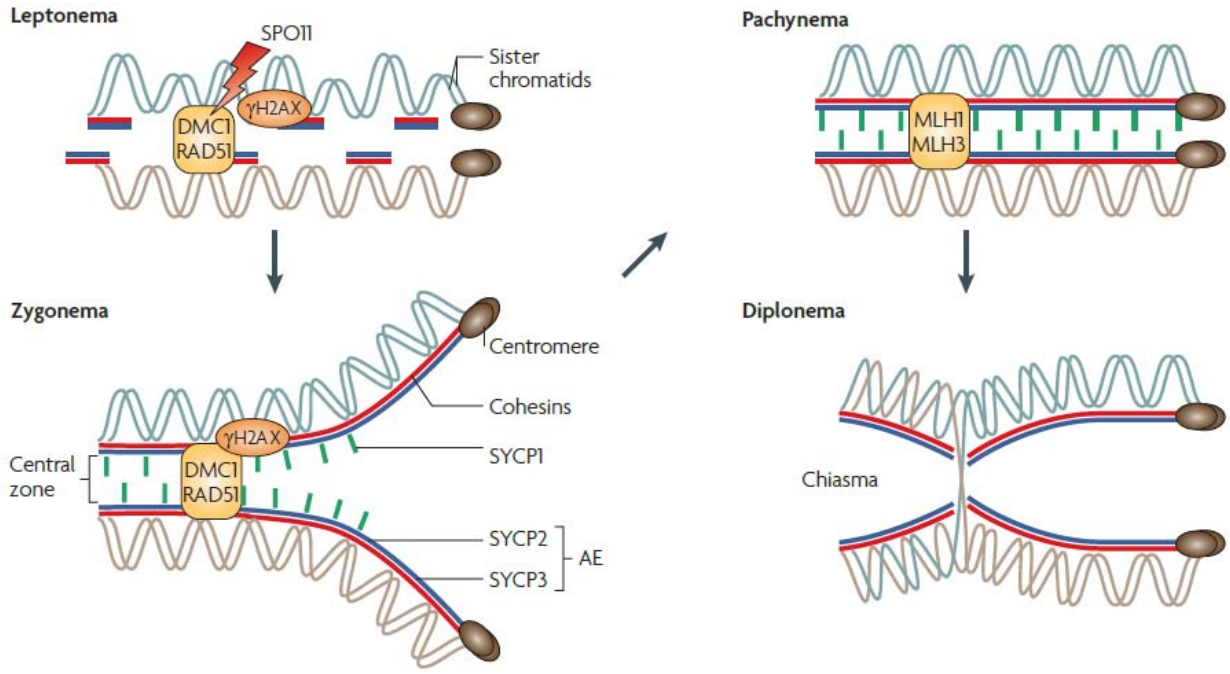

Figure 5.2: Dynamics of meiotic synapsis. From (Handel and Schimenti, 2010).

The DSB's are recognized by homologous recombination repair proteins like phosphorylated H2AX (γH2AX), ataxia telangiectasia mutated (ATM) machinery and recombinase A (RECA)-

related proteins like RAD51 and DMC1 which co-localize with densely stained foci called recombination nodules along the axial elements (Bishop et al., 1996; Mahadevaiah et al., 2001; Handel and Schimenti, 2010). At zygonema sister homologs find each other; pairing is established and synapsis begins where the axial elements of sister homologs started to zip (Mahadevaiah et al., 2001). In this process axial elements become lateral elements of the SC's and central element proteins like SYCP1, SYCE1, SYCE2 and TEX12 (de Vries et al., 2005; Bolcun-Filas et al., 2007; Bolcun-Filas et al., 2009; Hamer et al., 2006) form the central zone of synapsed structure. By the pachytene stage maturation of meiotic recombination sites is established by MutL protein homolog 1(MLH1) and MLH3 (Edelmann et al., 1996; Holloway et al., 2008). Only <10% of sites previously marked by RAD51 and DMC1 are marked by MLH1 (Plug et al., 1998). After recombination completion desynapsis initiates diplotene stage of meiosis I. The SC's look condensed and the homologs are held together only at recombination sites. Figure 5.2 explains the dynamics of the process.

5.4 The structure and function of synaptonemal complex (SC).

The SC structure is multiprotein complex formed during meiotic prophase. It is mainly composed of three basic structures called axial element (AEs), transverse element (TEs) and central element (CEs)(Figure 5.3).The AEs elements along sister chromatids are made up of core proteins called cohesins. In mammalian meiosis different variants of cohesion proteins like structural maintenance of chromosome 1B (SMC1β), REC8 (related to RAD21) and STAG3 (related to STAG1) form the core of AEs (Figure 5.3) (Revenkova et al., 2001; Eijpe et al., 2003; Prieto et al., 2001). The knockout of *SMC1β* and *REC8* genes in mouse causes meiotic disruption and sterility in males as well as females. Moreover meiotic chromosomes in those knockout animals are shorter with longer chromatin loops. When AEs of one pair of sister chromatid get associated with its homologous counterpart; they are called lateral elements (LE). The LEs are mainly composed of SYCP2 and SYCP3 (Figure 5.3) (Yang et al., 2006; Yuan et al., 2000).Recent discoveries showed LEs are also made up of axis-associated HORMA domain protein HORMAD1 and HORMAD2 which are required to prevent non-homologous synapsis during meiotic prophase (Shin et al., 2010; Wojtasz et al., 2012; Wojtasz et al., 2009).

In mice null allele of SYCP3 leads to male sterility and reduced female fertility with oocytes showing higher rate of aneuploidy (Yuan et al., 2002; Yuan et al., 2000; Pelttari et al., 2001;

Kolas et al., 2004). Similar phenotype was observed in SYCP2 mutants (Yang et al., 2006). HORMAD1 mice mutants showed defective DSB formation and/or repair and SC formation in both male and female and hence both sexes are sterile (Shin et al., 2010). But in HORMAD2 mouse mutant's sterility is male limited. Though the males are infertile no major defects were observed in DSB formation and/or repair and SC formation. It was also found HORMAD1 can perform the function of HORMAD2 in the mutant mice (Fukuda et al., 2010; Wojtasz et al., 2012; Wojtasz et al., 2009). In these mice the male limited sterility was linked to failure of meiotic sex chromosome inactivation check point (discussed later). The difference in phenotypes between male and female shows different sensitivity of spermatocytes than oocytes in relation to meiotic checkpoints. The transverse element (TEs) is mainly composed of SYCP1, which connects to central element (CEs) composed of synaptonemal complex central element protein 1 (SYCE1), SYCE2, SYCE3 and testis expressed sequence 12 (TEX12) (Figure 5.3). Mice with SYCP1 null allele form normal AE or LEs, which align to homologs, but do not synapse (de Vries et al., 2005). Both sexes are sterile. Similar sterility phenotypes were observed in SYCE1, SYCE2, SYCE3 and TEX12 mutant mice (Bolcun-Filas et al., 2007; Bolcun-Filas et al., 2009; Schramm et al., 2011; Hamer et al., 2008). In spite of detailed studies on SC formation and its constituents, their role in meiosis is still far from clear.

5.5 Importance of meiotic checkpoints in mouse meiosis.

The error free execution of meiotic process during meiotic prophase is essential for proper chromosomal segregation and preventing aneuploidy. To assure the quality of healthy egg and sperm quality control mechanisms are in place during meiosis. Any kind of defects linked to meiotic recombination, homologous pairing and repair of DSBs are under surveillance systems or checkpoints. Any kind of unresolved defects results in elimination of the meiocytes. An additional checkpoint monitors the crossover frequency in each chromosome. In mammals checkpoint linked genes are yet to be identified (Hochwagen and Amon, 2006). Mouse orthologs of yeast meiotic checkpoint genes ataxia telangiectasia mutated (ATM) and thyroid hormone receptor interceptor 13 (TRIP13) do not show any checkpoint activity, instead null alleles of this genes show severe recombination defects causing meiotic arrest and infertility (Handel and Schimenti, 2010).

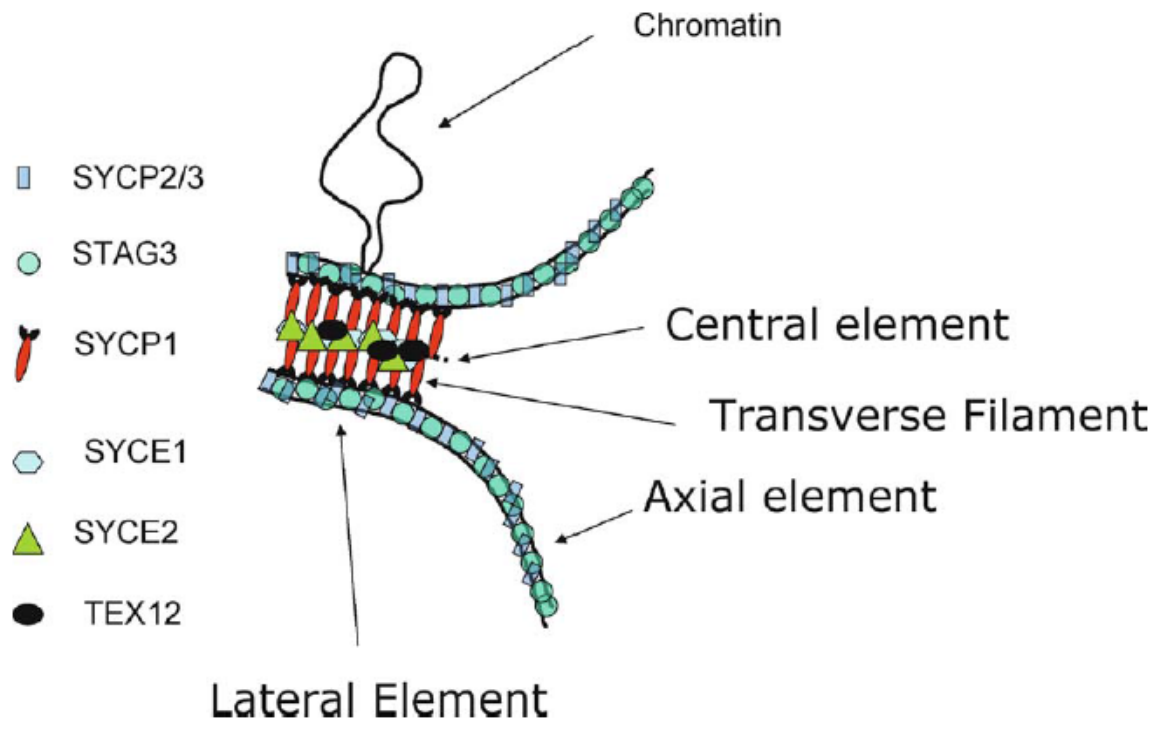

Figure 5.3: Cartoon showing nomenclature and major components of synaptonemal complex. From (Costa and Cooke, 2007).

The known mitotic DNA damage checkpoint may have a role in meiosis too but it needs further investigation to prove its meiotic function. The molecular dissection related to synapsis checkpoint is still unclear and its sensitivity is still debated between male and female meiosis. Some recent studies on ataxia telangiectasia and RAD3-related (ATR) show that this serine/threonine kinase checkpoint protein has a role in mammalian pachytene checkpoint. In particular it is supposed to trigger transcriptional silencing of unsynapsed autosomes or autosomal segments at pachytene stage during male and female meiosis commonly known as meiotic silencing of unsynapsed chromatin or MSUC (Schimenti, 2005). However, direct evidence on ATR role in MSUC is still missing. ATR null allele in mouse is lethal (Schimenti, 2005; Turner et al., 2005).

One interesting aspect of male germline control is the meiotic sex chromosome inactivation or MSCI originally proposed 30 years ago by Forejt (Forejt, 1984; 1996). According to McKee and Handel (McKee and Handel, 1993) transcriptional silencing of X and Y chromosomes takes place during the pachytene substage of male meiosis. MSCI is MSUC effecting on X and Y

chromosome (Figure 5.4). In mammals silencing of sex chromosomes is an important prerequisite for gamete viability in heterogametic sex. The repair proteins ATR and BRCA1 recognize unsynapsed X and Y and lead to phosphorylation of H2AX and heterochromatinization, compartmentalization and silencing in sex body (Kouznetsova et al., 2009; Mahadevaiah et al., 2008; Mahadevaiah et al., 2009). In mice with XYY genotype pachytene arrest and sterility is due to failure of MSCI (Royo et al., 2010). The expression of Y-linked *Zfy2* gene promotes apoptosis of germ cells (Vernet et al., 2011). Other than that HORMAD2 male mutants show failure of MSCI causing pachytene block (Wojtasz et al., 2012). Chromosomal translocation model of meiotic checkpoint showed chromosomal asynapsis interference with MSCI process leading to male limited sterility (Homolka et al., 2007). Thus silencing of sex chromosome in mammalian males is an essential step for proper completion of meiosis and most probably acts as a meiotic checkpoint.

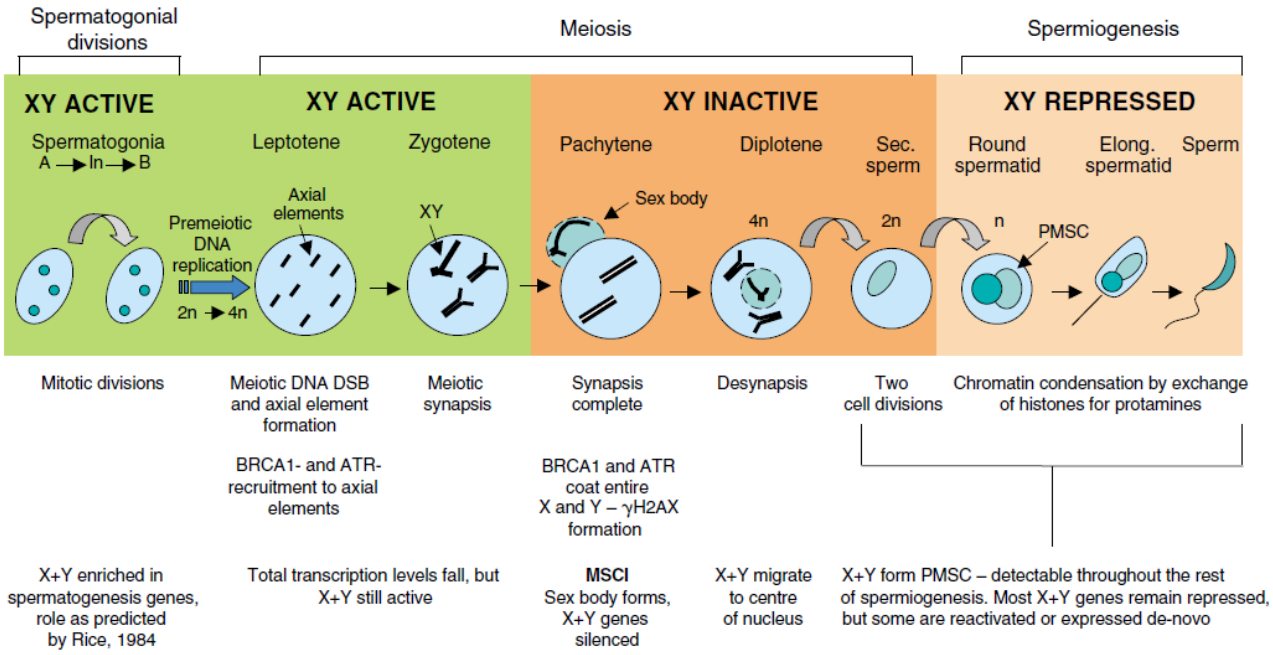

Figure 5.4: Overview of XY transcriptional activity during meiotic prophase I. From (Turner, 2007).

5.6 Failure of homologous synapsis and sex-specific phenotypic manifestation.

Sexual dimorphism in the manifestation of phenotypes in mutants of meiotic genes and translocation models showed that spermatogenic cells are more vulnerable to the pachytene checkpoint then female meiocytes. Females oocytes tend to bypass these checkpoints generating other problems such as metaphase arrest, aneuploidy and pregnancy loss. Mouse experiments have demonstrated the presence of MSUC in both males and females (Turner et al., 2005). The explanation for male specific infertility might be that the MSUC itself inactivates essential meiosis genes leading to the elimination of the cells. Otherwise inactivation of autosomal segments might interfere with sex body formation leading to male specific sterility. Alternatively MSCI failure means the abnormal expression of sex chromosome genes like *Zfy2* resulting in apoptosis (Mahadevaiah et al., 2008). Also heterosynapsis between autosome and sex chromosomes might interfere with the MSCI process causing expression of sex chromosomal genes in males. MSCI failure is only possible in males which can explain the sexual differences between male and female gametogenesis. The failure to eliminate oocytes with extensive asynapsis in HORMAD1 mutant females give rise to speculation that HORMAD1 might itself act as checkpoint protein (Kurahashi et al., 2012). Both SPO11 knockout males and females are sterile. The HORMAD1/SPO11 double knockout males show pachytene arrest due to MSUC and subsequently effecting MSCI, but the block is relaxed from zygonema in SPO11 knockout mice to pachytene in HORMAD1/SPO11 double knockout males (Kurahashi et al., 2012). SPO11 null females are sterile with small number of follicles but the HORMAD1/SPO11 double knockout females demonstrate same number of follicles as that of wild type controls. Thus the HORMAD1 might work in pachytene checkpoint pathway (Kurahashi et al., 2012). Further investigation of meiotic checkpoint proteins is essential to understand these sexual differences in the manifestation of meiotic phenotypes.

Aims and motivation

A. **Dissecting the genetic basis of F1 hybrid sterility.** Male-limited hybrid sterility contributes to speciation by restricting gene flow between related taxa. The only known mammalian speciation gene *Prdm9* was mapped in mouse (Mihola et al., 2009). One of the aims of this thesis was to investigate the genetic basis of hybrid male sterility in F1 hybrids between PWD female and B6 male. Using F1 hybrids between PWD and B6.PWD-Chr# consomic panel we tried to answer basic questions such as how many genetic loci control F1 hybrid sterility? Where in the genome are hybrid sterility loci located? Genetic studies in *Drosophila* species showed disproportionate contribution of Chr X on hybrid sterility. In our study we decided to genetically map the loci on Chr X contributing to F1 hybrid sterility. Using positional cloning strategies and expression profiling experiments we wanted to identify candidate genes that might be responsible for F1 sterility.

B. **Understanding the mechanistic basis of F1 hybrid sterility.** The mammalian speciation gene *Prdm9* perform dual role in hybrid sterility and in control of the meiotic recombination hotspots (Mihola et al., 2009; Parvanov et al., 2010; Baudat et al., 2010). The dual function of *Prdm9* prompted us to analyze the mechanistic basis of hybrid sterility, asking three specific questions: (a) which subcellular and molecular processes are involved in the spermatogenic breakdown? (b) Are the meiotic defects leading to hybrid male sterility indeed male specific (Haldane's rule)? (c) What can we learn about hybrid sterility by manipulating the individual components of its genetic architecture?

C. **Dissecting Muller's dominance theory as explanation for Haldane's rule.** The F1 hybrid sterility is male limited as explained by Haldane's rule (Haldane, 1922).The generally accepted explanation of Haldane´s rule is the dominance theory proposed by Herman Muller (Muller and Pontecorvo, 1942) stating that the sex dependent effect on hybrid fitness is due to recessive nature of X-linked mutations effective in hemizygous XY males but not in XX females. Here we asked whether the homozygosity of X-linked hybrid sterility gene in F1 hybrid females influences the fertility and meiotic phenotype similar as that of F1 hemizygous males. The results will show the results of the first experimental testing of dominance theory in mammals.

Materials and Methods

6.1 Ethics statement. The principles of laboratory animal care obeyed the Czech Republic Act for Experimental Work with Animals (Decree No. 207/2004 Sb. and Acts Nos. 246/92 Sb. and 77/2004 Sb.) was fully compatible with the corresponding EU regulations and standards, namely Council Directive 806/609/ EEC and Appendix A of the Council of Europe Convention ETS123.

6.2 Mice. The PWD/Ph and PWK/Ph inbred strain were created from a single pair of wild mice of the *Mus musculus musculus* subspecies trapped in 1972 in Central Bohemia, Czech Republic (Gregorova and Forejt, 2000). The C57BL/6J (B6), C3H/HeJ (C3H) and BALB/cByJ (BALB/c) inbred strains were imported from The Jackson Laboratory, USA. The congenic strain B6-Hst1^{f} carrying the Hst1^{f} allele of C3H origin on the B6 background was prepared in our laboratory (Mihola et al., 2009; Flachs et al., 2012). The conplastic B6.PWD-Mt, consomic B6.PWD-Chr # strains and sub-consomic strain B6.PWD-Chr X. # (Gregorova et al., 2008) have been maintained in the Specific Pathogen Free barrier facility on a 12 h light/12 h dark cycle. The mice had ad libitum access to a standard rodent diet (VELAZ, ST-1, 3.4% fat) and acidified water. All males were sacrificed at the age of 60 to 70 days. Heterozygous consomic females designated here as B6-X^{PWD}X^{B6} on B6 genetic background were prepared by repeated backcrossing of (PWD x B6) F1 females with B6 males (Storchova et al., 2004). The B6-X^{PWD}X^{B6} heterozygous consomic females were crossed in two independent experiments with PWD males to generate F1 recombinant male progeny and with B6 males to get B6.PWD-Chr.X1s sub-consomics for mapping experiments. The B6.PWD-Chr. # homozygous male and females were crossed with PWD/Ph male and females to dissect the genetic basis of F1 hybrid sterility phenotypes. F1 hybrid females from different hybrid experiment were mated with PWD males as per experimental requirements.

6.3 Fertility test, histology and apoptotic assay. To test the fertility of hybrid males, two males were mated with two C57BL/6J females at the age of 8 weeks for 3 months. Similarly, F1 hybrid females were tested by mating with PWD males. Wet weight of both testes was estimated to the nearest mg immediately after dissection. The periodic acid Schiff and hematoxylin-eosin stained testicular sections were observed under a Nikon Eclipse 200 microscope. The images were captured by a Penguin 150CL CCD color camera (Pixera) and processed with Adobe Photoshop

(Adobe Systems). Identification of apoptotic cells was done on paraffin embedded testis sections using DeadEnd Fluorometric TUNEL System (Promega; G3250). At least 15 tubules were counted for TUNEL positive cells. For sperm head abnormality analysis we stained sperms with eosin Y (Otubanjo et al., 2007) and observe them under light microscope.

Eight weeks old (B6.PWD-Chr $X^{PWD/B6}$ x B6) recombinant males were genotyped using SSLP X-linked markers listed in the Table below. Position for "SR" markers was computed using http://cgd.jax.org/mousemapconverter/. Genomic DNA for genotyping was obtained from the mouse tail by HotSHOT method (Truett et al., 2000) and phenol-chloroform isolation method (Homolka et al., 2011) respectively.

The 8 weeks old recombinant male progeny was then genotyped and tested for the following fertility parameters (1) testes weight (TW), (2) sperm count (SC) and (3) percentage of abnormal spermatozoa (SA) as was described in (Storchova et al., 2004). We determined the following borderlines between the subfertile and fertile phenotype: testes weight 185 mg and proportion of normal spermatozoa 80 %. Males with higher values of these parameters were considered as fertile and males with lower values as subfertile/fertile. Due to a high variance in the number of spermatozoa, we did not use this parameter for the determination of sterile/fertile phenotype. For (PWD x consomic) F1 hybrids, the testis weight up to 70 mg with no sperm in *cauda epididymides* were counted as sterile and above 70 mg with sperm as semisterile/fertile.

For mapping the borders of PWD sequence in X Chr consomics B6.PWD-Chr X# we used high density genotyping platform called Mega Mouse Universal Genotyping Array. The MegaMUGA genotyping platform carries 77000 markers on Illumina Infinum platform (http://csbio.unc.edu/CCstatus/index.py).

SSLP marker	Forward primer	Reverse primer
SR-09	AAGCCTTTTTCTTATCTCAG	TCATTTTATCAGAGCCTAGA
SR-12	ATATAGCACAATAGCCAAGA	TTAGCTCAAATATGATGCC
SR-22	GAGCTCCCAAAGTGTCAAAT	TCATCTTGTTCAGAACAGCC
SR-38	TTGCTTGAACTAAAACAGTG	AGGTTTGTTCTTTGATCAGT
SR-51	CAGGAGAAGATGGCACAATA	TAACCCTTTCACCATGTTTC
SR-62	GTCTTTTTACCCTAAATGTT	GACTGGGACCAATTTGT
DXMit55	CTGCTTCCAGAATATTATCACTACTCC	AAAACATCCATTTATGTTAACACACA
DXMit81	GAGGAGCATCAACCTTCTCG	GAGGTGGGGAGAAACAGAGG
DXMit49	TTGGGACGAGTCTGAGCAC	TTGTCACATTTGTCTTGAAGGC
DXMit166	GAGATAAACCTGACTAACCCTTTCC	GGATTTTCCCAAAAAAGAAACC
DXMit140	ACATGAAAGTTAGAAAGAGACCCG	GTGCACATTTGTGTGTGTATGC
DXMit92	GTATATCTTGCAGCAATAGAAACCC	TCCTCTATATCTGTGCTGTAAGATGC
DXMit76	CCTCCAACCACCAAGACCTA	ATAACACAGACACACATAGATACACCA
DXMit87	TGAGAAAAGTGGTGTGTTTCTAGC	CATTACCTAGGCCTACTTGTAGATCC
DXMit143	AGGAAATGTGTGTACTCTGTATCTATG	TGCTGCCTTGGCATGTATAG
DXMit109	AAGTGGTCAGGTCTAATGGCA	CCTCATAGCCTTCAAACCCA
DXMit142	TGGTGGATGTTTGCCTATCA	GCAGGCAACTGTGAGCCTC
DXMit25	TTCCCAAGCTGCTGTTTCTT	TGGCAGCACTTTAAGCATTG
DXMit119	CTTTAACCATAATAATGGCCTTGC	GGGTTCTGTGATCGCAAGTT
DXMit60	AATGCCTGGTTCTTAGAGGATG	CAGCAACAAGAGAGTTTCATGC
DXMit93	TTGTCAGAATGATCGATTCTTATATC	CACCCAAAGTAGTTAGATCTTATCATT
DXMit114	ATGGCATCCACAGTACCACA	GTAAAATCAATTTGTGAATAAGGAAGC
DXMit16	CTGCAATGCCTGCTGTTTTA	CCGGAGTACAAAGGGAGTCA
DXMit170	TGCAGGCACTAACAGTGAGG	TAGTTTCACTGTGCCATTGTATACA
DXMit173	ATTTGATGTCCTCGTCTGGTG	TAATTATACTGGGGACTAGAACTCAGG
DXMit234	ATTTATGTGTCAGTGGTGGGG	AAACTGGGACATAGTCTATAAGACCG
DXMit31	TTATGTGCTTATTAGCCAAGGTG	AAAATAGAACTTCAGCAGCATGC

Table 6.1. Primer sequences of SSLP markers used for finer *Hstx1/2* mapping.

6.4 QTL analysis

QTL mapping on the recombinant males from (B6-$X^{PWD}X^{B6}$ x PWD) was performed using the R 12.1 (R_Development_Core_Team 2008) and its qtl package (Broman, 2003; Sen et al., 2009) to perform statistical analysis. Marker positions were taken from MGI mouse genetic map (Bult et al., 2008). Standard interval mapping was implemented using *scanone* function. TW and logSC were modeled as continuous variables, fertility/sterile group as a binary variable. Genotype probabilities between the markers were calculated at a grid size of 5 cM and with genotyping error rate of 0.01%. Genome-wide significance was calculated by 1000 permutations and compared to α=5% threshold.

6.5 FACS isolation of spermatogenic populations

Three spermatogenic populations (early-mid pachytene, late pachytene-diplotene and spermatids) were isolated using fluorescence activated cell sorting (FACS) as described earlier (Bastos et al., 2005; Homolka et al., 2007) from PWD and B6 testis. Spermatogenic tubules of mice euthanized by cervical dislocation were incubated in enriched Krebs-Ringer bicarbonate medium (EKRB) and protocol was followed as described below.

10 x KRB (dil. and filtered)	30	ml
1M $CaCl_2$	0.39	ml
200mM	1.5	ml
L-Glu+antibiotics		
MEM AA (50x)	6	ml
MEM non.ess.AA (100x)	3	ml
$NaHCO_3$	4.54	ml
Lactate Na^+ (1.31g/ml)	0.114	ml
Sodium pyruvate	0.216	g
1M HEPES pH 7.25	6	ml

pH adjusted to 7.2 – 7.25 by NaOH, water added to 300ml EKRB

- The tunica was removed and the pair of testis was put into 10 ml EKRB with 100µl collagenase (50mg/lml; Sigma) and 50µl DNAse (1mg/ml; Sigma). Incubate in a shaker incubator at 32°C for 20min at120rpm.

- After incubation, tubules were pipetted with cut tip for 15 to 20 times and filtered using BD cell Strainer (40 micron mesh). Tubules were washed using 10 ml EKRB with 100µl collagenase (50mg/lml) and 50µl DNAse (1mg/ml) and incubated in a shaker incubator at 32°C for 20min at120rpm.

- After incubation, tubules were pipetted with cut tip for 15 to 20 times and filtered using BD Falcon cell Strainer (40 micron mesh).EKRB was added to single cell suspension to vol. 20ml, centrifuged at 1000rpm for 10min at room temperature on Jouan centrifuge. The process was repeated twice.

- The supernatant was removed and the cells were resuspended in 1 ml EKRB containing 1%Fetal calf serum (FCS; invitrogen) and transferred to an Eppendorf tube (20µl remove from the total 1 ml volume and added to 380µl EKRB for cell counting; kept at 4°C).

- The cell suspension was diluted to 1.5 ml using EKRB with 1%FCS.To the diluted single cell suspension, 7.5µl Hoechst (1mg/ml; invitrogen) and 7.5µl DNAse (1mg/ml) were added and incubated in dark at 32°C for an hour on a shaker.

- Before sorting, another 7.5µl of DNAse (1mg/ml) was added. Just before loading the cells for sorting 3µl propidium iodide (1mg/ml; invitrogen) was added and maintained at 32°C.

- The cells were directly sorted into QIAzol lysis reagent of the miRNeasy Mini isolation kit (QIAGEN).
- Small aliquots of cells were sorted in Krebs-Ringer bicarbonate medium (EKRB) for Immunofluorescence analysis. Population composition was determined based on anti-SYCP3, anti-SYCP1, anti-γH2AFX antibodies (details below) and cellular morphology stained by DAPI (Vectashield) .All sorted populations showed 85-90% purity of desired cell types.

6.6 Isotonic protocol for immunostaining of spread spermatocytes.

Isotonic protocol (Mahadevaiah et al., 2009) with modifications.

This part of the experiment has to be carried out very carefully to avoid any contamination. Autoclaved bottles were to be used for ddH2O or MilliQ H2O, falcon tubes, gloves, lab coat etc.

Slide preparation: Prepare following chemicals

CSK buffer

for 1000 µl:	
100 mM NaCl	
300 mM Sucrose	
3 mM $MgCl_2$	
10 mM PIPES	
0.5% triton X-100	Add just before use

1000 µl per slide needed; store at 4 °C

EKRB buffer

10 x KRB (dil. and filtered)	30	ml
1M $CaCl_2$	0.39	ml
200mM	1.5	ml
L-Glu+antibiotics		
MEM AA (50x)	6	ml
MEM non.ess.AA (100x)	3	ml
$NaHCO_3$	4.54	ml
Lactate Na^+ (1.31g/ml)	0.114	ml
Sodium pyruvate	0.216	g
1M HEPES pH 7.25	6	ml

300ml for 4 mice; store at 4 °C. pH adjusted to ~7.20 (770 ul 1M NaOH) . Volume made to 300 ml using MilliQ water.

0.5 x MAH-binding buffer

400 µl per slide (200 µl for blocking, each 100 µl for staining with primary and secondary antibodies

for 400 µl:	
1.5% BSA	
5 % Goat serum	
0.05% triton X-100	
0.2 x Protease Inhibitor	Add just before use
1 x PBS	Make the volume

Preparing single cell suspension:

Tunica was removed from pair of testis and put into 10 ml EKRB + 100µl collagenase (50mg/lml) + 50µl Dnase (1mg/ml). Incubate at 32°C for 20min at 120rpm

- Pipette it with cut tip for 20-25 times and filter it by 40 micron nylon cell Strainer.
- Put tubules in 10 ml EKRB + 100µl collagenase (50mg/lml) + 50µl Dnase (1mg/ml). Incubate at 32°C for 20min at 120rpm
- Pipette it with cut tip for 20-25 times and filter it by 40 micron nylon cell Strainer.
- Filter by 40 micron nylon cell Strainer and remove clumps.
- EKRB was added to single cell suspension to vol. 20ml, centrifuged at 1000rpm for 12min at room temperature on Jouan. Remove the supernatant
- 20 ml of EKRB was added, centrifuged at 1000rpm for 12min at room temperature on Jouan, supernatant removed.
- Cells were resuspended in 1ml EKRB for future use.

Slide preparation:

- Few drops of cell suspension was placed on clean slides (boiled in distilled water for 10 minutes; Silane-prep slides from Sigma S 4651 work well) and allowed to sink for 30 minutes at 4°C in a humidified chamber.

- The cells were permeabilised using 1ml ice cold CSK buffer for 10 minutes (Adjustable according to the requirement) at 4°C in a humidified chamber.
- CSK was drained off placing paper towels and cells were fixed by flooding the slides with ice-cold 1 ml of freshly prepared 4% PFA (in 1X PBS) and left for 10 minutes at 4°C in a humidified chamber.
- Wash the fixed cells by dipping the slide(s) into the coplin jar with PBS twice for 7 minutes or thrice for 5 minutes.
- Block the cells by 200ul 5%goat serum in 1x PBS (fresh) or 0.5x MAH for 1 hour at 4°C - cover the slides with 60mm cover slip .
- Incubate over night with primary antibodies at 4°C (covered with a cover glass). On the next day, wash the slides thrice in 1 x PBS, 5 minutes each. Add secondary antibodies in required dilution. Incubate for 2 to 3 hours (covered with a cover glass) in the dark at 4°C. Wash slides 3 times for 5 minutes each in the dark at room temperature (in 1 x PBS). Air dry the slides in the dark at room temperature and add vectashield DAPI (cover the slides with cover glass).
- Store at -20°C until observation.

6.7 Hypotonic protocol for immunostaining of spread spermatocytes.

Hypotonic protocol (Anderson et al., 1999) with modifications.

This part of the experiment has to be carried out very carefully to avoid contamination. Autoclaved bottles were to be used for ddH2O or MilliQ H2O, falcon tubes, gloves, lab coat etc. Slide preparation: Prepare following chemicals

1% PFA Solution

for 1000 µl:		**condition**
50 mM NaBorate (pH 9.2)	927 µl	
32 % PFA	34 µl	
15% triton X-100	10 µl	
7 x Protease Inhibitor	29 µl	Add just before use

200 µl per slide needed; store at 4 °C

Sucrose 0.1 M

for 500 µl		**condition**
1000 mM sucrose	50 µl	
millipore water	378.6 µl	
7 x Protease Inhibitor	71.43 µl	Add just before use

1000 µl per animal needed; store at 4 °C

0.5X MAH-binding buffer

400 µl per slide (200 µl for blocking, each 100 µl for staining with primary and secondary antibodies)

for 400 µl:	
1.5% BSA	
5 % Goat serum	
0.05% triton X-100	
0.2 x Protease Inhibitor	Add just before use
1 x PBS	Make the volume

- Dissect the testes from killed mouse, remove the tunica. Resuspend the tubules in RPMI buffer by vigorous shaking in hand for 3minutes. Let to sediment them, remove the supernatant. Resuspend the sedimented tubules again, and repeat as before. Macerate tubules in 200µl of RPMI.
- Allow to settle the cell clamps and large tubule clamps for 2min. Pipet the overlying cell suspension and aliquot equally into 2 microtubules.
- Centrifuge the cell suspension for 5 min at 2000 x g = 4600rpm (Eppendorf microfuge). During this time, arrange 7 new slides (boiled clean) in a level plastic dish that contained a damp paper towel.
- Drop 200 µl of an aqueous solution of 1% paraformaldehyde (pH 9.0) and 0.15% Triton X-100 with a cocktail of protease inhibitor and EDTA (Roche 1836153) was dropped onto each slide.
- The supernatants were removed, and the cell pellets in both microtubes were resuspended in 1000 µl of 0.1 M sucrose with the same protease inhibitor cocktail. A 100-µl aliquot of cell suspension was placed on each of 7 slides, and a cover was placed over the plastic dish so the slides would not dry. Incubate for 3 hours at 4°C.
- Rinse the slides gently in Millipore clean water and air dry. Unstained slides were examined using phase microscopy, and only slides on which the cells were well spread were immunostained.
- Slides were washed twice in PBS, 5 min each. Blocking: incubate the slides at room temperature with 200 µl 0.5 x MAH for 1 hour (covered with a cover glass). Go ahead for immunostaining using 0.5 x MAH for diluting the antibodies.
- Incubate over night with primary antibodies at 4°C (covered with a cover glass). On the next day, wash the slides thrice in 1 x PBS, 5 minutes each. Add secondary antibodies in required dilution. Incubate for 2- 3 hours (covered with a cover glass) in the dark at 4°C. Wash slides 3 times for 5 minutes each in the dark at room temperature (in 1 x PBS). Air dry the slides in the dark at room temperature and add vectashield DAPI (cover the slides with cover glass).
- Store at -20°C until observation.

6.8 Protocol for staining of RAD51, DMC1, MSH4 and MLH1 in spermatocytes.

Immunostaining protocol (Dumont and Payseur, 2011) with modifications.

This part of the experiment has to be carried out very carefully to avoid any contamination. Autoclaved bottles were to be used for MilliQ water, falcon tubes, gloves, lab coat etc.

Slide preparation: Prepare following chemicals

Hypo Extraction Buffer

3 ml per genotype is needed (prepare extra); pH has to be adjusted to 8.2 - 8.4 with NaOH and/or HCl (use immediately). Stable for 2 hours (watch out: 45 min incubation time!).

stock solution	**final concentraion**	**condition**
1000 mM Tris, pH 8.2	30 mM	
1000 mM sucrose	50 mM	
1000 mM citric acid	17 mM	
500 mM EDTA	5 mM	
500 mM DTT	2.5 mM	Add just before use
100 mM PMSF	0.5 mM	Add just before use
Tissue culture H2O	fill up to final volume	

1% PFA Solution

200 µl per slide needed; store at 4 °C

for 1000 µl:		**condition**
50 mM NaBorate (pH 9.2)	927 µl	
32 % PFA	34 µl	
15% triton X-100	10 µl	
7 x Protease Inhibitor	29 µl	Add just before use

Sucrose 0.1 M

for 500 µl		**condition**
1000 mM sucrose	50 µl	
millipore water	378.6 µl	
7 x Protease Inhibitor	71.43 µl	Add just before use

1000 µl per animal needed; store at 4 °C

0.5 x MAH-binding buffer

400 µl per slide (200 µl for blocking, each 100 µl for staining with primary and secondary antibodies)

for 400 µl:	
1.5% BSA	
5 % Goat serum	
0.05% triton X-100	
0.2 x Protease Inhibitor	Add just before use
1 x PBS	Make the volume

Slide preparation:

- Remove testes from the mouse, weigh them, remove tunica and place in a PBS-filled watch glass. Rinse in PBS (2 times PBS for washing).
- Transfer to a new watch glass containing 3 ml hypo extraction buffer. Gently tease apart tubules to expose them to the hypo extraction buffer.
- Use two forceps only to push the tubules apart without destroying them. Incubate for approximately 45 minutes in hypo extraction buffer at room temperature.
- After Incubation, macerate the tubules in ~ 50 µl of cold 0.1 M sucrose solution. Make the volume up to 450 µl by using 0.1 M sucrose solution. Remove cell clumps by the 40 µm dense mesh filter into new eppendorf tubes. (Measure the number of cells using a

Neubauer chamber and dilute it to 3000 cells/µl using 0.1 M sucrose solution.)

- Add 180 µl of cold 1% PFA on (boiled cleaned) dry slides in humid chambers to form a thin layer of PFA on the slides. Add 90 µl of diluted cells from a height of ~ 10 cm onto the slides as drops at 3 different spots. Cover the humid chamber to avoid drying of the slides. Incubate at 4 °C for 2 hours (whole step carried out in the cold room at 4°C).
- Rinse the slides gently in millipore clean water and air dry for 15-20 minutes. Wash twice in 1 x PBS, each 5 minutes (rehydration step). Blocking: incubate the slides at room temperature with 200 µl 0.5 x MAH for 1 hour (covered with a cover glass). Go ahead for immunostaining using 0.5 x MAH for diluting the antibodies.
- Incubate over night with primary antibodies at 4°C (covered with a cover glass). On the next day, wash the slides thrice in 1 x PBS, 5 minutes each. Add secondary antibodies in required dilution. Incubate for 4 - 6 hours (covered with a cover glass) in the dark at 4°C. Wash slides 3 times for 5 minutes in the dark at room temperature (in 1 x PBS). Air dry the slides in the dark at room temperature and add vectashield DAPI (cover the slides with cover glass).
- Store at -20°C until observation.
- The images were adjusted with Adobe Photoshop CS (Adobe Systems) and the RAD51,DMC1, MSH4 and MLH1 foci were counted using Image J software (http://rsbweb.nih.gov/ij/).

6.9 Staging the first meiotic prophase of oocytes. To determine the developmental stages of PB6F1, B6PF1, B6 and PWD oocytes, we took an advantage of the synchronous development of oocytes in embryonic ovaries(Dietrich and Mulder, 1983). We visualized chromosomal axes and centromeric regions in oocytes derived from 17.5 dpc (*postcoitum*), 19.5 dpc and 1 dpp (*postpartum*) hybrid ovaries and wild-type controls. The meiocytes found mainly in 17.5 dpc ovaries were classified as pachynema and those prevalent in 19.5 dpc ovaries as diplonema.

6.10 Immunostaining of spread meiocytes.

Meiocyte spreads were prepared by isotonic or hypotonic protocol (Anderson et al., 1999; Turner et al., 2005). For immunocytochemistry, the spread nuclei were immunolabeled with the following antibodies: rat polyclonal anti-SYCP3 (Abcam, #15092), mouse monoclonal anti-

SYCP1 (Abcam, #15087), guinea pig anti-histone linker H1t (Inselman et al., 2003), mouse monoclonal anti-γH2AX (Upstate, #05-636), human autoantibody anti-centromere (AB-Incorporated, #15-235), mouse monoclonal antibody anti-SYCP3 (Santa Cruz, D-1, #74569), rabbit polyclonal antibody anti-Rad51 (Santa Cruz, H-92, #8349), rabbit polyclonal antibody anti-DMC1 (Santa Cruz, H-100, # 22768), rabbit polyclonal antibody anti-MSH4(Abcam, #58666), rabbit polyclonal antibody anti-ATR (Santa Cruz, H-300, # 28901), mouse monoclonal anti-MLH1 (Abcam; #14206), rabbit polyclonal antibody anti-HORMAD1 and HORMAD2 (kind gift from Attila Toth), rabbit polyclonal antibody anti-STAG3 (gift from Rolf Jessberger) and the secondary antibodies: goat anti-Rabbit IgG-AlexaFluor488 (Molecular Probes, A -11034), goat anti-Mouse IgG Alexa Fluor 568 (Molecular Probes, A-11031), goat anti Rabbit IgG-Alexa Fluor 568 (Molecular Probes, A-11036), goat anti-Mouse IgG-Alexa Fluor 350 (Molecular Probes, A- 21049), goat anti Mouse IgG-Alexa Fluor 647 (Molecular Probes, A-21236), goat anti Rabbit IgG-Alexa Fluor 647 (Molecular Probes, A-21245) and goat anti-Guinea pig IgG-Cy3 (Chemicon, #AP108C). The immunocytochemistry was performed directly after RNA FISH, and the images were acquired and examined in a Nikon Eclipse 400 (Tokyo, Japan) microscope with motorized stage control using Plan Fluor objective, 60x (Nikon, MRH00601) and captured using a DS-QiMc monochrome CCD camera (Nikon) and NIS elements program. The images were adjusted with Adobe Photoshop CS software (Adobe Systems).

6.11 RNA Fluorescence In-Situ Hybridization (FISH).

RNA FISH Protocol (Mahadevaiah et al., 2009); Methods in Molecular Genetics with modifications.

This part of the experiment has to be carried out very carefully to avoid any contamination. Autoclaved bottles were to be used for ddH2O or MilliQ H2O, falcon tubes, gloves, lab coat etc.

Probe preparation.

The BAC's were obtained from Source BioScience LifeSciences (http://www.imagenes-bio.de/). Individual probes for RNA FISH were prepared from BAC DNA carrying the genomic region of interest, namely RP23-234F8 for *Scml2*; RP23-70P13 for *Ott*; RP23-34L18 for *Ndufa1* and RP23-364L1 for *Egfl6*, and CITB-288D7 (a gift from Paul S Burgoyne) for *Zfy2*.

- BAC-containing bacteria were streaked onto LB broth (500 ml) containing relevant antibiotic (usually 12.5 µg/mL chloramphenicol) and grown overnight at 37°C in a shaker incubator.

- BAC-DNA was isolated using NucleoBond Xtra Maxi kit (Macherey-Nagel) as per the provided protocol.

- 1 µg of BAC DNA was labeled using BioNick^{TM} DNA Labeling System for biotin labeling or the DIG-Nick Translation Mix for digoxigenin labeling exactly according to manufacturer's instructions (16µl of BAC DNA + 4 µl of mix; Roche).

- The mix was incubated at 15°C for 45 minutes in water bath then store on ice.

- 2µl of the reaction mix was loaded on 2% agarose gel to check the size of the smear. If too large the mix was incubated for 37°C for various time intervals until probes were 200bp long.

- 4µl of the labeled DNA were combined with 2µl of salmon sperm (invitrogen) and 6µl of mouse Cot1 DNA. Precipitate by adding 2.5 volume 100% EtOH. Flicked and spanned (13000 rpm at 4°C for 5 minutes).

- Pellet was washed twice with 70% EtOH, air dried for 5 minutes and later resuspended in 10 µl Formamide. The probe was stored at -20°C.

Meiocyte spread preparation and hybridization.

- Single cell suspensions from the testis were prepared in ice-cold RPMI including L-glutamine.

- Few drops of cell suspension was placed on clean slides (boiled in distilled water for 10 minutes) and allowed to sink for 20 minutes on an ice cold-frozen platform.

- The cells were permeabilised using 1ml ice cold CSK buffer (100mM NaCL, 300mM Sucrose, 3mM $MgCL_2$, 10mM PIPES) with supplements (0.5% Triton X-100 and 2 mM Vanadyl Ribonucleoside) for 10 minutes.

- CSK was drained off placing paper towels and cells were fixed by flooding the slides with ice-cold 1 ml of freshly prepared 4% PFA (in 1X PBS) and left for 10 minutes.

- In meantime, the labeled probes were denatured at 80°C for 10 minutes and 10 µl hybridization buffer (4X SSC,50% dextran sulphate,2mg/ml BSA, 2mM Vanadyl Ribonucleoside) was added into it. Later the mix was vortexed and pre-hybridized at 37°C at least for 30 minutes.

- Slides were dehydrated through ice-cold ethanol series (70% twice, followed by 80%, 95% and100%) for 3 minutes each. Air dried slides were used for probe hybridization.

- Pre-hybridized probe was directly added onto slide centre avoiding air bubble. Cover slip was placed and sealed with rubber cement. Slides were hybridized overnight at 37°C in a Formamide filled chamber.

- Next day cover slip were carefully removed washed twice in wash solution A (50% Formamide in 1 X SSC, pH 7.2-7.4, warmed to 42°C) for 5 minutes with gentle shaking.

- Next slides were washed 3 times in wash solution B (2 X SSC, pH 7.0-7.2, warmed to 42°C) for 5 minutes each with gentle shaking.

- The slides were washed with wash solution C (4XSSC, 0.1% Tween-20, pH 7.2-7.4) for 5 minutes.

- Slides were placed in the humidified chamber (H2O) and 200 µl of blocking buffer (4XSSC, 4mg/ml BSA, 0.1% Tween-20) was added, cover slip was placed and incubated at 37°C for 30-45 minutes.

- Cover slip was removed and 50 µl of diluted (1:10) anti-biotin or anti-DIG secondary antibody conjugated with FITC (Roche or Millipore) in detection buffer (4XSSC, 1mg/ml

BSA, 0.1% Tween-20) was added to the slide. Cover slip was placed and incubated at 37°C for 90-120 minutes.

- After incubation, slides were washed for 3 times in wash solution C for 2 minutes each with shaking.
- For Immunostaining 100µl of diluted primary antibody in detection buffer was added onto the slide and incubated overnight at 4°C.
- Next day slides were washed thrice in wash solution C and diluted secondary antibody was added. Cover slip was placed and incubated at 4°C for 2 hours.
- Later slides were washed thrice in wash solution C for 5 minutes each and mounted in vectashield mounting media with DAPI. The slides were stored at -20°C until observation.

6.12 DNA Fluorescence In-Situ Hybridization (FISH).

DNA FISH Protocol (Kauppi et al., 2011) with modifications.

This part of the experiment has to be carried out very carefully to avoid any contamination. Autoclaved bottles were to be used for ddH2O or MilliQ H2O, falcon tubes, gloves, lab coat etc.

Probe source: MetaSystems and Cambio (ready to use-50µl).

Slide preparation: Testicular nuclear spreads were prepared as per Anderson et.al 1999 with brief modifications described above. Slides were immunostained as described earlier and treated for DNA FISH. All steps to be carried out in dark with little exposure to light.

- Immunostained slides were washed twice in 1x PBS (5 minutes each).
- Slides were dehydrated gradually in 70%, 90% and 100% ethanol (ethanol /water) for 3 minutes each.
- Slides were air dried at room temperature (15-20 minutes) and incubated at 65°C for 1 hour (Ageing).

- The slides were denatured in 70% Formamide in 0.6 x SSC at 72°C (+1°C increase per slide) for 7 minutes.
- After denaturation slides were immersed in 70% ethanol (-20°C; ice-cold) for 3 mins. Afterwards slides were dehydrated gradually in 70%, 90% and 100% ethanol (ethanol /water) for 3 minutes each.
- Slides were air dried at room temperature (15-20 minutes).
- Probes (MetaSystems and Cambio) were prepared as per manufactures instruction (10µl ready to use probe + 1.1 µl mouse cot1 DNA; Invitrogen).
- Probes were denatured at 75°C for 5 minutes and renatured (Pre-annealed) it at 37^{o}C between 30min to 1 hour.
- 10 µl Pre-hybridized probes were directly added onto slide centre avoiding air bubble. Cover slip (24 x 24) was placed and sealed with rubber cement. Slides were hybridized over the weekend (72 hours) at 42°C in a water filled (saturated) chamber.
- Hybridized slides were washed in 4x SSC at 42°C (3 times; 5 minutes each) and mounted in a vectashield mounting media with DAPI. The slides were stored at -20°C until observation.

6.13 In vitro culture, MI and MII spreads and video microscopy of oocytes. We used fully grown germinal vesicle (GV) oocytes from both inter-subspecific hybrids together with C3B6F1 intra-specific oocytes isolated from the ovaries of animals 10–16 weeks old without prior hormonal stimulation. The cells were harvested and processed for chromosome spreads 7 hours after releasing into maturation media. Techniques used for oocyte culture, micromanipulation, microinjection as well as for chromosome spreads and kinetochore counting assay were described previously (Sebestova et al., 2012). Images were scanned with Leica SP5 confocal microscope equipped with AOBS and HCX PL APO 40x/1.3 OIL CS objective. For detection of DAPI, Alexa Fluor 488 and Alexa Fluor 555 excitation wavelengths 405nm, 488 nm and 561nm were used. Spreads were scanned using Leica AF6000 inverted fluorescence microscope equipped with HCX PL APO 100x/1.4-0.7 OIL objective. Live imaging experiments were performed on Leica SP5 confocal microscope equipped with EMBL microscope incubator allowing prolonged

time-lapse experiments in 5% CO_2 and 37ºC. For detection of EGFP and mCherry fluorescent proteins inside live oocytes; 488 and 561 nm excitation wavelengths, HCX PL APO 20x/0.7 IMM CORR λ_{BL} and HCX PL APO 40x/1.3 OIL CS objectives, tandem scanner and internal PMTs or HyDs were used. The 9-11 stacks were captured every 10–12 min for 18 hr. Quantification and data analysis was performed using ImageJ (http://rsb.info.nih.gov/ij/), Imaris (http://www.bitplane.com) and Huygens (http://www.svi.nl) software. For measuring securin signal the mean fluorescence intensity was normalized to the value at the time of GVBD. Mean and standard deviation values were calculated using MS Excel, statistical significance of the difference between the control and experimental groups were tested using Student's t-test (GraphPad Prism software for Macintosh).

6.14 Microarray analysis and real time PCR

RNA was isolated from the sorted cells and 14.5 dpc testes using the miRNeasy Mini isolation kit (QIAGEN) as per recommended protocol. RNA concentration was determined spectrophotometrically at A_{260nm} by NanoDrop (NanoDrop Technologies) and the integrity was checked on Agilent 2100 bioanalyzer - RNA Lab-On-a-Chip (Agilent Technologies). The Total RNA (20–30 ng for gene expression and 120 ng for miRNA expression) was converted in cRNA using the Affymetrix Two-Cycle Target Labeling kit according to the manufacturer's instructions or using the Affymetrix 3′ IVT Express Kit. Affymetrix GeneChip Mouse 1.0ST and Affymetrix GeneChip miRNA 1.0 Array was hybridized with cRNA. The data obtained from the experiments were analyzed using Bioconductor (Gentleman et al., 2004) (http://www.bioconductor.org/) and the R project for statistical computing (version 2.12; http://www.r-project.org/). The probes were annotated to Entrez gene identifiers using the custom chip description file, which is based on NCBI build 37. The data were normalized using gcRMA. We used Linear Models for Microarray Data Package, limma version 3.6 (Smyth, 2004) for statistical evaluations of expression differences. A linear model was fitted for each gene in a given series of arrays by using the lmFit function. To rank the differential expression of genes, we applied the eBayes function of the empirical Bayes method. A correction for multiple testing was performed using the Benjamini and Hochberg false discovery rate method. Genes were considered to be expressed if average expression in all samples was ≥100. The microarray dataset is deposited in the NCBI Gene Expression Omnibus (GEO) with series accession number GSE41707 (Bhattacharyya et al.,

2012). Expression of different X-linked protein coding genes on spermatogenic populations were derived from NCBI GEO profiles or NCBI GEO database GSE7306 (Homolka et al., 2007).

For real time PCR of protein coding genes, reverse transcription of isolated RNA sample was carried out using Applied Biosystems (ABI) high-capacity cDNA reverse transcription kit. The quantification of mRNAs was performed using FastStart DNA Master SYBR Green I kit (Roche) and cycled in the LightCycler 2000 (Roche). Reactions without reverse transcriptase were utilized as negative control. The assays were done in biological and technical triplicates. Data were analyzed using LightCycler Software version 3.5.3 (Roche).For miRNA expression revalidation we used ABI TaqMan MicroRNA assays and followed the manufacturer's instructions. The reactions were cycled in Applied Biosystems 7300 Real-time PCR system and associated software was used for data analysis. The reactions were also carried out using biological and technical triplicates and proper negative controls. Most high and stable expressed miRNA (U6 non-coding RNA for sorted cells and Mir152 for 14.5 dpc testis) were used as a reference for the data normalization. The primers are designed using primer 3 software (http://frodo.wi.mit.edu/) and sequences of primers are in table 5.2

6.15 Sequencing and SNP analysis.

A whole genome exome sequence analysis was carried out for PWD mice at BGI Europe using Illumina HiSeq 2000 sequencers. The reads where aligned against published B6 genome (http://www.sanger.ac.uk/resources/mouse/genomes/). The sequence specifically aligned to the region of interest was discussed in the manuscript. All the non-synonymous mutations between PWD and B6 for 4.7 Mb Hstx2 locus were tabulated. Resequencing experiments on PWD cDNA (for protein coding genes) and BACs (for miNRAs) (Jansa et al., 2005) were carried out as described (Mihola et al., 2007) using sequencing capillary machine ABI310 (Applied Biosystems). The sequences of primers are listed in the table 5.2 Brief sequencing protocol is described below.

Initial PCR

Total: 20ul per reaction:

2.1ul 10X buffer with $MgCl_2$, MBI Fermentas (without ammonium sulfate)
0.35ul 10mM dNTPs

0.2ul of each primer (0.4 total)
0.4ul Taq polymerase, MBI Fermentas
1ul DNAmQ H_2O to 20 ul (15.75)

PCR I: 94°C 1.15, 37X (94°C 0.30, annealing Temperature 0.15, 72°C according to expected length) 10°C forever.

- HOT START: 80-85°C → pause → put samples for 20-25 sec → resume

Band quantification

(On the plate) pipet 0.8ul of 10X loading buffer add 6 or 7 ul of amplificated DNA and load on the 1.5 to 2 % agarose gel with marker-ladder (5ng/ul-load 3 ul)

Run the gel for at least 1 hour, on the imager export the photo to GeneSnapTool and do the manual band quantification.

Calculate quantity – comparison with marker band as a standard (15ng), background adjustment.

ExoSapIt

(Exonuclease I for removing primers, Sap-alcalic phosphatase for removing dNTPs)

At least 1ul of ExoSapIt was added to 4ul of sample and mix with tip.

Reaction : 37°C – 20:00 min, 80°C – 15:00 min, 25°C - 55:00 min. (stop first after reach 25°C)

Sequencing PCR

Total: 10ul per reaction:
2ul of RR mix *
1ul of 5X seq buffer *
0.3ul of one sequencing primer (20uM)
DNA after ExoSapIt (calculated volume) †
mQ H_2O to 10 ul (also calculated)

* General Mix;

- For more than 1kbp pcr product add 4 ul of RR and no seq buffer

- For less than 0.3kbp pcr product add 1ul of RR and 1.5ul of seq buffer

† Quantity of DNA per one 10ul-reaction

100 – 200 bp: 1 – 2 ng
200 – 500 bp: 2 – 5 ng
500 – 1000 bp: 5 – 10 ng
1000 – 2000 bp: 10– 20 ng
more than 2000 bp: 20 – 50 ng

PCR II: 96°C 0.05, 28X (96°C 0.10, 50.0°C 0.05, 60°C 4.00) 10°C forever

- HOT START: 80-85°C → pause → put samples for 20-25 sec → resume

Repurify/condensation

Condensation with 1/10 of sodium acetate (pH 5.2) plus ethanol (2.5 times of reaction volume). It means 1ul of NaAc and 25ul of ethanol

Add 26 ul of mixture to all new marked tubes needed

Add 10 ul of final pcr reaction – above the surface (because of condensation) and mix by finger flicking

Incubate 15 min in room temperature and microfuge 13200rpm (max) for 20 min in defined orientation (expecting location of invisible pellet)

Remove supernatant and add 80 ul of 75% EtOH and microfuge 10 min (13200rpm)

Remove supernatant and dry in 80-85°C for 1 min.

Dissolve in 20ul of formamide (vortex and spin-slightly), denaturate in 95°C for 1-2 min and quickly transfer on ice (let it on ice at least 5 min)

Some of the SNPs were also confirmed using Mouse phenome database (http://phenome.jax.org/).

6.16 Statistical analysis

Multiple biological replicates of each genotype were analyzed for cellular phenotypes and RNA expression. Significance of BW, TW, sperm morphology and breeding phenotypes was computed using Welsch's t-test. Differences between cellular phenotypes were determined with $\chi 2$ test, ANOVA, and Mann-Whitney U test. All computations were done using R 2.15.0 or Graphpad prism. The dN:dS ratio (an indicator of evolutionary selective pressure on genetic processes) of

different X-linked protein coding genes between rat and mouse was calculated using ensemble (http://www.ensembl.org/biomart/martview/bcc06f42e7f96c64c420679e0520676e).

RTPCR primers	
Sequence	Name
GGCTGTATTCCCCTCCATCG	RT-Actb1-F
CCAGTTGGTAACAATGCCATGT	RT-Actb1-R
ATCCAGCAGCAGCAAGTGAT	RT-Ctag2-ex2-3-CF
AGGATCTTCTGTGGTCCACCT	RT-Ctag2-ex2-3-CR
GCTCAGGTAACATTGACTCCAA	RT-4930447F04Rik-F1
TCTGTCTTGATTCTTGTCCTTTGT	RT-4930447F04Rik-R1
TTCAAAGGCTGACCCCTACA	RT-Slitrk2-F1
TGGCTTTTGGAGCTCTGGT	RT-Slitrk2-R1
AGGGACCTTACTTAGGTT	RT-4933436I01Rik-F1
GAGGCTTCACAATGGAC	RT-4933436I01Rik-R1
GTGAGGATGATAAAGGGTGAG	RT-Fmr1-ex5-6F
CATAAGTTACAGAGAAGGCAC	RT-Fmr1-ex5-6R
GAGGAGGAAGAGGATGAACAG	RT-Fmr1nb-ex5-6F
TTTCAATGGGACAGTAAAGCTC	RT-Fmr1nb-ex5-6R
Re-sequencing primers	
ATCGAAGGCCAAGTCAGAGA	SEQ-Fmr1nb-ex1to3-F
ATCGAAGGCCAAGTCAGAGA	SEQ-Fmr1nb-ex1to3-R
AGGTGGTGGTGGCATGTAAT	SEQ-Fmr1nb-ex3to6-F
GCATGCAATGGAACTTTAATTTG	SEQ-Fmr1nb-ex3to6-R
CGTGGATATGTGCAAGCTCATCCATAAT	SEQ-MiR465b-LRP-F1
ACAGCAGGCCTTAAACCCATTGAGAGAT	SEQ-MiR465b-LRP-R1
AACAAGCGGCAGAAAAAGAA	SEQ-4933436I01Rik-F1
ATTGTCCCAGCTATGCATCC	SEQ-4933436I01Rik-R1
GGCCCTTAACGGCTATGATT	SEQ-Pri-Mir-465b-F
GAAAGGCCCTGATCAATTTTT	SEQ-Pri-Mir-465b-R
TGACCCTTTACTTGGCCATT	SEQ-Mir-465a-F
TGTGGATATGTCCAAGCTCATC	SEQ-Mir-465a-R
AGTAGTAGGATTCTGTATGACCCTTT	SEQ-Mir-465b-F
AAGAATGTGGCCATGTGGA	SEQ-Mir-465b-R
AAGTTTGTAGAGCAGGTGGTGAA	SEQ-Ctag2A-F
ATGAAATGCCTTTGCCTTGT	SEQ-Ctag2D-R

Table 6.2: Primer sequences for RT-PCR and sequencing of candidate genes.

Results

7. Genetic basis of hybrid sterility

7.1 Asymmetry of reciprocal F1 hybrid male sterility is controlled by the middle part of Chr X.

The asymmetry in hybrid sterility was reported in *Drosophila* (Zeng and Singh, 1993; Turelli and Moyle, 2007; Reed et al., 2008) and in experimental mouse crosses (Pialek et al., 2008; Mihola et al., 2009). In our model, hybrids between PWD female and B6 male (henceforth PB6F1) were sterile with testis weight (TW) 62.8 mg and no sperm in *ductus epidydimis*, while males from the reciprocal cross between B6 female and PWD male (henceforth B6PF1) were affected only by a partial spermatogenic arrest compatible with fertility (TW 112.6 mg and 13.7 million sperm). The asymmetry in F1 sterility could be explained by one of the following five mechanisms: (1) X-autosomal interaction, (2) Y-autosomal interaction, (3) X-Y incompatibility, (4) mitochondrion-nuclear incompatibility, or (5) by incompatibility of the imprinted autosomal gene(s). To experimentally validate these options, we crossed B6.PWD-Chr X.1, X.2 or X.3 consomic females identical with B6 but carrying the proximal, middle or distal part of Chromosome (Chr) X of PWD origin (Gregorova et al., 2008) with PWD males. In all three crosses the offspring received B6 and PWD autosomal sets from the opposite parents compared to original PB6F1 males, but the Chr Y was of PWD origin. The F1 male progeny of B6.PWD-Chr X.2 females and PWD male (henceforth DX.2PF1) showed typical F1 hybrid sterility phenotype with small testes (TW 60.9mg) and no sperm, while crosses of B6.PWD-Chr X.1 or X.3 consomic females with PWD males (henceforth DX.1PF1 and DX.3PF1 respectively) yielded fertile males with testis weighing more than 110 mg and 10 to 15 million sperm (Figure 7.1). Based on the known distal PWD border of B6.PWD-Chr X.1 and proximal border of B6.PWD-Chr X.3, the region carrying the PWD-specific incompatibility locus was delimited to 61.0 Mb – 94.3 Mb interval (Gregorova et al., 2008). The X-Y interaction as one of the possible causes of asymmetry was tested using hybrids between PWD female and B6.PWD-Chr Y consomic male. The (PWD x B6.PWD-Chr Y)F1 males carried both sex chromosomes of PWD origin but were sterile (Figure 7.1). Moreover, the effect of PWD mitochondria was excluded because fertility parameters of F1 hybrids of B6.PWD-Mit conplastic females and PWD males were not significantly different from fertile B6PF1 hybrids (Figure 7.1). In conclusion, we can exclude the X-Y interaction, the

autosome-Y or mitochondrial incompatibility and monoallelic expression of imprinted autosomal genes as the cause of asymmetry of the F1 hybrid fertility, leaving the Dobzhansky-Muller (D-M) incompatibility (Dobzhansky, 1951) of the middle part (61.0 Mb – 94.3 Mb; NCBIM37) of the X^{PWD} (*M. m. musculus)* chromosome with the heterospecific hybrid autosomal genome as the sole cause of the asymmetry in reciprocal F1 hybrids.

7.2 Estimating the number of F1 hybrid sterility gene: major locus on Chr.17 and 19.

The actual number of hybrid sterility gene participating in reproductive isolation mechanism in PB6F1 hybrid sterility model was not known. In an experiment to test the role in hybrid sterility of each autosome separately, we checked the fertility parameters of F1 male progeny of PWD females and B6.PWD-Chr# consomic males genes (Gregorova et al., 2008). The hybrid sterility phenotype is a culmination of D-M interactions of recessive to underdominant or dominant alleles in hybrid background. None of the 17 autosomes PWD/PWD homosomic on F1 background revealed recessive PWD hybrid sterility genes. Out of all F1 hybrids between PWD females and B6.PWD-Chr# males analyzed only (PWD x B6.PWD-Chr 17)F1 and (PWD x B6.PWD-Chr 19)F1 males resulted in full (TW 198mg, SC 33.9 million) and partial fertility (TW 73 mg, SC 0.193 million) rescue respectively (Figure 7.2). The action of hybrid sterility gene at Chr 17, most probably *Hst1/Prdm9*, was clearly underdominant because both its homozygous forms, PWD/PWD and B6/B6, rescued hybrid sterility when situated on F1 hybrid background or in N2 hybrids (Dzur-Gejdosova et al., 2012). The effect of Chr 19^{PWD} homosomy can be interpreted as the action of a dominant B6 hybrid sterility locus in PB6F1 sterile hybrid. In contrast introgression of the X^{PWD} chromosome into the B6 genetic background resulted in male-limited sterility associated with incomplete postmeiotic arrest and production of abnormal sperm unable to fertilize eggs (Storchova et al., 2004). Further, the *Hstx1* hybrid sterility locus responsible for the X-linked male sterility was localized to the middle region of the X^{PWD}. Its phenotype depends on epistatic *cis*-interaction with at least one proximal and one distal region on Chr X (Storchova et al., 2004). This work was done in collaboration with Dr.Sona Gregorova.

7.3 Fine-scale genetic mapping of X-linked F1 hybrid sterility locus- *Hstx2*

In the section 7.1 we have shown that asymmetry in male limited hybrid sterility phenotype between PWD and B6 is controlled from the middle region of chromosome X (61.0 Mb – 94.3

Mbp, NCBIM37). To further dissect the role of X–linked genes in F1 hybrid sterility, we produced 124 F1 males by crossing heterospecific consomic female B6-$X^{PWD}X^{B6}$ with PWD male. The hybrid males produced from such a cross have the same heterospecific PWD/B6 autosomes, Chr Y^{PWD}, and mitochondrial^{B6} DNA while recombinant Chr X loci were either PWD or B6. Eight-weeks-old hybrid males were tested for reproductive phenotypes such as testis weight (TW) and sperm count (SC) and genotyped using 27 X-linked SSLP markers (see materials and methods). Single QTL analyses were performed using the TW and SC phenotypes. The cross yielded males with a wide range of TW (from 56 to 186 mg) and SC (from zero to 13.5 million) in *cauda epididymis*. The QTL analysis of the TW phenotype of the F1 progeny revealed a 1.5-LOD support interval between 62Mb - 66.5 Mb (NCBIM37), located at the middle of Chr X (Figure 7.3A). The maximum LOD score of 30 was at 63.9 Mb (NCBIM37) marked by DXMit87 (Figure 7.3B). The QTL analysis for SC detected a 1.5-LOD-support interval mapped also between 62 Mb and 66.5 Mb (Figure 7.3C) with peaks on 63.9Mb (NCBIM37) with LOD score of 20 again localized at DXMit87 (Figure7.3D). The region from 62 and 66.5 Mbp (NCBIM37) segregates with male fertility phenotypes was named as hybrid sterility X 2 locus or *Hstx2*.

7.4 Preparation of consomic mice carrying F1 hybrid sterility locus- *Hstx2*

To further refine the position of *Hstx2*, a new subconsomic strain B6.PWD-Chr X.1s was created. We crossed heterospecific consomic females B6-$X^{PWD}X^{B6}$ with B6 male to specify the position of X-linked locus (loci) controlling the sterility phenotype. We analyzed 38 PWD/B6 single-recombinant males between 62 and 66.5 Mb (NCBIM37) to further narrow down the critical region. For genotyping 27 SSLP markers uniformly covering the X chromosome were used. Genotyping data revealed two very short recombination intervals around the borders of the 4.5Mb critical region harboring *Hstx2* locus. Further breeding experiment failed to narrow the region. Thus, the suppression of recombination inside the critical region prevented further reduction of the *Hstx2* interval. For functional studies on *Hstx2*, two homosomic subconsomic strains carrying recombinant Chr X of PWD origin on otherwise B6 genetic background were established. Using high resolution Mouse Universal Genotyping Arrays we found that the strain B6.PWD-Chr.X.1 carries the PWD segment from 5.4Mb – 64.8Mb (GRCm38), while other subconsomic strain B6.PWD-Chr.X.1s harboring *Hstx2* locus carries the PWD segment from 5.4Mb – 69.5 Mb (GRCm38). The difference between the two subconsomic strains was

remapped to 4.7Mb (GRCm38) harboring the *Hstx2* locus. This work was done in collaboration with Dr. Radka Reifova.

7.5 Asymmetry of reciprocal F1 hybrid male sterility is controlled by $Hstx2^{PWD}$ locus.

To further localize the *Hstx2* region B6.PWD-Chr.X.1s subconsomic females were crossed with PWD males (henceforth (B6.PWD-Chr.X.1 x PWD)F1 or DX.1sPF1). The (B6.PWD-Chr.X.1 x PWD)F1 and (B6.PWD-Chr.X.2 x PWD)F1 (henceforth DX.1PF1 and DX.2PF1 respectively) hybrid males were used as controls. The crosses are explained in Figure 7.4. The DX.1PF1 hybrid males were fertile with 113 mg TW and 10.9 million sperm in *cauda epididymis*. But DX.1sPF1 hybrid males were sterile with 61mg TW ($p < 0.0001$, Welch's t-test) and no sperm (Figure 7.4). Meanwhile DX.1sPF1 hybrid males were similar to DX.2PF1 male hybrids with no significant difference in sterility phenotype (Figure 7.4). Thus, DX.1sPF1 hybrids fully reconstructed the HS phenotype of PB6F1 hybrid males, showing azoospermia in both hybrid males. The position of *Hstx2* was localized to 4.7 Mb interval delineated by UNC30904273 for the distal end of B6.PWD-Chr X.1 PWD sequence and UNC30934795 for the distal end of B6.PWD-Chr X.1s (X: 64,880,641-69,581,094 bp; GRCm38).Hence, using DX.1PF1 and DX.1sPF1 F1 hybrids, the asymmetry in F1 hybrid sterility phenotype was mapped back to 4.7-Mbp $Hstx2^{PWD}$ Chr X region.

7.6 *Hstx2* locus also harbors *Hstx1* hybrid sterility locus.

Previously, it has been shown that introgression of the proximal part of chromosome X^{PWD} on B6 background can causes male limited infertility (Storchova et al., 2004). In contrast to F1 hybrid sterility phenotype of reduced TW and azoospermia, the males with introgressed X^{PWD} showed teratozoospermia and failure to produce offspring (Storchova et al., 2004). To further dissect the region and to acquire a high resolution genetic map we crossed heterospecific consomic females B6-$X^{PWD}X^{B6}$ with B6 male. Seventy one single recombinant males with recombinant PWD/B6 X chromosome on mixed PWD/B6 genetic background from 4-9 backcross generations of (PWDxB6) x B6-BC4-9 cross were genotyped and considered for various male reproductive phenotypes (Figure 7.5). The recombinant males with the PWD segment encompassing the proximal 64.8 Mb (GRCm38) were fertile (except for 2 out of 20 no offspring, but other fertility parameters similar to fertile males). When the recombination breakpoint moved 4.7 Mb distally to 69.5 Mb (GRCm38) the males became sterile or sub-fertile (Figure 7.5) indicating the region

harboring *X-linked hybrid sterility 1* (*Hstx1*) gene. The 4.7 Mb *Hstx1* locus overlaps same interval on chromosome X carrying *Hstx2*. To further localize *Hstx1*, four homosomic subconsomic males (Gregorova et al. 2008 and B6.PWD-Chr.X.1s) carrying recombinant Chr X of PWD origin on otherwise B6 genetic background were studied for reproductive phenotype (Figure 7.4). In pair- wise comparison with all the three subconsomics and B6 controls, the B6.PWD-Chr.X.1s strain displayed a significant low TW (171mg) and higher sperm abnormality (62%; SA; $P < 0.05$, Welch's t-test; Figure 7.4). The 4.7 Mbp locus between 64.8Mb to 69.5 Mb (GRCm38) overlaps with the region containing *Hstx2* mentioned above. However, in spite of the presence of $Hstx1^{PWD}$ allele, the B6.PWD-Chr X.2 subconsomic males showed significant difference in reproductive phenotypes to that of B6.PWD-Chr X.1s. Such divergence in the phenotypes between B6.PWD-Chr.X.1s and B6.PWD-Chr.X.2 (both carrying *Hstx1*) indicates epistasis between *Hstx1* loci with another locus on the proximal region of Chr X^{PWD}. This work was done in collaboration with Dr.Radka Reifova.

7.7 Dissecting epistasis between *Hstx2* and *Prdm9*.

To understand the consequence of epistasis between two major hybrid sterility loci, $Hstx2^{PWD}$ and $Prdm9^{PWD/B6}$, we crossed B6.PWD-Chr.X.1s female with B6.PWD-Chr.17 male. The resulting F1 hybrids represent a unique model to evaluate the interaction between $Hstx2^{PWD}$ and $Prdm9^{PWD/B6}$ on B6 genetic background. As controls, we used (B6.PWD-Chr.X.1 x B6.PWD-Chr.17)F1 and (B6x B6.PWD-Chr.17)F1 hybrid males both lacking $Hstx2^{PWD}$. The (B6.PWD-Chr.X.1s x B6.PWD-Chr.17)F1 hybrids were sterile with TW 127.7 mg, SC 13.9 million and SA of 88.3% in *ductus epididymis* whereas (B6.PWD-Chr.X.1 x B6.PWD-Chr.17)F1 and (B6x B6.PWD-Chr.17)F1 hybrid males had TW above 212 mg, SC above 42 million and 13 to 15% SA ($P<0.05$; Welch's t-test; Table 7.1).These results suggest that the epistasis between *Hstx2* and hetrozygosity of Chr 17 (may be due to *Prdm9*) does contribute to the manifestation of the teratozoospermia phenotype in a homogenous genetic environment. The data suggest other weak recessive interacting loci on other autosomes or background heterozygosity must be complementing the D-M interactions of major hybrid sterility genes in PB6F1 sterile hybrids to produce F1 sterility phenotype.

7.8 Behavior of *Hstx2*^{PWD} depends on genetic background of the hybrid animals

The co-occurrence of *Hstx1* and *Hstx2* in a single region made us to investigate the incompatibilites between various genetic backgrounds and *Hstx2* locus. To test it, we introduced *Hstx2*^{PWD} to a different (*M.m.m* x *M.m.d*)F1 hybrid background, where F1 hybrids lack the meiotic block phenotype. PWD and PWK are related inbred strains derived from *M.m.m* subspecies (Gregorova and Forejt, 2000). However, the F1 hybrids resulting from the cross of PWK female and B6 males are semi-fertile, whereas hybrids between female PWD and male B6 are sterile due to azoospermia (Table 7.2). Therefore, we asked whether the presence of *Hstx2*^{PWD} in (PWK x B6)F1 hybrid background can influence its meiotic phenotype. We crossed B6.PWD-Chr.X.1, X.1s, X.2 and X.3 subconsomic females with PWK male. The 8-weeks-old (B6.PWD-Chr.X.1 x PWK)F1 males were fertile with 173.6 mg TW and 29.5 million SC, whereas (B6.PWD-Chr.X.1s x PWK)F1 hybrid males had 79.5mg TW with no sperm in *cauda epididymis* (Table 7.2). Surprisingly, 24 weeks old (B6.PWD-Chr.X.1s x PWK)F1 hybrid males showed partial rescue in its sterility phenotype with a significant increase in TW to 109.8 mg and 0.6 million sperm in *cauda epididymis* (Table3, $P<0.05$, Welch's t-test). The phenotypes in 8 and 24- weeks-old (B6.PWD-Chr.X.1s x PWD)F1 and (PWD x B6)F1 hybrid males remained similar (Table 7.2). This delayed fertility phenotype in (B6.PWD-Chr.X.1s x PWK)F1 hybrid males suggested that the *Hstx2*^{PWD} locus cannot manifest the same phenotype in (PWK x B6)F1 background as in (PWD x B6)F1 background. The above experiment concludes that the manifestation of *Hstx2*^{PWD} locus depends on epistasis involving other interacting locus on genetic background.

7.9 Candidates for *Hstx1* and *Hstx2*

Our mapping experiments with introgression model and F1 hybrids of B6.PWD-Chr.X# subconsomic strains indicated a single 4.7-Mbp region on PWD Chr X involved in multiple hybrid sterility phenotypes. The QTL showed an overlap with previous studies on a different hybrid sterility model (Storchova et al., 2004; Oka et al., 2004; Good et al., 2008a). In this 4.7 Mbp hybrid sterility locus, there are eleven known protein coding and 20 miRNA genes (Figure 7.6). Out of these, six genes (cancer/testis antigen 2 or C*tag2,* RIKEN cDNA 4930447F04 gene or *4930447F04Rik,* SLIT and NTRK-like family, member 2 or *Slitrk2,* RIKEN cDNA 4933436I01 gene or *4933436I01Rik,* fragile X mental retardation syndrome 1 homolog or *Fmr1*

and fragile X mental retardation 1 neighbor or *Fmr1nb*) and all 20 miRNAs show expression in meiotic prophase (Figure 7.6A and Table 7.3). Out of the six genes; *4933436I01Rik* with an unknown function is abundantly expressed in post meiotic round spermatids; whereas *Fmr1* and *Fmr1nb* are predominantly expressed in early prophase. The other three genes (C*tag2; 4930447F04Rik, Slitrk2*) showed expression in both pre and post-meiotic cells (Figure7.6A). All the six genes showed similar expression in sorted spermatogenic population in PWD and B6 strain (Table 7.3). They showed expression on 14.5dpp testis of PB6F1 and reciprocal B6PF1 hybrids with no significant difference between them (Table 7.4; Figure 7.6C). All 20 miRNAs present in *Hstx1/2* locus are expressed in adult testis and do not undergo meiotic sex chromosome inactivation ((MSCI) (Song et al., 2009); Table 7.3). Out of the 20 miRNAs Mir465a/b/c-3p showed approximately two fold upregulation in the early and late pachytene cells in PWD compared to that of B6 (Table 7.3; Figure 7.6B). The comparison of expression profiling of PB6F1 14.5dpp testis with that of B6PF1 showed 1.5 to 2 fold up regulation of Mir88b-3p, Mir465a/b/c-3p and Mir465a/b -5p, while Mir743a,Mir743-5p,Mir880 and Mir465c-5p showed 1.2 to 4 fold down-regulation (Table 7.4 and Figure 7.6D).

Re-sequencing experiment using PWD genomic DNA and BAC libraries showed number of non-synonymous mutations in protein coding genes listed in Figure 7.8. The inspection of exome sequencing data revealed seven nonsynonymous substitutions in the PWD allele of *4933436I01Rik* gene compared to B6. Of the remaining genes, *Aff2* has five, *Fmr1nb* has two, C*tag2; 4930447F04Rik, and Slitrk2* have one whereas *Fmr1* has no non-synonymous substitutions between PWD and B6. Among miRNAs Mir743a has a single nucleotide polymorphism in its seed sequence, which changes it from the AAAGACA in B6 to AAAGACG in PWD (Figure 7.8). These results were further confirmed by re-sequencing using the Sanger method and using mouse phenome database.

Genes involved in reproductive isolation in *Drosophila* and mouse (including *Prdm9*) have been shown to be rapidly evolving (Ting et al., 1998; Barbash et al., 2004; Barbash et al., 2003; Presgraves et al., 2003; Brideau et al., 2006; Mihola et al., 2009) and to undergo positive selection, an important prerequisite for Dobzhansky-Muller incompatibilities (Coyne et al., 2004; Orr et al., 2004). Two of the candidates for the *Hstx1/2* locus (*4933436I01Rik* and *Fmr1nb*) displayed an elevated rate of protein evolution in comparison with their rat orthologs (Figure

7.8). In particular, *4933436I01Rik* is among the most rapidly evolving genes on Chr X (Bono et al., 2003; Good et al., 2008b). As *4933436I01Rik* is under positive selection, it is likely to function both as *Hstx1* and *Hstx2* because of its pre and post-meiotic expression.

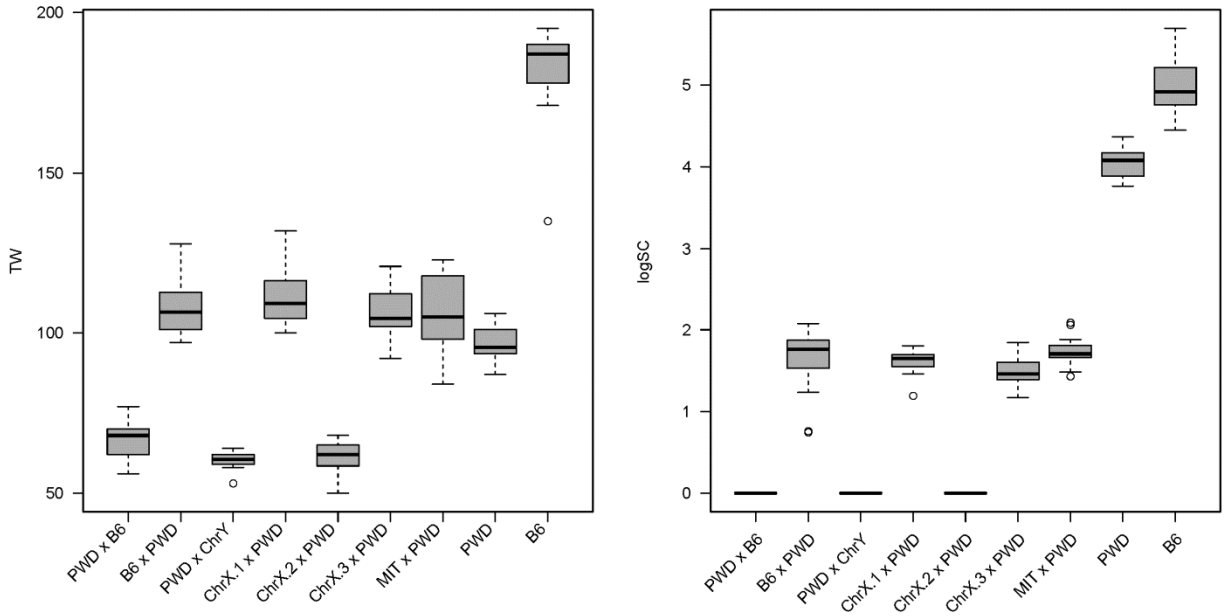

Figure 7.1: Box plot ranges for male fertility parameters of reciprocal F1 hybrids and hybrids of selected chromosome substitution strains. TW – Testes weight, LogSC - log sperm count. Chr # is an abbreviated designation for a B6.PWD-Chr# chromosome substitution strain.

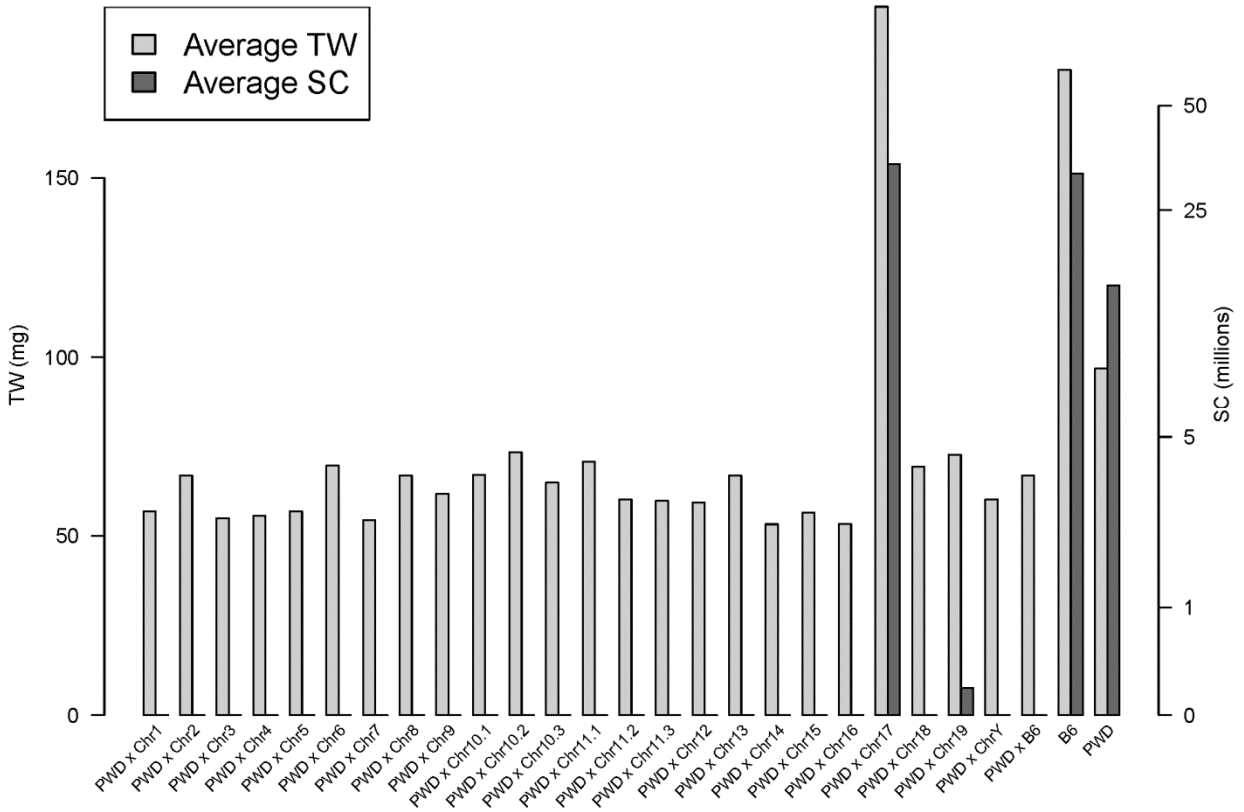

Figure 7.2: Fertility parameters of F1 hybrids between PWD and chromosome substitution strains. Bar plots represent average testis weight (mg) and log-sperm count across individual crosses. Chr # is an abbreviated designation for a B6.PWD-Chr# chromosome substitution strain.

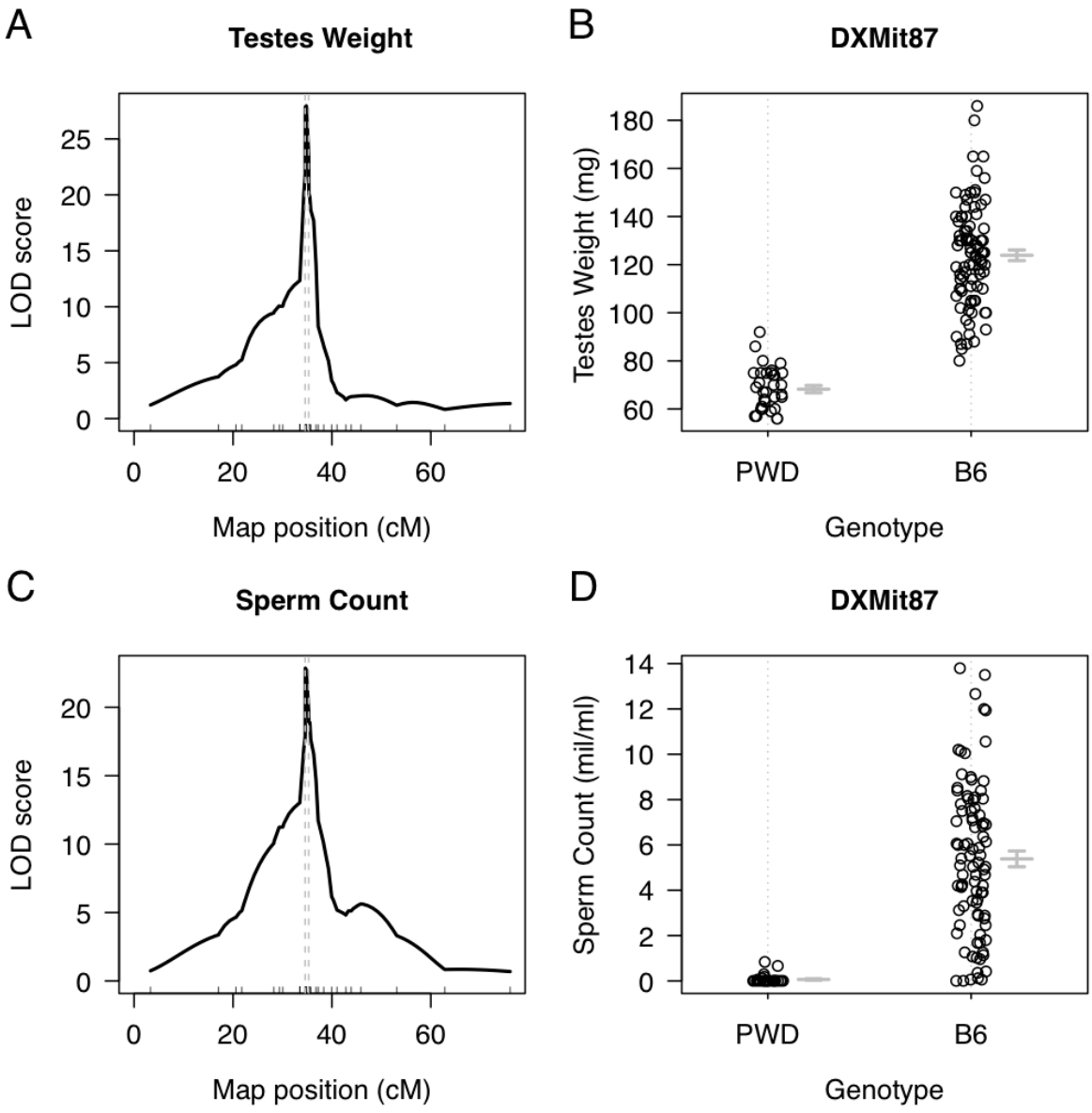

Figure 7.3: Single QTL mapping on X chromosome on F1 hybrid males from the cross between consomic females carrying heterozygous X (B6.Chr $X^{PWD}X^{B6}$) with PWD males. (a) QTL analysis using testis weight shows a 1.5-LOD support interval between 34.59 cM to 35.30cM, located in the central region of Chr X. (b) Testis weights of males carrying *DXMit87* (LOD score of 30) from PWD versus B6.(c) QTL analysis of sperm count shows 1.5 LOD support interval between 34.59 cM to 35.30cM. (d) Sperm counts of males with *DXMit87* (LOD score above 20) from PWD versus B6.

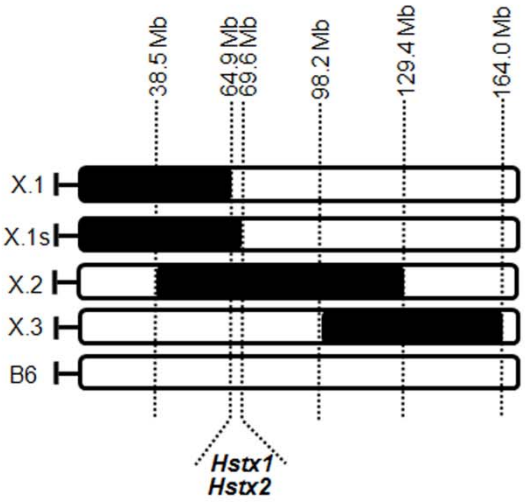

	Hstx1			*Hstx2*	
	B6.PWD-Chr X x B6			B6.PWD-Chr X x PWD	
	(B6 x B6)			(PWD x B6)	
	Testes weight (mg)	Sperm count ($x10^6$)	Abnormal sperm (%)	Testes weight (mg)	Sperm count ($x10^6$)
X.1	198±32	30.9±10.5	17.5±5.7	113±9	10.9±2.9
X.1s	171±11	24.8±6.5	**62.3±3.6**	61±5	**0**
X.2	183±12	26.5±2.5	24.3±6.4	61±5	**0**
X.3	179±22	20.8±7.5	16.3±2.6	106±8	15.4±3.5
B6	188±21	28.5±3.2	14.6±6.6	62.8±5.8	0

Figure 7.4: Phenotypic values of F1 hybrids resulting from the crosses of B6, PWD and B6.PWD-Chr.X# subconscomics and parental controls. The figure highlighted in the table are significant difference from the controls ($P<0.01$; Welch's t-test).Position of markers are as per GRCm38.

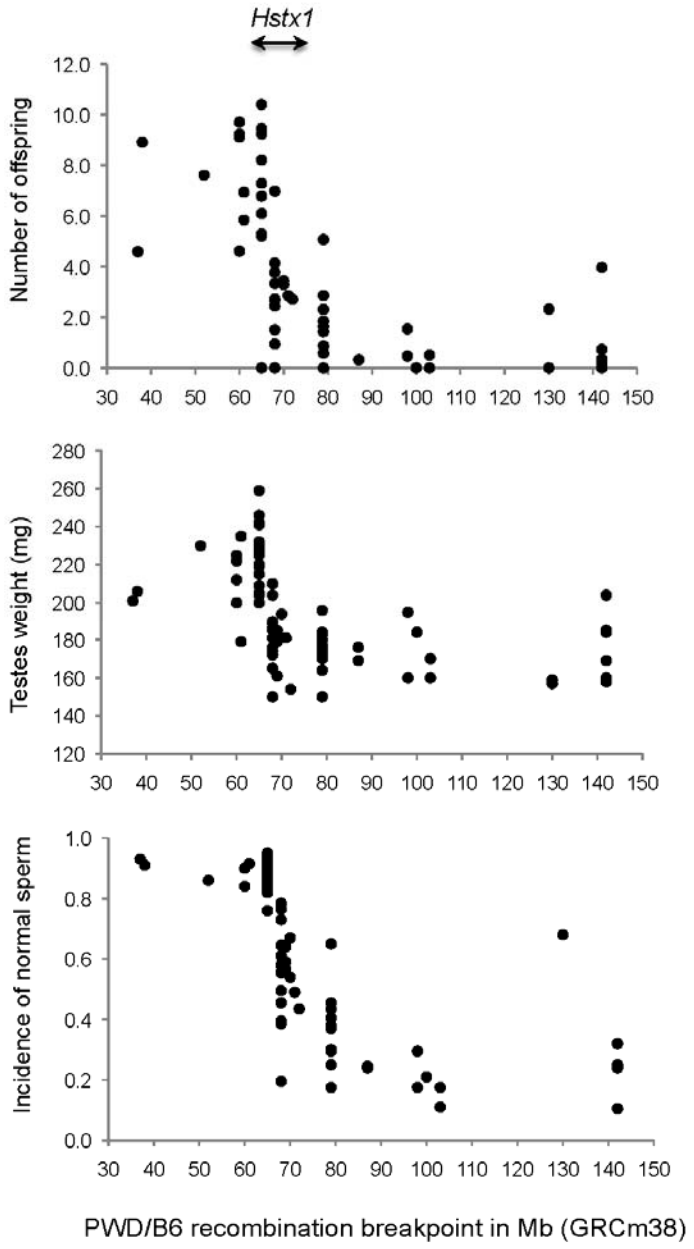

Figure 7.5: Values of three fertility parameters depending on the position of the recombination breakpoint on the X chromosome in 71 PWD/B6 single recombinant males. The fertility declines in males with recombination breakpoint between markers *DXMit76* (64.8 Mb) and *DXMit143* (69.5 Mb), indicating that this region encompasses *Hstx1* gene. The broken lines refer to borderlines between fertile and sterile/subfertile phenotypes.

Strain	Testis weight (mg)	Sperm count ($x10^6$)	abnormal sperm (%)
B6.PWD-Chr.17 (n=10)	195.6 ± 7.7	35.8 ± 7.9	-
B6.PWD-Chr.X1s (n=5)	173.0 ± 2.8	17.8 ± 7.5	56.7
(B6 x B6.PWD-Chr.17)F1 (n=3)	213.3 ± 9.5	47.3 ± 9.6	15.7
(B6.PWD-Chr.X1 x B6.PWD-Chr.17)F1(n=3)	212.7 ± 10.1	42.6 ± 7.6	13.5
(B6.PWD-Chr.X1s x B6.PWD-Chr.17)F1(n=6)	123.0 ± 8.8*	15.4 ± 6.7*	87.8*

Table 7.1: Fertility phenotypes of consomic hybrids showing epitasis between *Hstx2* and *Prdm9***.** * means P<0.05; Welch's t-test for the comparison of 8-weeks-old (B6.PWD-Chr.X1s x B6.PWD-Chr.17)F1 verses all other genotypes.

Cross	8 weeks old			24 weeks old		
	Testes (mg)	Sperm ($x10^{-6}$)	n	Testes (mg)	Sperm ($x10^{-6}$)	n
(PWD x B6)F1	62.8 ± 5.8**	0***	52	58.8 ± 8.1**	0**	10
(B6.PWD-Chr X.1s x PWD)F1	61.3 ± 5.2**	0***	32	60.3 ± 6.6**	0**	10
(PWK x B6)F1	110.2± 6.8*	1.7 ± 0.7	12	-	-	-
(B6.PWD-Chr X.1 x PWK)F1	173.6 ± 9.6	29.5 ± 3.9	11	-	-	-
(B6.PWD-Chr X.1s x PWK)F1	79.5 ± 6.2**	0***	15	109.8 ± 6.2	0.6 ± 0.2	15
(B6.PWD-Chr X.2 x PWK)F1	70.8 ± 6.9**	0***	10	-	-	-
(B6.PWD-Chr X.3 x PWK)F1	118.2 ±7.9*	9.0 ± 2.0*	8	-	-	-

Table 7.2: Fertility phenotypes of F1 hybrids resulting from PWD and PWK crosses.

**P<0.05 and ***P <0.00001; Welch's t-test; 8 weeks compared with all F1 hybrid genotypes compared to (B6.PWD-Chr X.1 x PWK)F1 ;whereas for 24 weeks hybrids were compared against (B6.PWD-Chr X.1s x PWK)F1.

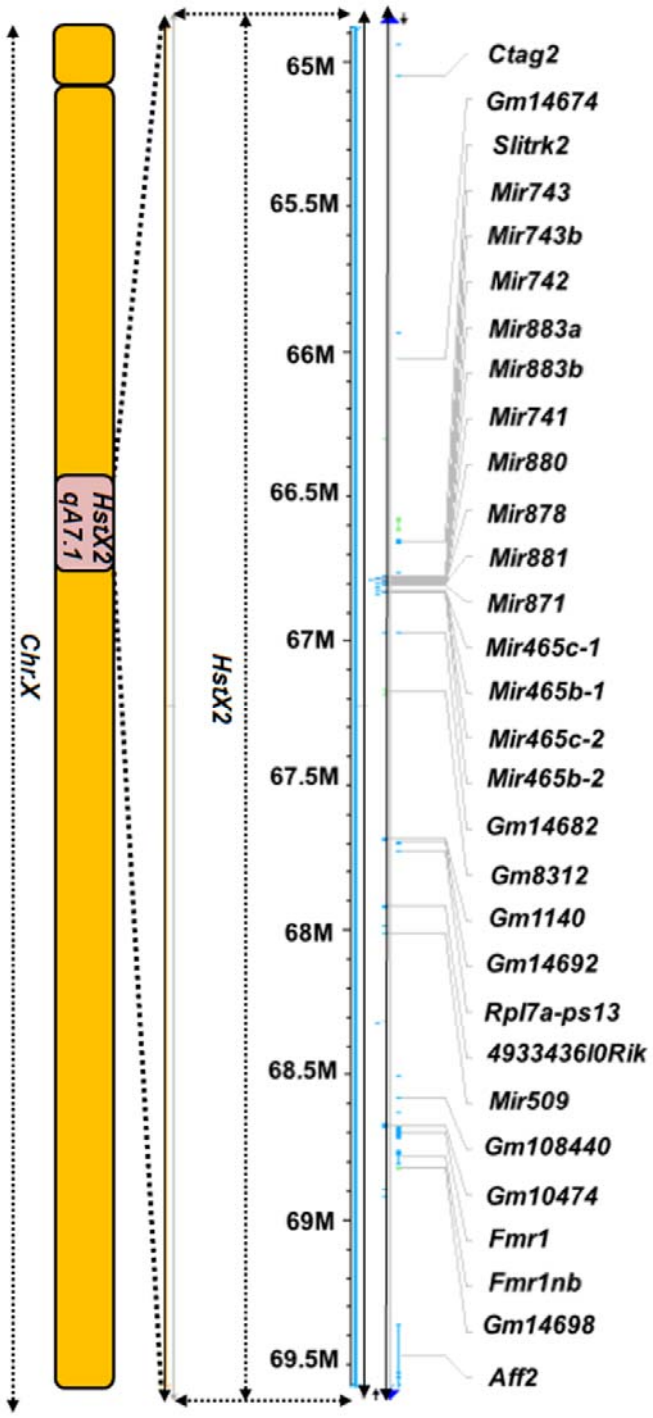

Figure 7.6: Schematic representation *Hstx1* and *Hstx2* loci on X chromosome (GRCm38).

symbol	AvgExp	LogFC			P-Value		
		LP(PWD VS B6)	RP(PWD VS B6)	ST(PWD VS B6)	LP(PWD VS B6)	RP(PWD VS B6)	ST(PWD VS B6)
Ctag2	8,03	0,51	0,14	-0,55	0,31	0,77	0,28
4930447F04Rik	4,48	-0,03	0,15	-0,58	0,72	0,13	0,00
4933436I01Rik	6,39	0,41	0,64	-0,58	0,54	0,36	0,40
Fmr1	7,45	-0,25	0,25	1,08	0,61	0,60	0,05
Fmr1	6,04	-0,41	-0,93	0,10	0,34	0,05	0,80
Fmr1nb	8,78	-0,45	-0,55	0,03	0,57	0,49	0,97
Aff2	3,10	-0,04	0,10	-0,06	0,37	0,05	0,22
Mir-743a	1,73	0,22	-0,99	-1,07	0,76	0,19	0,15
Mir-743b-3p	0,34	-0,51	0,24	0,02	0,16	0,49	0,94
Mir-743b-5p	0,12	-0,02	-0,13	0,32	0,92	0,49	0,12
Mir-742*	0,13	0,05	0,15	-0,20	0,84	0,54	0,41
Mir-742	0,53	0,35	-0,08	-0,25	0,12	0,71	0,26
Mir-883a-3p	0,35	0,01	0,09	0,01	0,97	0,79	0,98
Mir-883a-5p	0,45	-0,09	-0,07	-0,26	0,76	0,80	0,37
Mir-883b-3p	2,61	0,94	0,74	0,12	0,27	0,38	0,88
Mir-883b-5p	0,42	0,04	-0,10	0,02	0,91	0,76	0,94
Mir-471	0,22	0,06	-0,32	-0,23	0,79	0,18	0,34
Mir-741	0,38	0,11	-0,25	-0,12	0,74	0,45	0,71
Mir-463*	0,39	-0,06	-0,04	0,21	0,84	0,89	0,45
Mir-463	0,29	0,00	0,21	0,22	0,99	0,41	0,39
Mir-880	0,27	-0,17	0,22	-0,33	0,54	0,44	0,25
Mir-878-3p	1,57	-0,07	-0,16	-1,00	0,92	0,82	0,15
Mir-878-5p	0,27	-0,38	0,61	-0,11	0,20	0,05	0,70
Mir-881*	0,32	0,02	-0,13	0,11	0,96	0,68	0,74
Mir-881	0,20	-0,10	-0,18	0,20	0,70	0,46	0,42
Mir-871	0,37	0,09	0,21	-0,54	0,73	0,44	0,06
Mir-470*	0,22	0,06	0,48	0,30	0,82	0,07	0,25
Mir-470	6,39	0,04	-0,10	-0,03	0,88	0,69	0,92
Mir-465a-3p	2,41	**3,32**	**1,59**	0,40	**0,00**	**0,01**	0,45
Mir-465a-5p	0,20	0,16	0,69	0,10	0,48	0,01	0,67
Mir-465b-3p	2,18	**2,73**	**2,15**	-0,20	**0,00**	**0,01**	0,80
Mir-465b-5p	0,18	-0,24	0,19	0,59	0,44	0,54	0,07
Mir-465c-3p	2,63	1,26	**2,27**	0,03	0,13	**0,01**	0,97
Mir-465c-5p	0,24	-0,28	-0,03	0,30	0,25	0,89	0,22
Mir-201	0,05	-0,04	-0,13	-0,11	0,83	0,46	0,54
Mir-547	0,13	-0,02	0,16	-0,30	0,93	0,44	0,15

Table 7.3: Differential expression profiling of *Hstx1/2* linked genes and miRNAs between sorted spermatogenic cells from PWD and B6 testis. LP means leptonema, zygonema and early pachynema cells; RP stands for mid-late pachytene and Diplotene whereas ST stands for round spermatids. Significant differential expression is highlighted in the table.

symbol	AvgExp	logFC	P-value
		(PB6F1 vs B6PF1)	(PB6F1 vs B6PF1)
Ctag2	4,5213	0,1542	0,3599
4930447F04Rik	3,0405	-0,2115	0,1261
Slitrk2	4,5023	0,0386	0,7860
4933436I01Rik	2,7804	0,0745	0,5526
Fmr1	10,1064	0,2715	**0,0234**
Fmr1nb	8,7537	-0,9859	**0,0000**
Aff2	6,7561	-0,3164	0,0648
Mir-743a	8,9883	-1,1335	**0,0018**
Mir-743b-3p	4,0478	-0,4085	0,6599
Mir-743b-5p	1,1363	-1,5710	**0,0105**
Mir-742*	0,6496	-0,8107	**0,0287**
Mir-742	8,6757	0,0966	0,6650
Mir-883a-3p	4,0594	0,4024	0,6492
Mir-883a-5p	5,9751	0,4204	0,3407
Mir-883b-3p	1,0307	1,2569	**0,0247**
Mir-883b-5p	7,1262	-0,2453	0,3531
Mir-471	0,1933	0,2923	0,3947
Mir-741	7,6933	-0,2601	0,2985
Mir-463*	0,5841	-0,2129	0,6612
Mir-463	1,9609	-0,0419	0,9643
Mir-880	2,3231	-1,2864	**0,0109**
Mir-878-3p	10,1923	-0,2956	0,2269
Mir-878-5p	0,2159	-0,4168	0,2170
Mir-881*	1,2869	0,0326	0,9377
Mir-881	0,6124	0,4541	0,2390
Mir-871	4,2930	-0,5499	0,3840
Mir-470*	1,2962	-0,5856	0,2276
Mir-470	11,8064	-0,1177	0,6151
Mir-465a-3p	8,9695	**1,5959**	**0,0005**
Mir-465a-5p	3,4266	**2,4397**	**0,0009**
Mir-465b-3p	8,8471	**1,6438**	**0,0006**
Mir-465b-5p	4,6127	**2,4017**	**0,0033**
Mir-465c-3p	8,9632	**1,6967**	**0,0003**
Mir-465c-5p	2,1612	**-4,2762**	**0,0000**
Mir-201	0,4721	-0,0713	0,9001
Mir-547	0,8788	0,1635	0,6836

Table 7.4: Differential expression profiling of *Hstx1/2* linked genes and miRNAs between 14.5dpp PB6F1 and B6PF1 testis. Significant differential expression is highlighted in the table.

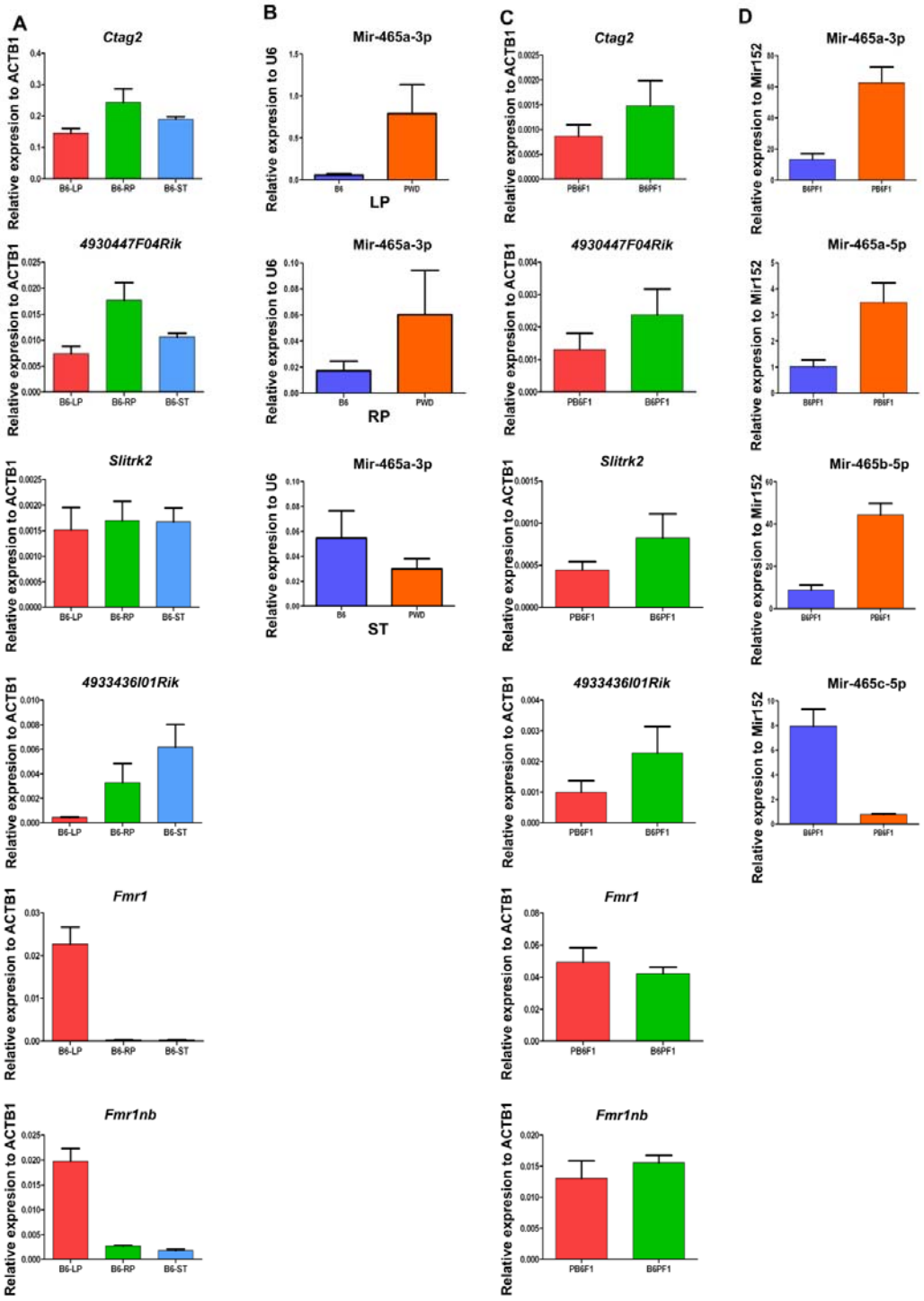

Figure 7.7: Expression profiling of Hstx2 linked genes and miRNAs. (A and B) Expression profiling of genes and miRNAs on sorted spermatogenic population in meiotic prophase. (C and D) RT-PCR quantification of candidate genes and miRNAs on 14.5dpp testis.

Gene Symbol	Position (Mb)[a]	Position (Mb)[b]	dN:dS[c]	Non-synonymous SNP (B6 vs PWD)[d]	Spermatogenetic expression[e]	Candidate for
Ctag2	65.04	62.3	0.57	62301128: T to G	Pre and post meiotic	
4930447F04Rik	66.3	63.5	0.54	63556739: A to C	Pre and post meiotic	
Slitrk2	66.6	63.9	0.11	63909049: A to G	Pre meiotic	
Mir743	66.7	64.02	-	64029949: T to C	Pre and post meiotic	*Hstx1/Hstx2*
Mir465c-1 / 2	66.82 / 66.83	64.07 / 64.08	-	64079188 / 64085750: G to A	Pre and post meiotic	
4933436I01Rik	67.9	65.1	0.82	65173312: C to T 65173318: T to G 65173487: G to T 65173606: T to A 65173980: T to A 65173993: C to T 65173997: T to G 65174232: C to T	Pre and post meiotic	*Hstx1/Hstx2*
Fmr1	68.6	65.9	0.06	-	Pre and post meiotic	
Fmr1nb	68.7	66.01	0.65	66015200: C to G 66022239: T to A	Pre and post meiotic	*Hstx1/Hstx2*
Aff2	69.3	66.6	0.20	66798088: A to G 67083920: C to T 67083935: C to G 67083957: A to T 67087955: G to A	Pre meiotic	

Figure 7.8: Candidate genes from the X-linked hybrid sterility region.

a. Physical position of the candidates genes based on GRCm38.

b. Physical position of the candidates genes based on NCBI mouse build 37(Ensemble 67, May 2012).

c. Rate of protein evolution based on one to one comparison with rat orthologs. (NCBIM37, May 2012).

d. SNPs for protein coding genes taken from PWD exome sequencing compared with B6 reference genome (NCBIM37, May 2012).SNPs were confirmed by classical re-sequencing method and mouse phenome database.

e. Expression in spermatogenetic germ cells; for miRNAs this thesis and (Song et al., 2009).Confirmed by quantitative RT-PCR.

8. Mechanistic basis of hybrid sterility.

8.1 Spermatogenic block and apoptosis of primary spermatocytes at pachytene stage.

The F1 adult males derived from the crosses between PWD female with B6 males (PB6F1) were invariably infertile, azoospermic with more than 50% reduction of testes, whereas a reverse interspecific hybrid between B6 female with PWD males are fertile (B6PF1) having testis weight (TW) of 112.6 mg with 13.7 million sperm (SC) in cauda epididymis. In intra-species hybrids between PWD female with PWK male (both *M. m. musculus*; henceforth PKF1) are fertile (TW 102.9 mg; SC 14.4 million); similarly hybrids between B6 female with BALB/C male (both *M m domesticus*; henceforth B6CF1) are fertile (TW 175.4 mg; SC 28.8 million).

Analysis of hematoxylin - eosin (HE) and Periodic acid-Schiff (PAS) stained histology sections of sterile PB6F1 hybrids showed huge disruption of spermatogenesis with section showing the formation of large vacuole like structure and enlarged pachytene cells completely devoid of postmeiotic cell types, smaller tubule diameter and no progression beyond epithelial stage IV. Large vacuole-like structures and enlarged multinuclear cells were also detected in most of the tubules (Figure 8.1A). Testicular histology of fertile reverse inter-species B6PF1 hybrids showed incomplete spermatogenic block in some tubules with reduced numbers of round and elongated spermatids. Some of the sections showed vacuole like structure, while other tubules seem to have normal spermatogenesis; overall it looked significantly different from normal fertile controls (Figure 8.1A). In intra-species hybrids B6CF1 and PKF1 shows normal spermatogenesis similar to fertile inbred controls of PWD and B6 males (Figure 8.1A).

Absence of round spermatids and mature sperms in sterile hybrids made us to investigate the fate of germ cells. Using fluorometric DeadEnd TUNEL assay system on testicular sections from 2 months old PB6F1, B6PF1 hybrids and B6 as inbred controls we determined the rate of apoptosis in due course of spermatogenesis. Sterile PB6F1 hybrids displayed 24-fold increase in TUNEL positive apoptotic cells compared to B6 ($P<0.00001$, Mann-Whitney U test) and 4-fold more TUNEL positive cells to that of fertile B6PF1 hybrids ($P<0.00001$, Mann-Whitney U test; Figure 8.1B and C). The reverse fertile B6PF1 hybrid showed 7- fold more TUNEL positive cells than that of B6 controls ($P<0.0001$, Mann-Whitney U test; Figure 8.1B and C).The TUNEL assay revealed that in sterile PB6F1 hybrid, high amount of germ cells undergoes apoptosis causing the

stage IV arrest leading to sterility, while the fertile B6PF1 hybrids shows partial but significant apoptosis of germ cells than that of B6 inbreed controls ($P<0.0001$, Mann-Whitney U test).

We also checked the cellular composition of spermatogenic populations from 13.5 dpp till adult in PB6F1, B6PF1 and B6 animals. Adult intraspecific hybrids PKF1 and B6CF1 were also analyzed for germ cell composition during meiotic prophase. We analyzed the course of meiotic prophase I using antibody against testis specific histone H1t (differentiates leptonema, zygonema and early pachynema from mid-late pachynema and diplonema) and synaptonemal complex protein 3 (SYCP3, protein present in axial element of synaptonemal complex; differentiate meiotic prophase I based on its structure) on spermatocyte spreads. The pachytene spermatocytes first occur on day 13.5 after birth (13.5 dpp) in the first wave of spermatogenesis. Until 14.5dpp we did not find any significant differences in the cellular composition between the hybrids and B6 controls. The first significant deviation in sterile hybrids was the deficiency of mid-pachytene cells at 15.5 dpp ($P<0.001$, chi-square test; Figure 8.1D). Another block was observed at 17.5 dpp with excessive accumulation of early pachytene cells, apoptosis of remaining mid-pachynemas and almost complete absence of diplotene cells (both $P<0.000001$, chi-square test; Figure 8.1D). By 8 weeks of age PB6F1 sterile mouse shows significant difference to its fertile counterpart ($P<0.000001$, chi-square test; Figure 8.1D). As expected, intra-specific hybrids PKF1 and B6CF1 showed normal spermatogenesis similar to inbred controls of PWD and B6 males.

8.2 Cause of germ cell elimination: dissecting meiotic recombination in PB6F1 hybrids.

Meiotic recombination is dependent on the formation and subsequent repair of programmed Spo11-induced DNA double-strand breaks (DSBs) (Baudat et al., 2000; Romanienko and Camerini-Otero, 2000). To investigate whether pachytene arrest could result from the disturbance of these earlier processes, we visualized the early recombination intermediates using antibodies for RAD51 and DMC1 DNA repair recombinases to mark DSBs (Smagulova et al., 2011), ATR foci to monitor DSBs repair (Turner et al., 2006) (Figure 8.2D), and STAG3 cohesin to check integrity of the synaptonemal complex (Prieto et al., 2001). The average number of RAD51/DMC1 foci did not differ between the sterile PB6F1 hybrids in comparison to B6PF1 and B6 controls (256± 18, 258±17 and 257±18 foci respectively) in zygotene spermatocytes, but was higher at the pachytene stage of sterile hybrids (50.7± 18; 40.8± 11 and 42.2± 10 foci; $P<0.01$, Mann-Whitney U test; Figure 8.2B). MSH4, a mismatch repair protein of the MutS

family showed foci at late zygonema – early pachynema at lower frequency (55.2 ± 10.3; foci Figure 8.2B) in PB6F1 sterile hybrids compared to B6 and B6PF1(76.9 ± 13.7;Figure 8.2B). Additionally, MLH1, a mismatch repair protein of the MutL family, displaying foci at mid-pachynema also have lower frequency (24.1 ± 2.2 foci) in PB6F1 sterile hybrids compared to B6 and B6PF1(24.9 ± 2.1 and 27.0 ± 2.3 foci respectively; Figure 8.2C) indicating changes in the rate of meiotic recombination. However analysis of other genotypes including fertile (PWD × B6.*Hstl*^{f}) F1; (PWD × B6.PWD-chr17) F1 and (PWD × B6.PWD-chr19) F1 hybrids showed similar MLH1 frequency (on average 24.5 foci; Figure 8.2C) to PB6F1 sterile hybrids pointing to an X-linked polymorphism controlling the meiotic recombination rate (Dumont and Payseur, 2011), rather than the meiotic arrest (Figure 8.2C). To obtain an insight into DSB's repair process for pachytene cells we used anti-ATR antibody which showed decorated sex chromosomes and autosomal univalents in mid-pachytene cells (Figure 8.2D). Thus the failure of DSB repair mechanism can now explain the elimination of pachytene spermatocytes. The mammalian STAG3 protein is a component of the synaptonemal complex that is specifically expressed in germinal cells. STAG3 has a role in sister chromatid arm cohesion during mammalian meiosis I. Immunofluorescence results in prophase I cells suggest that STAG3 is a component of the axial/lateral element of the synaptonemal complex. STAG3 interacts with the structural maintenance chromosome proteins SMC1 and SMC3, which have been reported to be subunits of the mitotic cohesin complex (Prieto et al., 2001). The knockout mutants of subunits of the mitotic cohesin complex show asynapsis in the prophase 1 of mammalian meiosis where sister homologs fails to pair (Prieto et al., 2001). So we looked at the mitotic cohesin complex using anti-STAG3 antibody along with anti- SYCP3 antibody. In PB6F1 sterile hybrids STAG3 showed complete co-localization with SYCP3 protein component of the lateral element of synaptonemal complex in spermatocytes similar to that of fertile control (Figure 8.2E).

8.3 Extent of chromosomal asynapsis contributes to germ cell elimination.

The most distinct aberration in pachynemas of sterile PB6F1 males was the asynapsis of homologous chromosomes during the first meiotic prophase. Examination of the synaptonemal complexes on meiotic spreads from sterile PB6F1 testes revealed multiple asynapsed autosomes (range 1-19 per cell, median 5) in over 95% of early, histone H1t negative, pachytene spermatocytes, while , 17.6% in B6PF1 and 7.7% in B6 showed asynapsis (Figure 8.3A,B,C and

D). The asynapsis of individual autosomal pairs was mostly complete with exceptional bizarre multivalents and ring-like chromosomes apparently resulting from partial and/or non-homologous synapsis (Figure 8.3B). The SYCP3-positive univalents were negative for SYCP1 protein component of transverse filaments of the central element of synaptonemal complex. The univalents were decorated by HORMAD2, a HORMA domain-containing protein coordinating chromosome synapsis and γH2AFX, the phosphorylated form of histone H2AFX. The unpaired chromosomes often formed domains of silenced chromatin, sometimes termed as pseudo-sex bodies (Bellani et al., 2005). However, unlike the fertile controls the early pachytene spermatocytes from sterile males rarely displayed a discernible sex body (Figure 8.3A and B).

In mid-pachytene stage the chromosomal asynapsis became limited to 2 or 1 autosomes. The early pachytene spermatocytes carrying multiple univalent of autosomes disappeared by mid-late pachytene stage, which might have been eliminated by apoptosis. In PB6F1 sterile hybrids 90.6% of mid-late pachynemas in sterile PB6F1 hybrids, and 32% in semisterile B6PF1 carried one, exceptionally two unsynapsed autosomes completely or partially embedded in the sex body (Figure 8.3A). Similar introgression of autosomal chromatin was reported in various male-sterile chromosomal translocations with incomplete synapsis of their rearranged chromosomes (Forejt, 1984; Forejt et al., 1981). The autosomal introgression into the sex body was non-existent in the B6, PKF1 and B6CF1 intra-specific fertile hybrids controls (Figure 8.3E). The synapsis of X and Y chromosome is restricted to a short ≈700 Kb pseudoautosomal region (PAR) and is a prerequisite of homologous recombination and for the proper segregation of the X and Y chromosomes (Kauppi et al., 2011; White et al., 2012). The X-Y synapsis failed in 34% of analyzable mid-pachytene spermatocytes of sterile males. The failure of pseudoautosomal synapsis in fertile B6PF1 hybrid was observed in 7.4% of mid- pachytene cells which are non-existent in B6 fertile inbreed controls (Figure 8.3F). We conclude that the autosomal asynapsis does not result from a failure of DSBs formation or DSBs repair. The elevated DSBs incidence in early pachynemas suggests a partial failure or delay of DSBs repair on unsynapsed autosomes. The unrepaired DSBs on asynaptic chromosomes are supposed to activate the pachytene checkpoint leading to apoptosis (Burgoyne et al., 2009).

8.4 Nonrandom engagement of individual autosomes in asynapsis.

Chromosomal asynapsis in the sterile PB6F1 hybrids proved to be the major cause of elimination of pachytene cells in two stages. The early pachynemas with multiple asynapsis could influence different meiotic check points to promote the process of cellular elimination and a major block in the progression of spermatogenesis. We further asked whether the asynapsis affected the autosomes at random by analysis ofsynapsis status of chromosome Chr 2, 16, 17, 18 and 19 (randomly chosen) using DNA FISH whole-chromosome-specific probes in combination with the antibodies against HORMAD2 as a mark for asynapsed chromosomes (Figure 8.4A to E). In PB6F1 male Chr 19 was asynapsed in 46.7% of pachynemas, where two Chr 19 DNA clouds colocalized with HORMAD2-labeled univalents. The Chr 17 was unsynapsed in 32.1% of pachytene cells (Figure 8.4F). The proportionality test comparing the probability of overall asynapsis with that of the individual chromosomes suggested that the Chr 2 (4.7%) and Chr 16 (6%) were asynapsed significantly less frequently and Chr 19 was asynapsed significantly more frequently than would be expected by random asynapsis (expected random asynapsis, 27%; $P < 0.01$), but there was no significant deviation from the random involvement of Chr 17 (32.1%) and Chr 18 (26.2%). However, Chr 19 and Chr 17 were prevalent in a small fraction of supposedly mid–late pachynemas with only one or two unsynapsed autosomal pairs.

8.5 The extent of asynapsis is genetically modulated.

Previously we identified four main components of the genetic control of hybrid sterility, which together represent the minimal genotype necessary to reconstitute the sterility of PB6F1 male hybrids on the B6 genetic background (*Mus m. domesticus*). They include a region on the Chr X^{PWD} carrying the *Hstx2* locus, $Prdm9^{PWD/B6}$ heterozygosity on Chr 17, and heterozygosity of a poorly defined portion of the F1 genetic background. The fourth component resides on Chr 19 (also (Dzur-Gejdosova et al., 2012)). Using the reciprocal F1 hybrids and B6.PWD-Chr# chromosome- substitution strains to switch the subspecies origin of these components, we examined the extent of rescue of pachytene arrest and asynapsis (Table 8.1). The reciprocal B6PF1 hybrids carrying the middle region of Chr X^{B6} on an F1 hybrid background were semifertile, with partial spermatogenic arrest and significantly increased apoptosis as compared with B6 controls (Figure 8.1 A, B and C). Compared with PB6F1 sterile hybrids, the asynapsis

was reduced to 32% (39/120). In half of the pachynemas with asynapsis, the Chr 19 univalents were observed. Interestingly, asynapsed Chr 17 was not found with detectable frequency. At the mid–late pachytene stage, six of the seven examined cells revealed Chr 19 asynapsis. We conclude that a gene in the middle part of Chr X^{B6} controls the partial rescue of pachytene arrest and more than threefold reduction in the occurrence of pachynemas with asynapsis. The difference between the male reciprocal F1 hybrids was in contrast to the equal frequency of meiocytes with asynapsis in reciprocal F1 female hybrids (section 9). Complete suppression of the sterilizing effect of the F1 hybrid genome was observed in the (PWD × B6.PWD-Chr 17)F1 males. Elimination of Chr $17^{PWD/B6}$ heterozygosity in an otherwise complete F1 hybrid genotype resulted in a total rescue of fertility, release of pachytene block, and complete disappearance of asynaptic chromosomes. The rescue cannot be explained by a dominant sterilizing effect of Chr 17^{B6}, because it was shown elsewhere (Dzur-Gejdosova et al., 2012) that homozygosity for Chr 17^{B6} is incompatible with a full pachytene block.

8.6 Heterospecific homologs of Chr 17 and 19 are more prone to asynapsis.

The occurrence of asynaptic chromosomes can result from aberrant gene function, such as *Spo11*, *Mei1* or *Hormad2* null mutations (Baudat et al., 2000; Romanienko and Camerini-Otero, 2000; Libby et al., 2002; Kogo et al., 2012) or from structural or sequence incompatibility between the individual members of homologous pairs. We found that asynapsis of Chr 17 and 19 pairs was limited to genotypes where they are heterospecific, each composed of a PWD and B6 homolog. In (PWD x B6.PWD-Chr 19)F1 hybrids where all autosomal pairs but Chr 19 are heterospecific, asynapsis occurred in 59.6% of the pachynemas but strikingly, did not affect Chr $19^{PWD/PWD}$ (0/100). The males were sterile but displayed the range of 0 – 1.2 million sperm count and 72.6 mg testes weight (Figure 8.5A). The other example of the predisposition of heterospecific homologs to asynapsis was found in (B6.PWD-Chr X.1s × B6.PWD-Chr 17) pachynemas where the only heterospecific was Chr 17 pair. Seventeen per cent of pachynemas displayed a single pair of asynapsed chromosomes (Figure 8.5B). In all cells (25/25) examined it was identified as Chr 17 by DNA FISH. The results on pachytene asynapsis in F1 males of various genotypes are summarized in Table 8.1.

8.7 The disturbed inactivation of sex chromosomes in sterile males.

To evaluate the transcriptional activity of sex chromosomes in the spermatocytes of sterile F1 hybrids we carried out RNA FISH for Chr X genes *Scml2, Egfl6, Ndufa1* and *Ott,* and for Chr Y *Zfy2* (Figure 8.6 A to F). All examined Chr X genes but *Scml2* are known to be silent at the pachytene stage of primary spermatocytes in control males. While all five genes were silenced by MSCI at mid-pachytene in fertile B6 controls with the exception of weak positivity (3.6%) of *Scml2*, their transcripts were detected with frequency ranging between 30% to 45% of mid-pachytene cells in PB6F1 sterile males (Figure 8.6G). The activation of *Zfy2* (30%) in mid-late pachynemas is known to induce apoptosis (Royo et al., 2010). In B6PF1 fertile hybrids 2.1% of mid-pachytene cells showed expression of *Scml2*, whereas 8.9% of mid-pachytene cells showed expression of *Ott* showing failure of MSCI to a certain extent (Figure 8.6G).

Next we searched for genome-wide changes in the gene expression pattern by comparing transcription profiles of whole testes from sterile 14.5 dpp PB6F1 males and fertile controls (B6PF1, B6 and PWD) of the same age using Affymetrix GeneChip Mouse Gene 1.0 ST Array. Using the approach described recently (Good et al., 2010) we confirmed similarity of cellular compositions of testes of 14.5 dpp reciprocal hybrids by comparing the expression pattern of the dataset of spermatogenesis stage-specific genes (Chalmel et al., 2007; Good et al., 2010), (Figure 8.7A). Since the immunofluorescence microscopy and RNA FISH revealed the absence of the regular sex body or its aberration in pachynemas and active transcription of probed Chr X and Chr Y genes, we focused mainly on the genome-wide expression pattern of genes on the sex chromosomes. Comparison of the expression profile of sterile hybrids to fertile controls B6PF1, B6 and PWD showed that the sterile PB6F1 hybrids displayed misregulated genes more frequently on the Chr X (Figure 8.7B and 8.8A and C, Poisson model, p-value < 0.01). The most extensive genome-wide disturbance of gene expression was observed on the Chr X A7.1 cytogenetic band (Figure 8.8B, permutation test, p-value<0.01). However, the misregulation was not significantly biased in either direction, as 140 Chr X genes were upregulated and 116 Chr X genes were downregulated (Figure 8.8C, binomial test, p-value = 0.15). The same conclusion was reached by Gene Set Enrichment Analysis (GSEA) (Subramanian et al., 2005), which further revealed enrichment of functionally predetermined gene sets among differentially expressed genes upregulated in PB6F1 sterile hybrids or B6PF1 fertile controls. Many enriched gene sets in

fertile controls were connected to gametogenesis with GO terms such as SEXUAL REPRODUCTION, GAMETE GENERATION, DNA REPAIR, DNA RECOMBINATION or MEIOTIC CELL CYCLE, probably reflecting the activation of genes necessary for later stages of spermatogenesis. The gene sets enriched in sterile (PB6F1) hybrids were frequently connected with ion channels and membrane receptors for reasons not obvious to us. This work was carried out in collaboration Dr. Petr Simecek and Dr. Paul Denny.

8.8 Effects of *Hstx2* on meiotic pairing and spermatogenic differentiation

Meiotic arrest of PB6F1 hybrid males is associated with the failure of proper pairing and synapsis of homologous heterospecific autosomes, delay of DNA double strand break repair on unsynapsed autosomes and dysregulation of meiotic sex chromosome inactivation (MSCI) at the first meiotic prophase. Here we focused on the fertility parameters and pachytene chromosome synapsis in F1 hybrid males differing at *Hstx2* locus. The hybrid males (B6.PWD-Chr X.1s x PWD)F1 or DX.1sPF1 carrying $Hstx2^{PWD}$ alleles were fully sterile without sperm, whereas the (B6.PWD-Chr X.1 x PWD)F1 or DX.1PF1 males carrying $Hstx2^{B6}$ were semifertile (more on section 7). Analysis of hematoxylin and eosin (HE) and Periodic acid-Schiff (PAS) stained histology sections of sterile DX.1sPF1 hybrids showed a huge disruption of spermatogenesis with section showing the formation of large vacuole like structure and enlarged pachytene cells with complete lack of postmeiotic cell types, smaller tubule diameter and spermatogenic block at epithelial stage IV, similar to that of PB6F1 hybrids (Figure 8.9A). The fertile DX.1PF1 hybrids showed incomplete spermatogenic block in some tubules similar to that of B6PF1.The B6 control showed normal spermatogenesis (Figure 8.9A). Analysis of meiotic prophase on 2 month old adult testis from DX.1sPF1 showed reduced occurrence of mid-late pachynemas, almost absent diplotene spermatocytes (Figure 8.9B and C). The DX.1PF1 males showed greatly reduced meiotic arrest at the late pachytene stage (Figure 8.9C). Identification of synaptonemal complexes by immunostaining SYCP3 and SYCP1 components of lateral and central element or HORMAD2 protein revealed unsynapsed autosomes in >90% of pachynemas in DX.1sPF1 males similar to that of PB6F1 hybrid (Figure 8.9D). Similar pattern between DX.1sPF1 and PB6F1 males were followed by the number of univalents per cell (Figure 8.9E). The examination of meiocytes using super resolution microscopy revealed irregular spots of SYCP1 on some univalents and clear examples of nonhomologous synapsis (Figure 8.10). In contrast, DX.1PF1

males carrying *Hstx2*^{B6} showed only 34% of pachynemas with asynapsis restricted to one or two pairs of unsynapsed univalents. It can be concluded that the presence of the *Hstx2*^{B6} allele in F1 hybrid males partially restores the fertility and significantly reduces the frequency of pachynemas with asynapsis and the number of unsynapsed autosomes per cell.

8.9 Heterochromatinization of autosomal univalents and relaxation of the Chr X chromatin in sterile male hybrids

To further analyze the effect of *Hstx2* gene on spermatogenic differentiation, we used the whole chromosome DNA FISH probes in combination with HORMAD2 protein immunostaining to visualize Chr 17 and Chr 19 known to get frequently unsynapsed in PB6F1 pachynemas (section 8.4 and (Bhattacharyya et al., 2012)). The F1 hybrid males DX.1sPF1 and PB6F1 displayed very similar frequencies of pachynemas with asynaptic Chr 17 (27% and 30%) and Chr 19 (42% and 40%) (Figure 8.11 A and B). During this experiment we noticed significant differences in chromatin areas covered by the hybridization signal between synapsed and unsynapsed autosomes ($P<0.01$ Mann-Whitney U test, Figure 8.11 A and C). For both chromosomes the chromatin was more condensed in univalents, suggesting their heterochromatinization and meiotic silencing of unsynapsed chromatin (MSUC). Next we inspected the chromatin area defined by Chr X DNA FISH and found two-fold increase in Chr X chromatin area in PB6F1 and DX.1sPF1 sterile hybrid males compared to fertile parental (PWD) control ($P<0.01$ Mann-Whitney U test, Figure 8.11 A and C). This finding provides the cytological counterpart to the transcriptional reactivation of X-linked genes during MSCI failure in PB6F1 sterile males as described earlier (section 8.7).

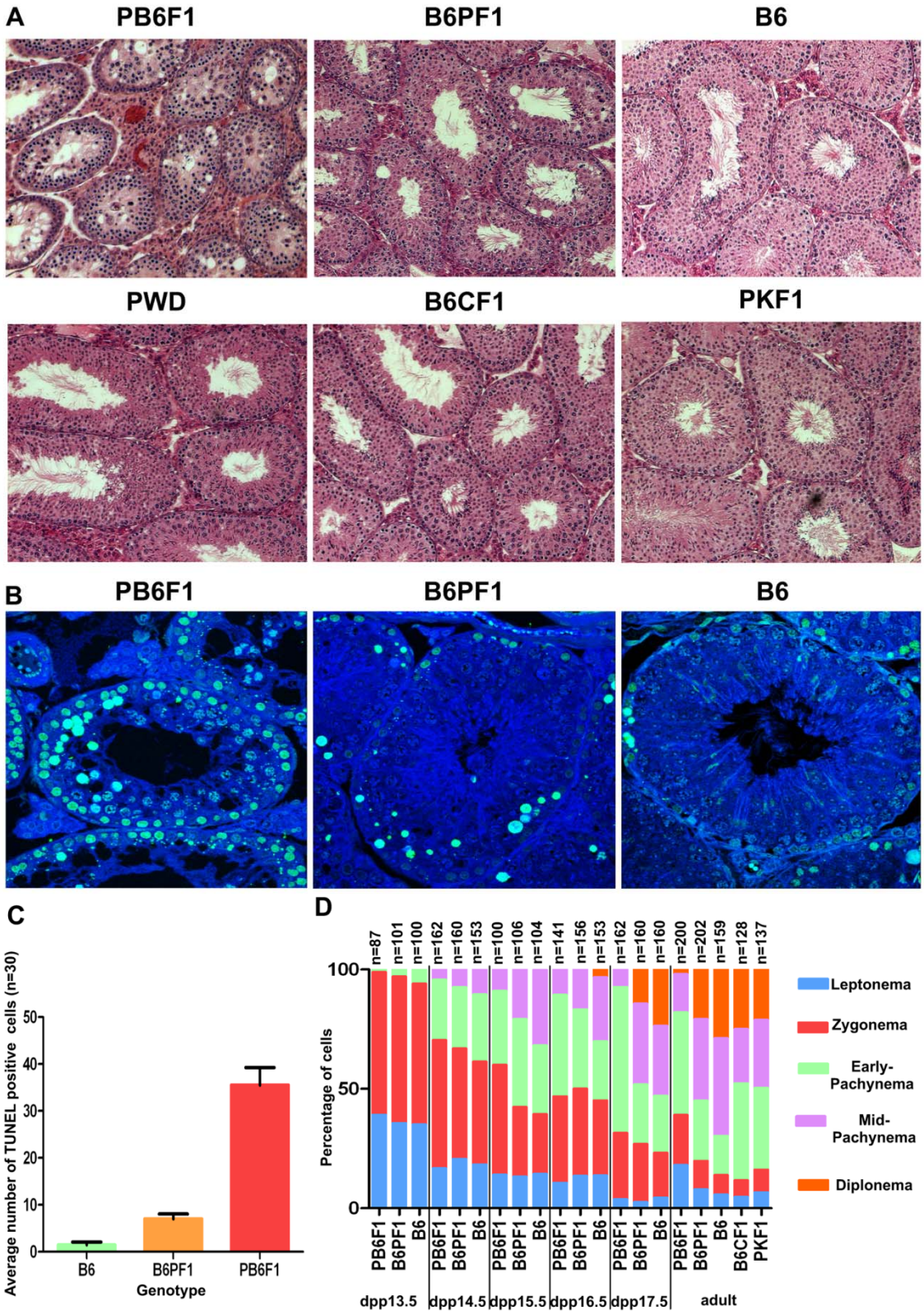
A
PB6F1
B6PF1
B6
PWD
B6CF1
PKF1
B
PB6F1
B6PF1
B6
C
Average number of TUNEL positive cells (n=30)
0
10
20
30
40
50
B6
B6PF1
PB6F1
Genotype
D
Percentage of cells
0
50
100
n=87
n=101
n=100
n=162
n=160
n=153
n=100
n=106
n=104
n=141
n=156
n=153
n=162
n=160
n=160
n=200
n=202
n=159
n=128
n=137
PB6F1
B6PF1
B6
B6CF1
PKF1
dpp13.5
dpp14.5
dpp15.5
dpp16.5
dpp17.5
adult
Leptonema
Zygonema
Early-Pachynema
Mid-Pachynema
Diplonema

Figure 8.1: Spermatogenesis during the first wave of spermatogenesis and in adults in interspecific and intraspecific hybrids. (A) Histological cross-sections of spermatogenic tubules stained with H&E show a block at epithelial stage IV, giant multinuclear cells, and the absence of haploid phase in sterile PB6F1 hybrids. The B6PF1 testes display complete spermatogenic development but a reduced number of postmeiotic cells. (B) Apoptosis of spermatogenic cells detected by TUNEL assay in histological cross-sections from 8-wk-old mice. (C) Average number of TUNEL-positive cells per cross-section of a seminiferous tubule. Sterile PB6F1 hybrids show significantly higher numbers of apoptotic cells than B6PF1 and B6 mice ($P<0.01$ for both comparisons; Mann–Whitney U test). n= n,total number of cross-sections examined. (D) Frequency of individual stages of primary spermatocytes in the suspensions of testicular cells from males during the first wave of spermatogenesis and from adults. The first difference in cellular composition was found in 15.5-dpp sterile PB6F1 males ($P < 0.001$; $\chi 2$ test). The second significant difference was observed at 17.5 dpp in PB6F1 cell populations, showing reduced mid–late pachynemas and the absence of diplotene spermatocytes. Three males per genotype were analyzed. n= number of cells examined.

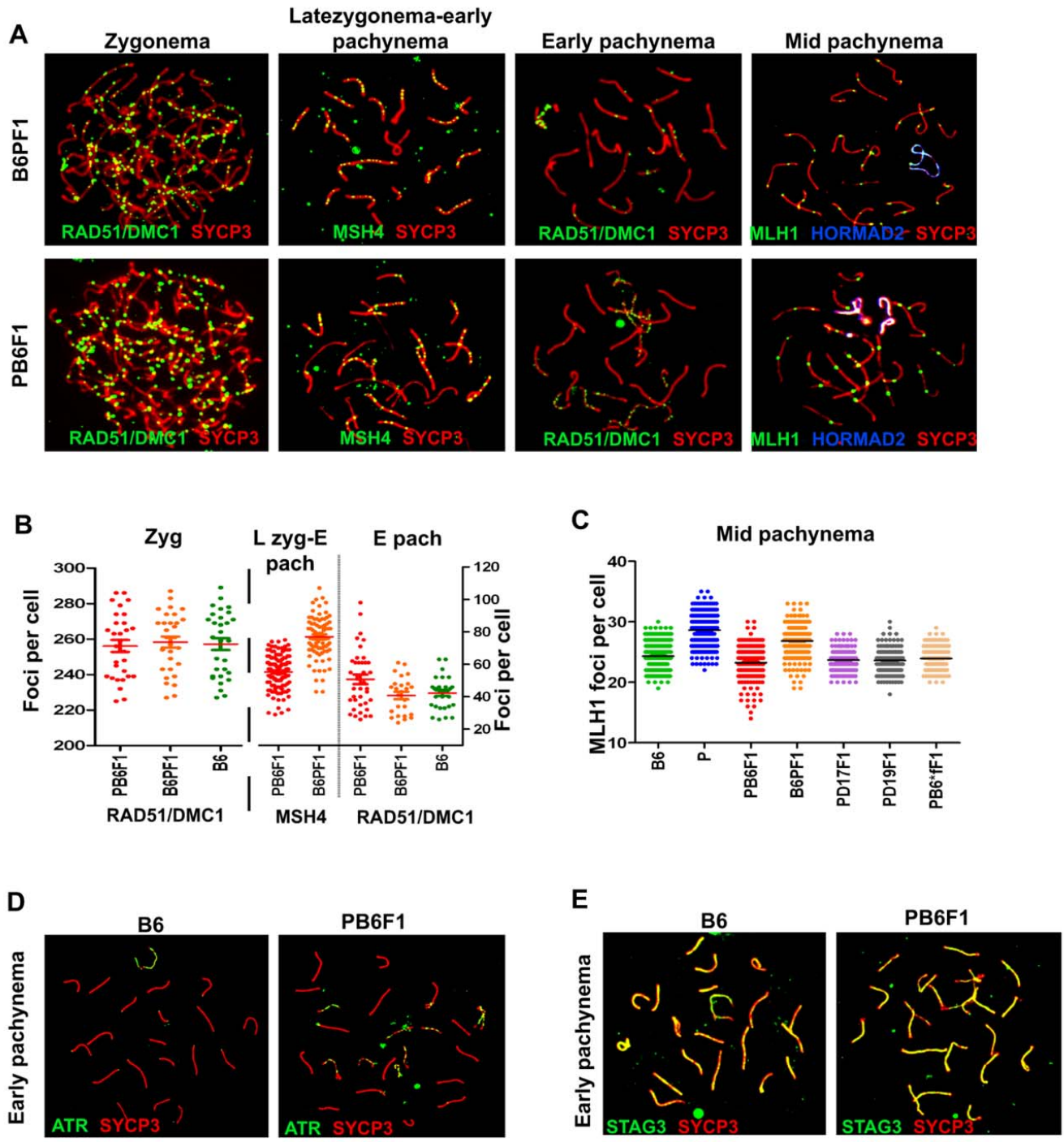
A
Zygonema
Latezygonema-early pachynema
Early pachynema
Mid pachynema
B6PF1
PB6F1
RAD51/DMC1 SYCP3
MSH4 SYCP3
RAD51/DMC1 SYCP3
MLH1 HORMAD2 SYCP3
RAD51/DMC1 SYCP3
MSH4 SYCP3
RAD51/DMC1 SYCP3
MLH1 HORMAD2 SYCP3
B
Zyg
L zyg-E pach
E pach
Foci per cell
300
280
260
240
220
200
120
100
80
60
40
20
PB6F1
B6PF1
B6
RAD51/DMC1
MSH4
RAD51/DMC1
C
Mid pachynema
MLH1 foci per cell
40
30
20
10
B6
P
PB6F1
B6PF1
PD17F1
PD19F1
PB6*fF1
D
B6
PB6F1
Early pachynema
ATR SYCP3
ATR SYCP3
E
B6
PB6F1
Early pachynema
STAG3 SYCP3
STAG3 SYCP3

Figure 8.2: DSBs, repair, and meiotic recombination in sterile males. (A) RAD51/DMC1, MSH4, and MLH1 foci are visualized by immunolabeling on meiotic spreads from sterile hybrids and fertile controls. Synaptonemal complexes are labeled by anti-SYCP3 antibody; unsynapsed chromosomes of mid-pachynemas are labeled by HORMAD2. (B and C) The increased frequency of RAD51/DMC1 in early pachynemas of sterile hybrids reflects stalled repair of DSBs in asynapsed autosomes. The difference between reciprocal hybrids in MSH4 and MLH1 probably is controlled by an X-linked polymorphism of the meiotic recombination rate locus (39). N = number of mice, n = number of cells analyzed: RAD51, DMC1 and MSH4 (N = 3, n = 30 for zygotene, n = 60 for early pachytene; MSH4 N = 3, n = 100; MLH1, N = 5, n = 150. (D) ATR decorates only the XY pair in B6 mice; in sterile hybrids it also persists on unsynapsed autosomes (N = 4 n = 100 per genotype). (E) STAG3 cohesin labels all chromosomes irrespective of their synapsis status (N = 3, n = 50).

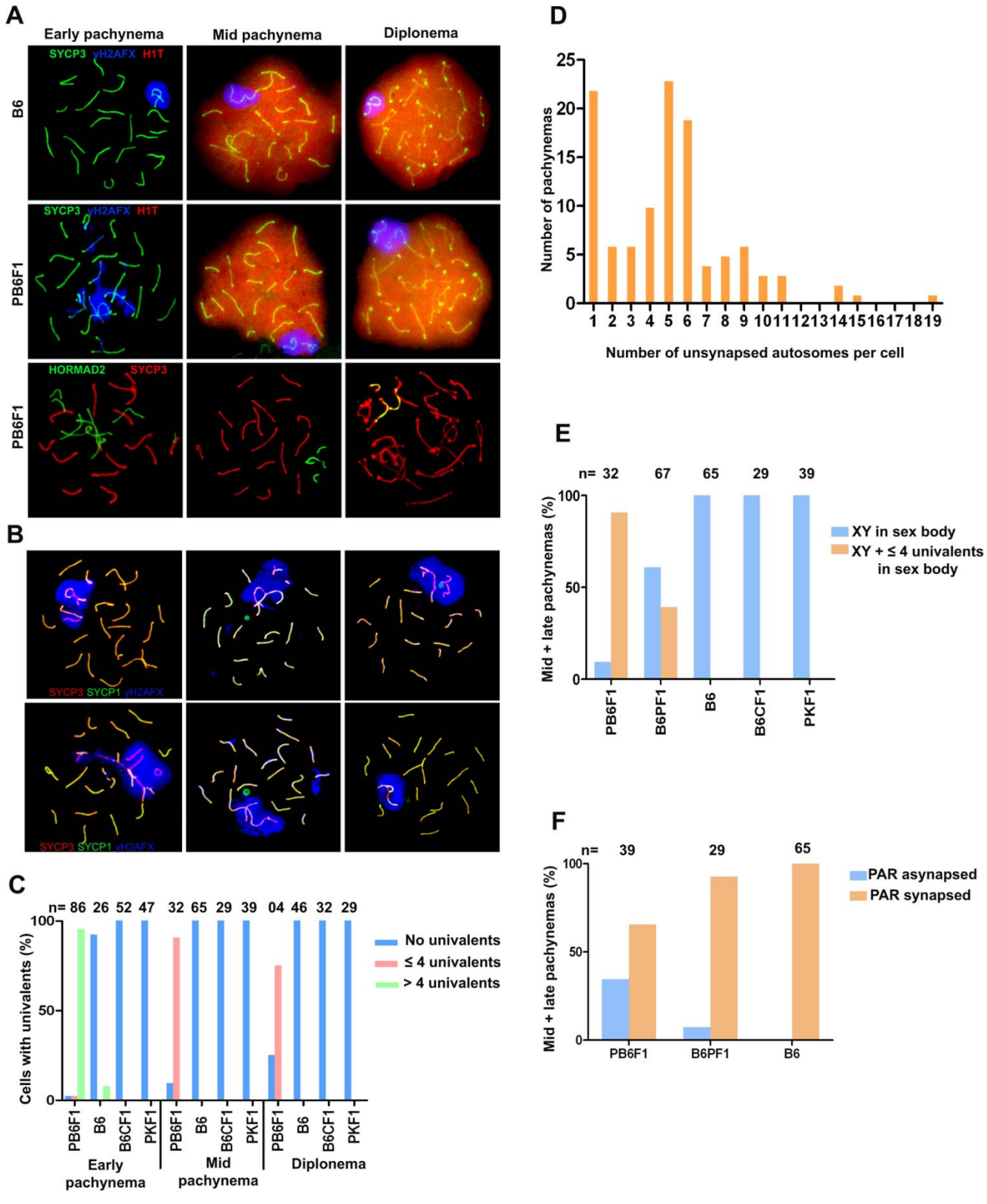
A
Early pachynema
Mid pachynema
Diplonema
B6
PB6F1
PB6F1
SYCP3 γH2AFX H1T
SYCP3 γH2AFX H1T
HORMAD2 SYCP3
B
SYCP3 SYCP1 γH2AFX
SYCP3 SYCP1 γH2AFX
C
n= 86 26 52 47 32 65 29 39 04 46 32 29
Cells with univalents (%)
100
50
0
No univalents
≤ 4 univalents
> 4 univalents
PB6F1 B6 B6CF1 PKF1 PB6F1 B6 B6CF1 PKF1 PB6F1 B6 B6CF1 PKF1
Early pachynema
Mid pachynema
Diplonema
D
Number of pachynemas
25
20
15
10
5
0
1 2 3 4 5 6 7 8 9 10 11 12 13 14 15 16 17 18 19
Number of unsynapsed autosomes per cell
E
n= 32 67 65 29 39
Mid + late pachynemas (%)
100
50
0
XY in sex body
XY + ≤ 4 univalents in sex body
PB6F1 B6PF1 B6 B6CF1 PKF1
F
n= 39 29 65
Mid + late pachynemas (%)
100
50
0
PAR asynapsed
PAR synapsed
PB6F1 B6PF1 B6

Figure 8.3: Asynapsis of homologous chromosomes in sterile F1 males. (A) Asynapsis of pachytene spermatocytes revealed by immunostaining of SYCP3 or HORMAD2. Early (histone H1t-negative) pachynemas show multiple asynapsed autosomes decorated by the phosphorylated form of histone H2AFX (γH2AFX). H1t-positive mid–late pachynemas show one or two pairs of asynaptic autosomes engulfed in the sex body. (B) The exceptional multivalents and ring-like chromosomes indicate partial and/or nonhomologous synapsis. (C) Asynapsis was rare in B6 mice and was absent in intraspecific hybrids (B6 × BALB/c) F1 (abbreviated B6CF1) and (PWD × PWK)F1 (abbreviated PKF1). PB6F1 meiocytes with more than four univalents disappear in mid-pachynema and diplonema. (D) Distribution of pachynemas according to the number of asynapsed autosomes estimated by counting the CREST-stained centromeres on SYCP3- labeled synaptonemal complexes. Individual pachytene stages could not be identified in this experiment. In total, 111 aberrant pachynemas were counted. (E) Frequency of mid–late pachynemas with autosomal univalents within the sex body in sterile PB6F1 and semifertile reciprocal B6PF1 hybrids. (F) X–Y asynapsis correlates with male sterility; however, the sex chromosomes could not be reliably identified in the majority of early pachynemas. PAR, pseudoautosomal region.

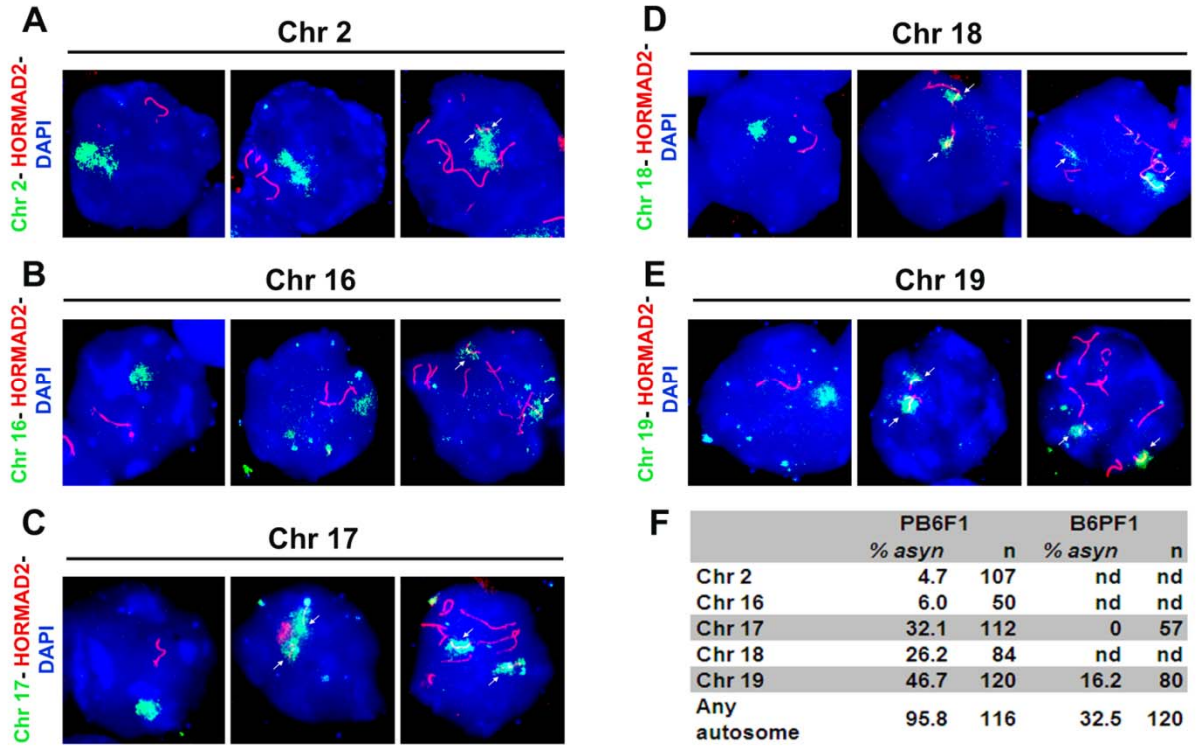

F

	PB6F1		B6PF1	
	% asyn	n	*% asyn*	n
Chr 2	4.7	107	nd	nd
Chr 16	6.0	50	nd	nd
Chr 17	32.1	112	0	57
Chr 18	26.2	84	nd	nd
Chr 19	46.7	120	16.2	80
Any autosome	95.8	116	32.5	120

Figure 8.4: Five autosomes were tested for asynapsis by DNA FISH and HORMAD2 immunolabeling on pachytene spreads from PB6F1 sterile males. (A and B) (Left) A single DNA cloud signals properly aligned chromosomes and HORMAD2-positive axes restricted to sex chromosomes. (Center) A cell in which asynapsis does not involve the studied chromosome. (Right) Arrows show partial asynapsis of Chr 2 and complete asynapsis of Chr 16, respectively. (C–E) Separate DNA clouds and HORMAD2-labeled univalents demonstrate asynapsis of Chrs 17 (C), 18 (D), and 19 (E). (F) The frequency of asynapsis of five examined chromosomes in sterile PB6F1and semifertile reciprocal B6PF1 hybrids. n, total number of cells scored; nd, not done.

A

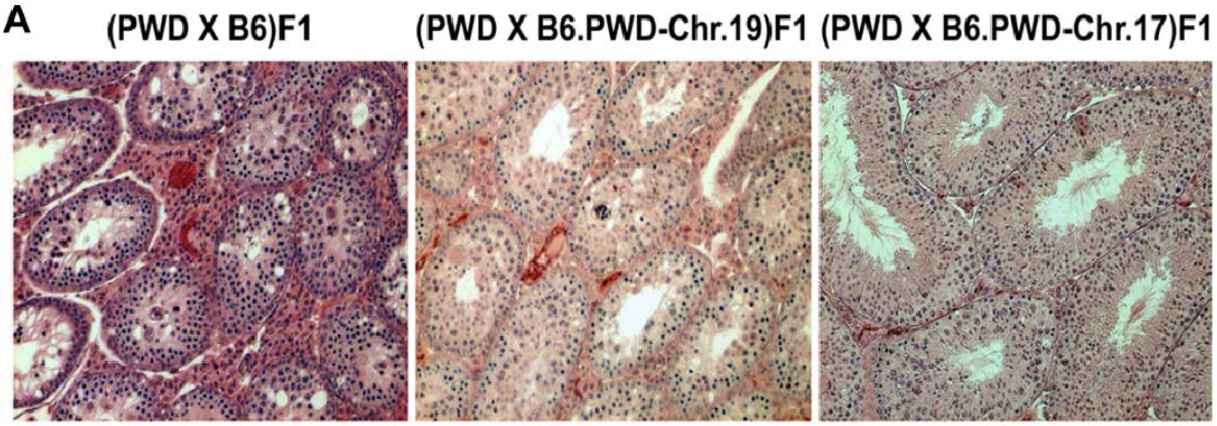

B

Genotype		Chr 17	Chr 19	Any autosome
(PWD x B6)F1	% asyn	32,1	46,7	95,8
	N	112	120	116
(B6 x PWD)F1	% asyn	0	16,2	32,5
	N	57	80	120
(PWD X B6.PWD-chr.19) F1	% asyn	ND	0	59,6
	N	ND	100	104
(PWD X B6.PWD-chr.17) F1	% asyn	ND	ND	0
	N	ND	ND	62
(B6.PWD.Chr.X X B6.PWD.Chr.17) F1	% asyn	100	ND	17
	N	25	ND	100

Figure 8.5: (A) Histological cross-sections of spermatogenic tubules stained with H&E display a block at epithelial stage IV, giant multinuclear cells, and the absence of haploid phase in sterile PB6F1 hybrids. The (PWD x B6.PWD-Chr19)F1 testes display partial relaxation of spermatogenic block with reduced number of postmeiotic cells. The (PWD x B6.PWD-Chr17)F1 testes display normal spermatogenesis. (B) The frequency of asynapsis of Chr 17 and 19 examined in sterile PB6F1, semifertile / fertile crosses (PWD x B6.PWD-Chr17 or 19)F1 and (B6.PWD-Chr X.1s × B6.PWD-Chr 17)F1 hybrids .N= total number of cells scored; ND means not done.

Genotype	autosomal constitution	Chr X	Fertility	Pachytene block	Pachytene asynapsis
PWD × B6	All $A^{PWD/B6}$*	PWD	ST	Complete	Multiple. Excess of Ch17 and Chr 19 univalents
B6 × PWD	All $A^{PWD/B6}$	B6	F/ST	Weak	Limited. Excess of Chr 19 univalents
PWD × B6.PWD-Chr 19	**Chr 19$^{PWD/PWD}$** All other $A^{PWD/B6}$	PWD	ST	Partially released	Multiple. **Chr 19 univalents missing**
B6.PWD-Chr X.1s × B6.PWD-Chr 17	**Chr 17$^{PWD/B6}$** All other $A^{B6/B6}$	PWD**	ST	None	Limited. **Only Chr 17 univalents present**
PWD × B6. PWD-Chr 17	Chr $17^{PWD/PWD}$ All other $A^{PWD/B6}$	PWD	F	None	None

Table 8.1: Heterospecific autosomes and pachytene asynapsis in F1 hybrid males of various genotypes.

*All heterospecific autosomal pairs consist of one *Mus m. musculus* (PWD) copy and one of *Mus m. domesticus* (B6)

** Chr X.1s shows a 4.5 MB extension of the distal end of proximal PWD interval, when compared to Chr X.1

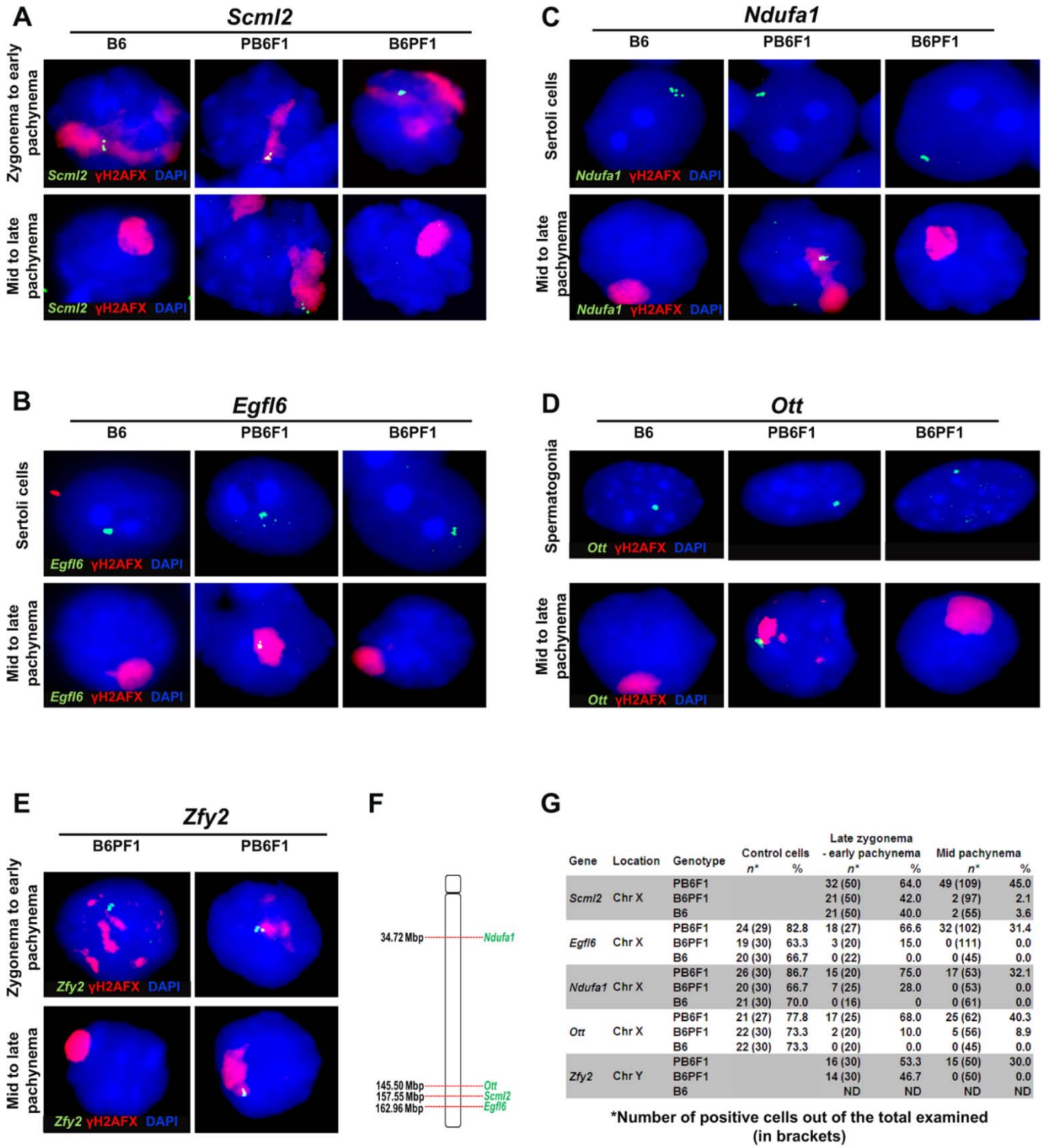

G

Gene	Location	Genotype	Control cells n*	Control cells %	Late zygonema - early pachynema n*	Late zygonema - early pachynema %	Mid pachynema n*	Mid pachynema %
Scml2	Chr X	PB6F1			32 (50)	64.0	49 (109)	45.0
		B6PF1			21 (50)	42.0	2 (97)	2.1
		B6			21 (50)	40.0	2 (55)	3.6
Egfl6	Chr X	PB6F1	24 (29)	82.8	18 (27)	66.6	32 (102)	31.4
		B6PF1	19 (30)	63.3	3 (20)	15.0	0 (111)	0.0
		B6	20 (30)	66.7	0 (22)	0.0	0 (45)	0.0
Ndufa1	Chr X	PB6F1	26 (30)	86.7	15 (20)	75.0	17 (53)	32.1
		B6PF1	20 (30)	66.7	7 (25)	28.0	0 (53)	0.0
		B6	21 (30)	70.0	0 (16)	0	0 (61)	0.0
Ott	Chr X	PB6F1	21 (27)	77.8	17 (25)	68.0	25 (62)	40.3
		B6PF1	22 (30)	73.3	2 (20)	10.0	5 (56)	8.9
		B6	22 (30)	73.3	0 (20)	0.0	0 (45)	0.0
Zfy2	Chr Y	PB6F1			16 (30)	53.3	15 (50)	30.0
		B6PF1			14 (30)	46.7	0 (50)	0.0
		B6			ND	ND	ND	ND

*Number of positive cells out of the total examined (in brackets)

Figure 8.6: Disrupted silencing of X- and Y-linked genes in mid–late pachynemas revealed by RNA FISH. (A) The *Scml2* gene is silenced in mid–late pachynemas in fertile controls but remains active in PB6F1 sterile males. (B and C) *Egfl6* (B) and *Ndufa1* (C) are active in Sertoli cells. They are silenced in mid–late pachynema of fertile controls but remain active in sterile hybrids. (D) Similarly, multicopy *Ott* is active in spermatogonia of all genotypes. It is silenced in mid–late pachynema of fertile controls but is active in mid–late pachytene of sterile hybrids. (E) *Zfy2* on the Y chromosome remains active in sterile hybrids. Its activity is thought to induce apoptosis. (F) Positions of the studied genes on Chr X. (G) Quantification of pachytene and control cells with active or silenced X/Y genes. ND is not done.

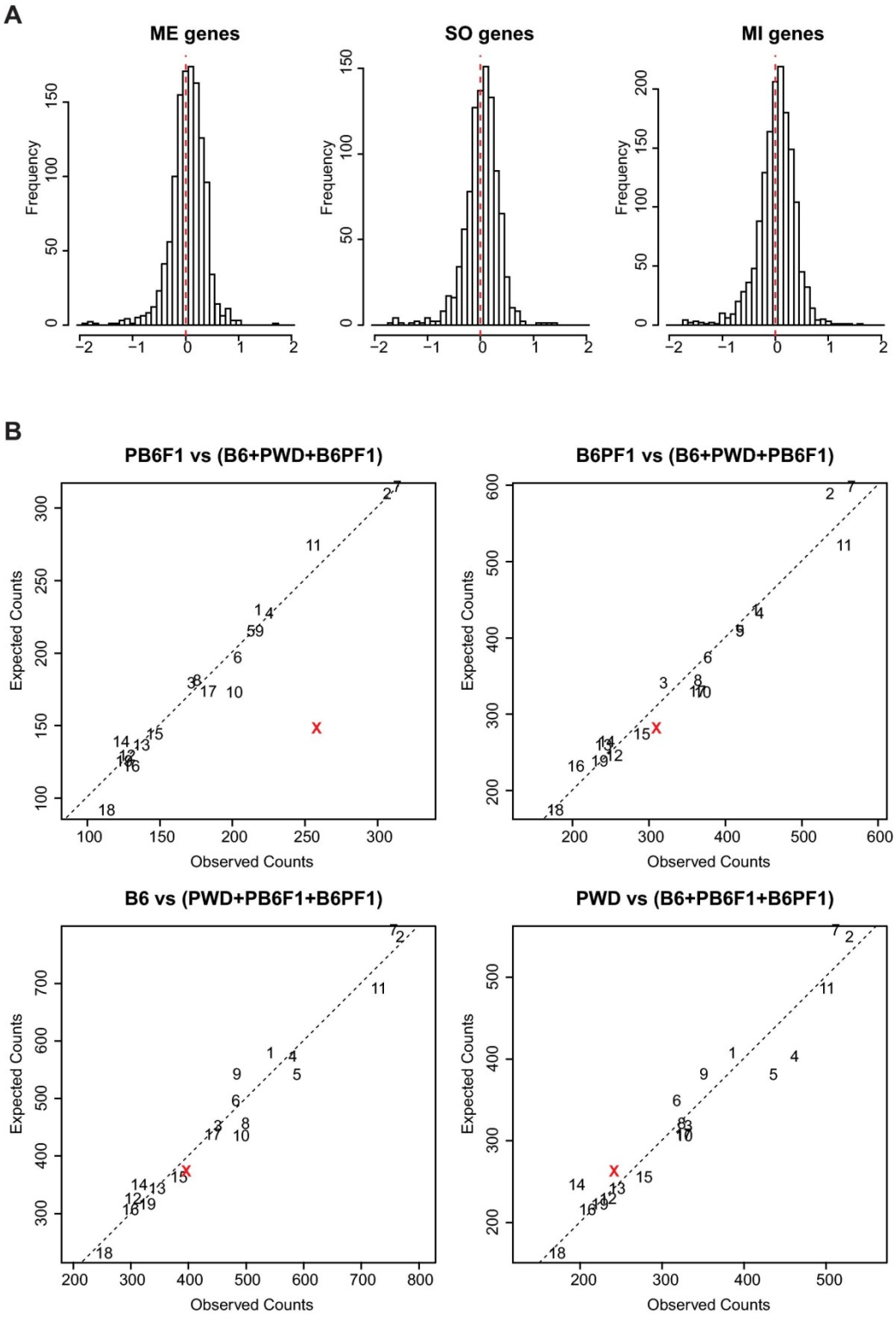
A
ME genes
SO genes
MI genes
Frequency
B
PB6F1 vs (B6+PWD+B6PF1)
B6PF1 vs (B6+PWD+PB6F1)
B6 vs (PWD+PB6F1+B6PF1)
PWD vs (B6+PB6F1+B6PF1)
Expected Counts
Observed Counts

Figure 8.7: Gene-expression profiling of 14.5-dpp sterile hybrids and fertile controls. (A) No apparent differences in the distribution of testicular cell types are indicated by histograms of log fold-changes in gene expression between sterile PB6F1 and fertile B6PF1 hybrids for each cell type. ME, meiotic (spermatocytes), 1,222 genes; MI, mitotic (spermatogonia), 1,544 genes; SO, somatic (Sertoli cells), 995 genes. (B) Number of genes with suggestive differences in expression ($P< 0.05$) specific for PB6F1, B6PF1, B6, or PWD strains, compared with the pool of remaining three strains, is calculated for each chromosome and compared with the counts expected by pure chance. The preponderance of misregulated genes on Chr X (shown in red) is apparent in the comparison of sterile PB6F1 hybrids with fertile controls.

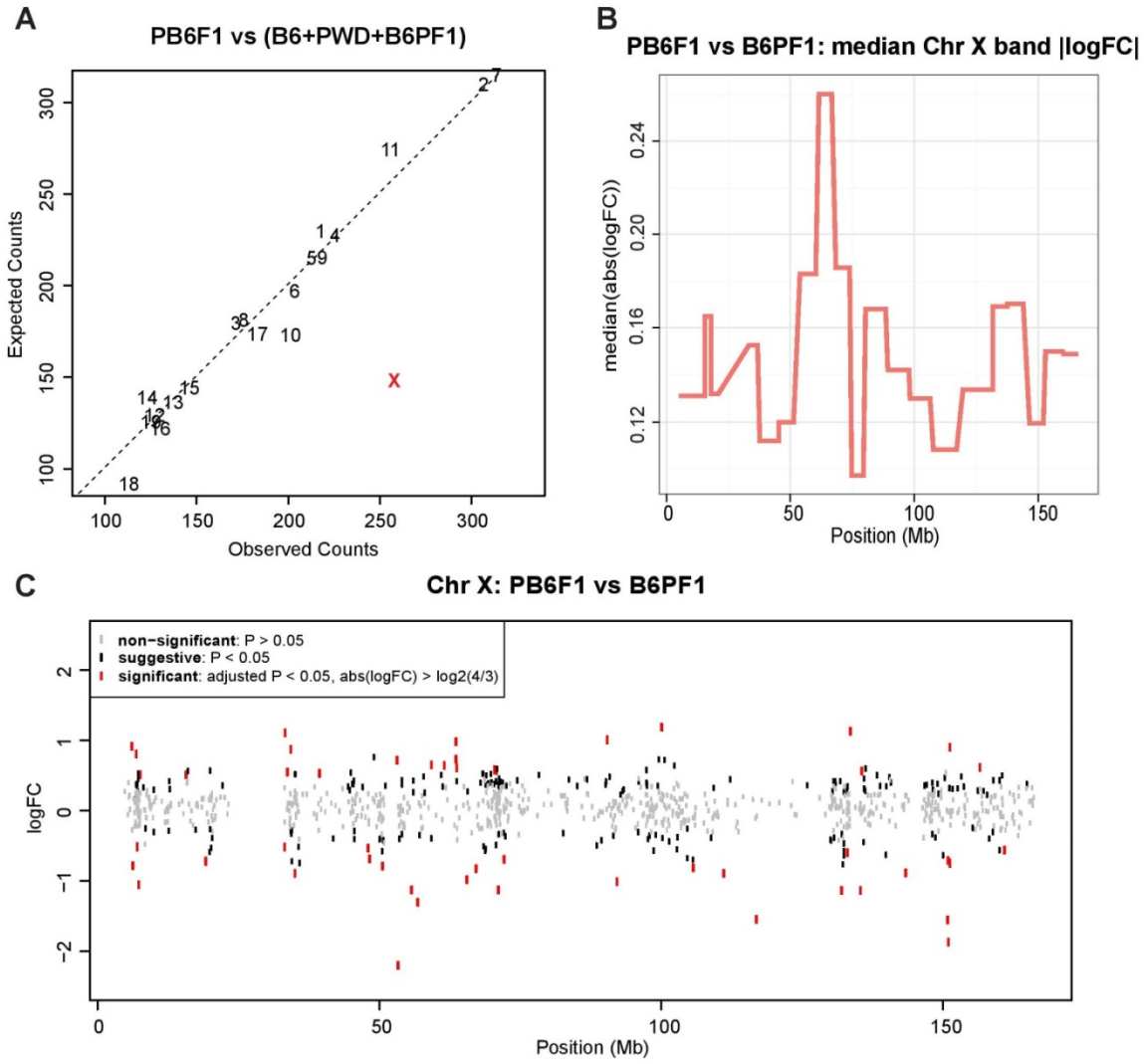
A
PB6F1 vs (B6+PWD+B6PF1)
Expected Counts
Observed Counts
B
PB6F1 vs B6PF1: median Chr X band |logFC|
median(abs(logFC))
Position (Mb)
C
Chr X: PB6F1 vs B6PF1
non−significant: P > 0.05
suggestive: P < 0.05
significant: adjusted P < 0.05, abs(logFC) > log2(4/3)
logFC
Position (Mb)

Figure 8.8: Gene-expression profiling of 14.5-dpp male testes of sterile males and fertile controls. (A) The number of genes with suggestive differences in expression per chromosome (unadjusted P value < 0.05) between sterile PB6F1 hybrids and a pool of fertile (B6PF1, B6, PWD) controls was compared with counts expected by pure chance (Poisson model, P < 0.01). The X chromosome showed a significantly high number of misexpressed genes compared with the autosomes. Three mice were analyzed per genotype. (B) Median absolute log fold-change between PB6F1 and B6PF1 average gene expression was calculated for Chr X cytogenetic bands. Maximum is attained for A7.1. (C) Log fold-changes of Chr X gene expression between PB6F1 and B6PF1.

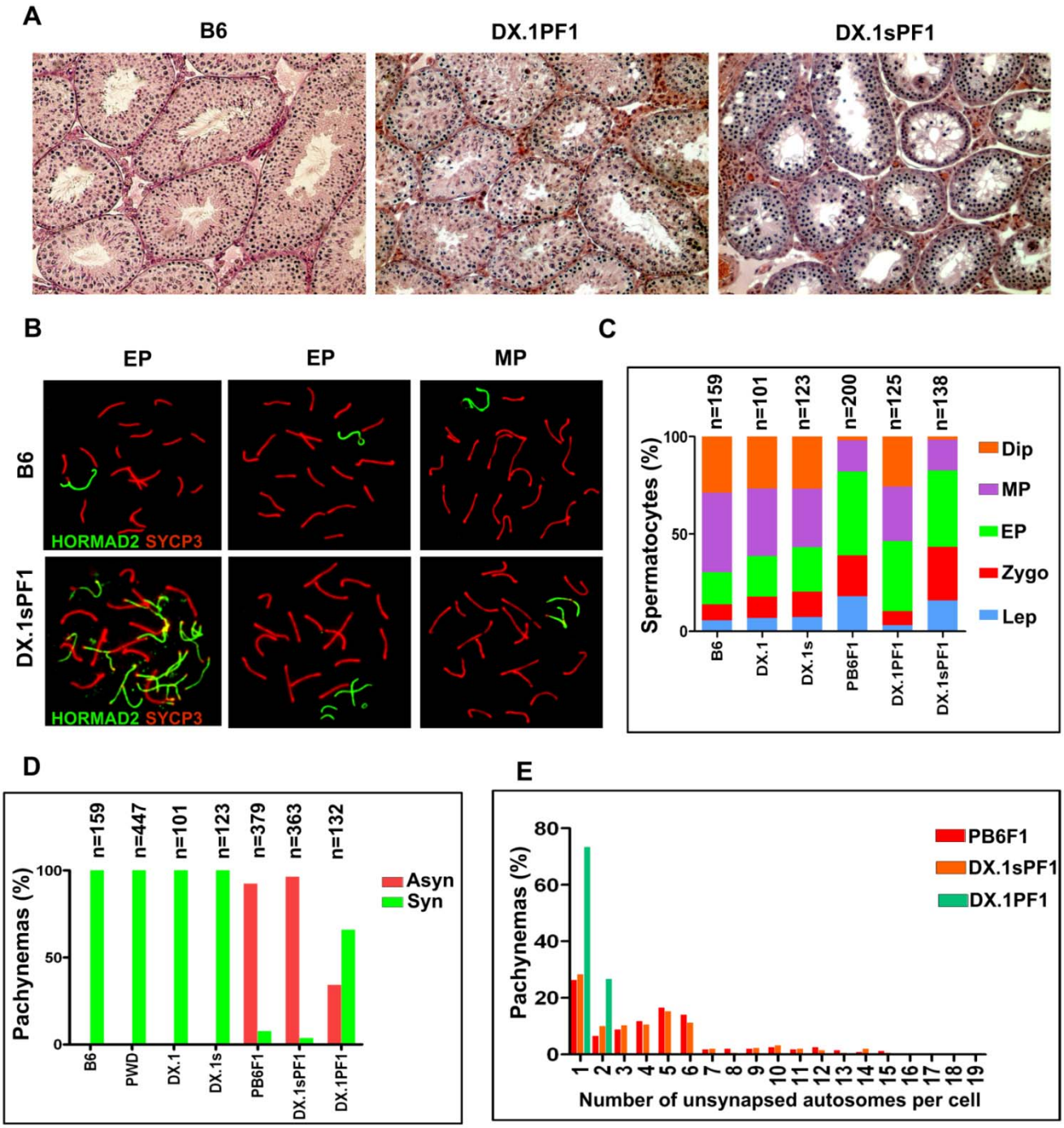
A
B6
DX.1PF1
DX.1sPF1
B
EP
EP
MP
B6
DX.1sPF1
HORMAD2 SYCP3
HORMAD2 SYCP3
C
n=159
n=101
n=123
n=200
n=125
n=138
Spermatocytes (%)
100
50
0
Dip
MP
EP
Zygo
Lep
B6
DX.1
DX.1s
PB6F1
DX.1PF1
DX.1sPF1
D
n=159
n=447
n=101
n=123
n=379
n=363
n=132
Pachynemas (%)
100
50
0
Asyn
Syn
B6
PWD
DX.1
DX.1s
PB6F1
DX.1sPF1
DX.1PF1
E
Pachynemas (%)
80
60
40
20
0
PB6F1
DX.1sPF1
DX.1PF1
1
2
3
4
5
6
7
8
9
10
11
12
13
14
15
16
17
18
19
Number of unsynapsed autosomes per cell

Figure 8.9: (A) Histological cross-sections of spermatogenic tubules stained with H&E display a block at epithelial stage IV, giant multinuclear cells, and the absence of haploid phase in sterile DX.1sPF1 hybrids. The DX.1PF1 testes display complete spermatogenic development with reduced postmeiotic cells while B6 testes showed normal spermatogenesis. (B) Asynapsis of pachytene spermatocytes as revealed by immunostaining of SYCP3 and HORMAD2. Early pachynemas show multiple asynapsed autosomes. Mid–late pachynemas showed one or two pairs of asynaptic autosomes engulfed in the sex body. (C) Frequency of individual stages of primary spermatocytes in the suspensions of testicular cells from adult males. A significant difference in the cellular composition was found in between sterile PB6F1 and DX.1sPF1 males with fertile controls ($P < 0.001$; $\chi 2$ test). In comparison to or compared to fertile controls striking difference was observed in the reduced number of mid–late pachynemas and rare presence of diplotene spermatocytes in PB6F1 and DX.1sPF1 sterile hybrids. n, number of cells examined. (D) PB6F1 and DX.1sPF1 meiocytes with more than four univalents disappear in mid-pachynema and diplonema. In DX.1PF1 asynapsis was restricted to one or two chromosome in 34% of the spermatocytes. In B6, PWD, DX.1 and DX.1s control males asynapsis was absent. (E) Distribution of percentage pachynemas according to the number of asynapsed autosomes estimated by counting the CREST-stained centromeres on SYCP3- labeled synaptonemal complexes. In total 350 aberrant pachynemas with asynapsis were counted for PB6F1 and DX.1sPF1 sterile hybrids, whereas 45 meiocytes with asynapsis were counted for DX.1PF1 fertile hybrid.

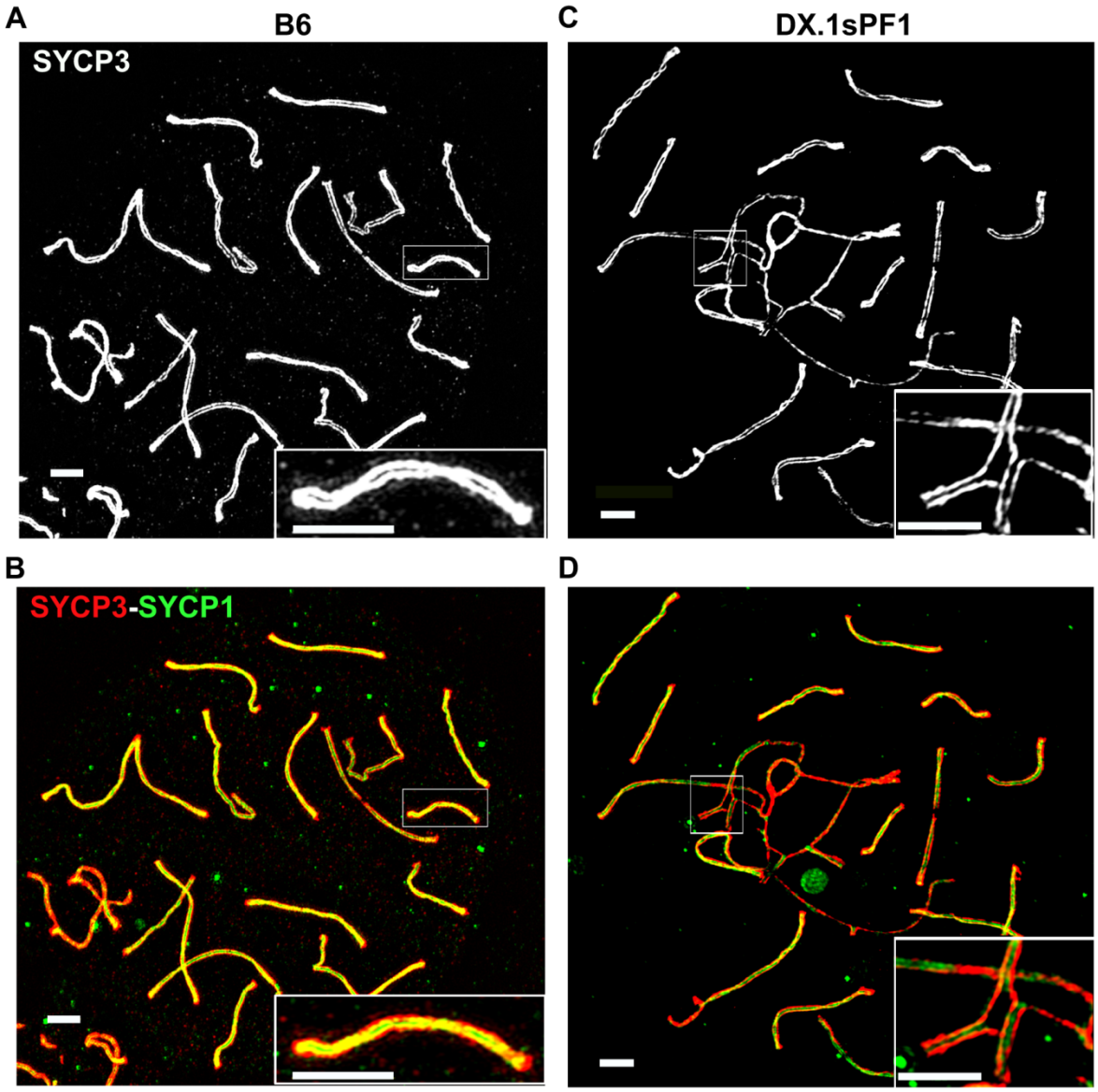

Figure 8.10: The examination of meiocytes using super resolution microscopy.(A) In normal pachytene spermatocyte the chromosome pair with their homologous partners shown here by SYCP3 (Red; stains Axial element of synaptonemal complex). (B). The synapsis process is marked by the presence of central element protein SYCP1 (Green) (C) In sterile PB6F1 and DX.1sPF1 hybrids pachynemas showed clear examples of nonhomologous synapsis and revealed irregular spots of SYCP1 on some univalent (D). The scale bar is 2µm in length.

A

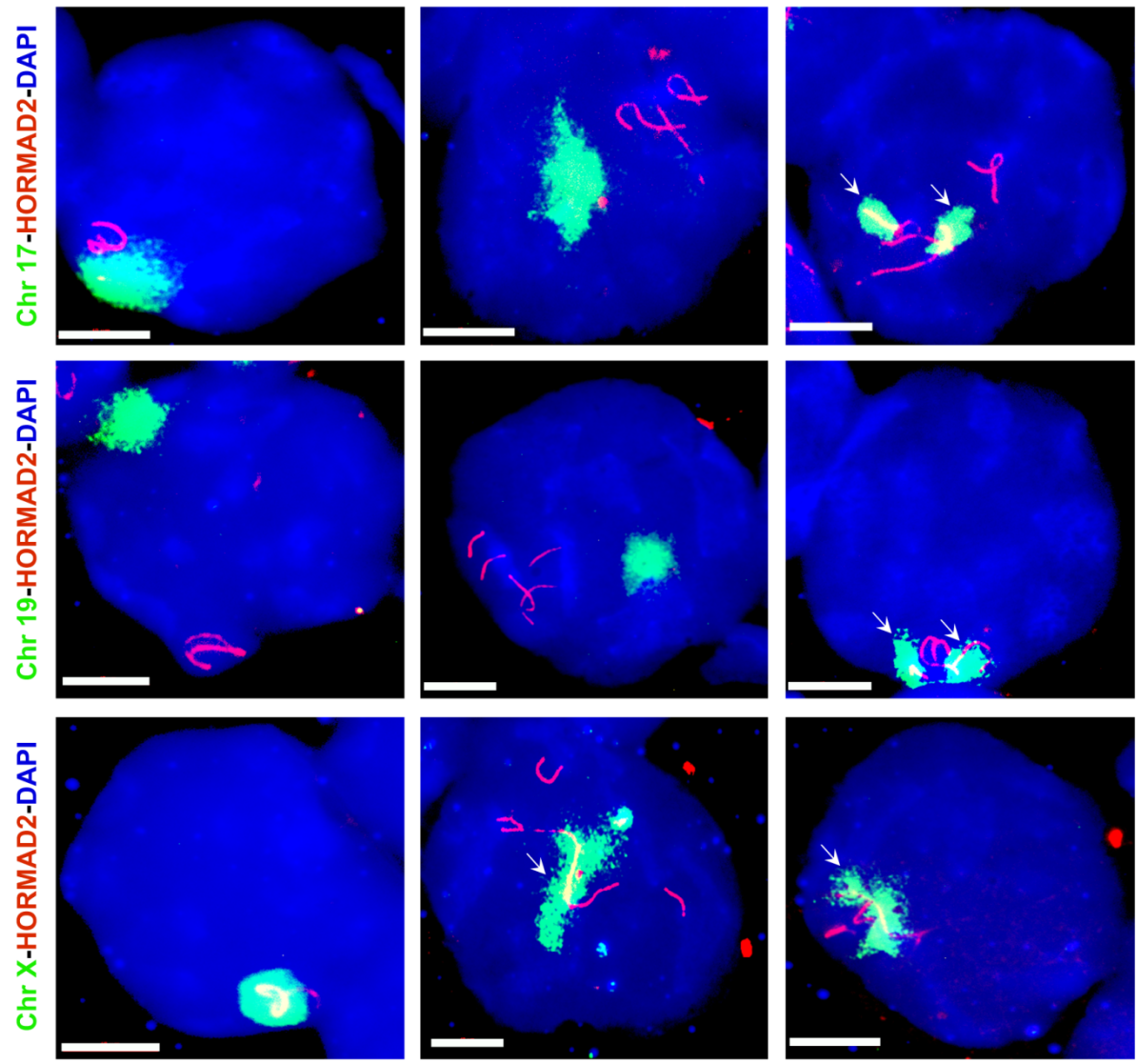

B

	PWD		PB6F1		DX.1sPF1	
	% asyn	*n*	*% asyn*	*n*	*% asyn*	*n*
Chr 17	0	94	27.1	144	29.9	117
Chr 19	0	95	41.7	120	40.5	121
Any autosome	0	447	92.3	379	96.4	363

C

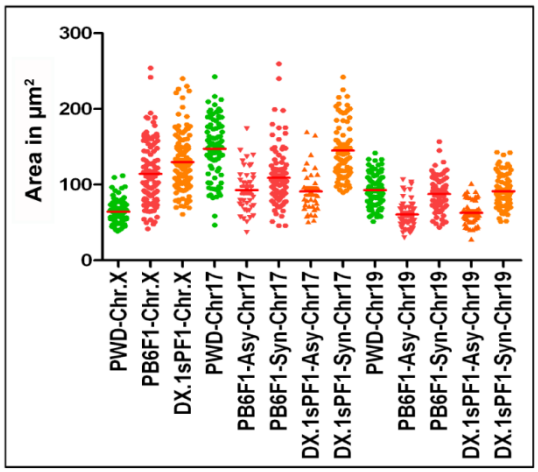

Figure 8.11: Two autosomes and chromosome X were tested for asynapsis by DNA FISH and HORMAD2 immunolabeling on pachytene spreads from PB6F1, DX.1sPF1 and PWD males. (A) (Left) A single DNA cloud signals the properly aligned autosomes or HORMAD2-positive axes restricted to X chromosome. (Center) A cell in which asynapsis does not involve the studied autosomes but on relaxed X chromosome. (Right) Arrows show complete asynapsis of Chr 17 and Chr 19, and relaxed chromatin of X chromosome. (B) The frequency of asynapsis of Chr17 and 19 in PB6F1, DX.1sPF1 and PWD males. n, total number of cells scored.(C) Graph displaying the area of chromatin in terms of synapsis status. The area of chromatin doesn't show any correlation with the area of DNA (DAPI).The unsynpsed autosomes (both Chr 17 and 19) in sterile hybrids showed significant ($P<0.01$; Mann-Whitney U test) decrease in the chromatin area to their synapsed counterpart which could be explained by meiotic silencing of the unsynapsed chromatin and the suppression of transcription. Meanwhile Chr. X in sterile hybrids showed significant ($P<0.01$; Mann-Whitney U test) spreading of chromatin area in comparison to fertile PWD control. The finding provides the cytological counterpart to the transcriptional reactivation of X-linked genes during MSCI failure in PB6F1 sterile males as described earlier (section7.7).

9. Meiotic phenotype in hybrid females.

The F1 hybrid sterility is male limited following the Haldane's rule (Haldane et al. 1922). Here we asked whether the meiotic defects leading to hybrid male sterility are indeed male specific. To answer this next question we decided to do molecular dissection of oogenesis in PB6F1 hybrid females and then compare it with intra-species hybrid and parental control females.

9.1 Asynapsis of homologous chromosomes in F1 hybrid pachytene oocytes.

According to Haldane´s rule, sterility or inviability of interspecific hybrids preferentially involves heterogametic sex. Indeed, PB6F1 females were fully fertile but their oocytes in the first and second meiotic division revealed a series of abnormalities. Meiotic spreads from ovaries revealed asynapsis in 40% and 50% of inter-subspecific (PB6F1) F1 hybrid pachynemas at 17.5 dpc and 19.5 dpc, respectively (Figure 9.1A and B). In about half of these cells one or two autosomes were asynapsed, while more than two asynapsed autosomes were observed in the remaining aberrant pachynemas. Clouds of phosphorylated histone H2AFX or γH2AFX decorated the univalents in a similar fashion as in spermatocytes from sterile males. Unexpectedly oocytes of B6 and PWD inbred strains and intraspecific (C3H × B6)F1 (abbreviated C3B6F1) hybrids also showed asynapsis, albeit at lower 12% and 23% frequency (Figure 9.1B). Unlike the male hybrids, the reciprocal F1(B6PF1) hybrid oocytes and (PWD × B6.*Hst1*^{f})F1 oocytes displayed the same high level (47%) of asynapsis (Figure 9.1B), thus not reflecting the alternate genotype of hybrid sterility genes. At 1 dpp the proportion of diplonemas was significantly reduced in PB6F1 (37.5%) and B6PF1 (33%) inter-subspecific hybrid oocytes compared to B6 (64.1%) and PWD (56.6%) controls ($P<0.01$, Chi-square test, Figure 9.2A). Partial elimination of the univalent-carrying oocytes is the likely explanation of this reduction. To test this possibility we counted the oocytes on histological cross-sections of 6-weeks-old ovaries of C3B6F1, PB6F1, B6PF1 and PWD females. The number of oocytes was decreased in PB6F1 and B6PF1 (321.7±109.8 and 351.2±55.1 respectively; $P<0.05$ ANOVA with Tukey's correction) when compared to C3B6F1 (941.66±335.9) females. However, a similar reduction was observed in PWD ovaries (320.7±45.9) probably reflecting the smaller body and ovary size of PWD females (Figure 9.2 B and C). Histological section analysis was done in collaboration wih Dr. Ondrej Mihola.

9.2 Chromosome pairing and segregation errors in female metaphase I and II.

The high frequency of asynaptic chromosomes observed in pachytene stage of developing oocytes prompted us to analyze the later stages of meiosis I. Oocytes in metaphase I with chromosomes without visible chiasmata were found with similar frequency, about 6%, in both inter-subspecific F1 hybrids (B6PF1 n = 77; PB6F1 n = 81; Figure 9.2 G and H). In contrast, control C3B6F1 oocytes (n = 78) had no univalent; Figure 9.2 F and H). The finding of a low frequency of univalents in MI indicated significant elimination of oocytes with meiotic pairing errors. It has been shown that the presence of univalent chromosomes at the first meiotic division is frequently accompanied by chromosome segregation errors and aneuploidy (Sebestova et al., 2012; Kouznetsova et al., 2007). Kinetochore counting at the metaphase II (MII) revealed 2% aneuploidy in C3B6F1 (n = 238) MII oocytes, while significantly higher frequency, 11% and 9%, was detected in MII from inter-subspecific hybrids B6PF1 (n = 129) and PB6F1 (n = 100, Figure 9.2 I, J and K). This work was done in collaboration with Dr. Martin Anger.

9.3 Live imaging analysis of chromosome segregation in MI oocytes.

The relatively low frequency of univalents detected in MI in inter-subspecific F1 hybrids could not fully explain the levels of aneuploidy in MII oocytes and therefore we monitored potential defects of chromosome segregation by live imaging microscopy. We did not observe any difference in duration of meiosis I between inter-subspecific and intraspecific hybrids, despite the presence of univalents in B6PF1and PB6F1 oocytes (Figure 9.2 D). Quantification of the securin expression levels showed that also the timing of anaphase-promoting complex (APC) activation was similar in all three hybrids (Figure 9.2 E). Both results are not surprising in the light of recently accumulating evidence showing that spindle assembly checkpoint in oocytes is unable to arrest cells with unaligned chromosomes (Nagaoka et al., 2011; Sebestova et al., 2012). However, the analysis of the time-lapse movies showed extensive chromosome congression defects in B6PF1and PB6F1oocytes compared to C3B6F1 (Figure 9.1 C and D). While C3B6F1 oocytes were able to align chromosomes properly on the metaphase plate when approaching to anaphase, B6PF1and PB6F1oocytes were both entering anaphase with the metaphase plate fairly disorganized. Quantification of density of DNA located near the equatorial plane in six intervals within the last two hours before anaphase showed significant differences between inter-

subspecific and intraspecific hybrid oocytes in all but the last interval (Figure 9.1D). This work was done in collaboration with Dr. Martin Anger.

9.4 *Hstx2* and *Hst1/Prdm9* regulate male but not female asynapsis

Our most critical observation was that asynapsis preferentially affects autosomal pairs with heterospecific homologs and their pairing failure is strongly influenced by *Prdm9* and *Hstx2* hybrid sterility genes in sterile hybrid males (section 8) (Bhattacharyya et al., 2013). Thus we asked whether the genetic control of meiotic asynapsis differs between male and female gametogenesis of intersubspecific hybrids. The examination of B6 and PWD parental strains did not reveal any asynapsis in pachynemas of primary spermatocytes but showed 14% and 29% of pachynema 18.5 dpc oocytes with one or more asynapsed autosomal pairs. In PB6F1 hybrid females over 40% of pachynemas showed asynapsis, but contrary to F1 hybrid males the frequency of asynaptic oocytes was not modified by *Prdm9* and *Hstx2* hybrid sterility genes. The conclusion was reached by comparing the asynapsis frequency in male and female meiosis of hybrids between consomics and PWD. In (PWD x B6.PWD-Chr 17)F1 or PD17F1 female fetuses 46% pachytene oocytes displayed asynapsis that was absent in spermatocytes of the same genotype. Moreover 46.5% and 44% of oocytes of (B6.PWD-Chr X.1 x PWD)F1 or DX.1PF1 and (B6.PWD-Chr X.1s x PWD) or DX.1sPF1 hybrids showed asynaptic autosomes, compared to 34.1% and 96.4% of pachynemas of the corresponding male genotypes of the same cross. These comparisons demonstrate the lack of control of asynapsis in female meiosis by the Chr 17 and *Hstx2* hybrid sterility gene (Figure 9.3 A and C). However, the detailed analysis of female hybrids conspecific for Chr 17^{PWD} showed lower number of unsynapsed autosomes per cell when compared with other intersubspecific F1 hybrid genotypes (Figure 9.3 D). Thus *Prdm9/Hst1* or some other gene on Chr 17 showed a limited effect on asynapsis in female hybrids.

The state of asynapsis in F1 hybrid females raised questions about the fate of these pachynemas with asynapsis. Earlier in this chapter we have shown that the majority of meiocytes with asynapsis gets eliminated before moving to diplotene stages. The state of asynapsis in DX.1sPF1 hybrid females brought questions about the fate of these pachynemas with asynapsis. So, we checked the progression of pachytene to diplotene in 19.5dpc ovary. The 19.5dpc DX.1sPF1 ovary had 66.7% pachynema and 33, 3% diplonema, whereas 19.5dpc PB6F1 hybrid have 71.5% and 28.5% pachynema and diplonema respectively. The inbreed control of PWD (45%) and B6

(47.5%) showed significantly (P< 0.01, Chi-square test, Figure 9.3B) higher percentage of diplonema's at same age. The decrease in number of diplotene in hybrid females can be explained by elimination of pachynemas as we have showed earlier.

9.5 Heterospecific homologs are prone to asynapsis in female meiosis

Previously we showed that the conspecific (PWD/PWD) homologous autosomes become resistant to asynapsis in otherwise heterospecific (PWD/B6) genomic background. The finding indicates cis-control of asynapsis based on some form of incompatibility between heterospecific homologs of *Mmm* and *Mmd* origin (Bhattacharyya et al., 2013). Considering the difference between male and female hybrids in the overall frequency of asynapsis and the role of hybrid sterility genes in their control we asked whether the incompatibility of heterospecific homologs resulting in decreased efficiency of their pairing and synapsis operates also in female meiosis.

We used the chromosome substitution strains carrying Chr 17^{PWD} and Chr X.1s ^{PWD} to analyze primary oocytes of intersubspecific F1 hybrid (18.5-19.5 dpc) conspecific (PWD/PWD) for these particular chromosomes. We compared efficacy of their meiotic synapsis with matching heterospecific pairs in (PWD x B6)F1 or PB6F1 pachytene oocytes. First, the chromosome synapsis was determined using SYCP3/SYCP1 immunostaining of synaptonemal complexes and/or visualization of univalents by HORMAD2 and SYCP3 on pachytene spreads prepared from PB6F1 oocytes. Besides Chr 17 and Chr X we also visualized Chr 2, Chr 16, Chr 18, and Chr 19 by whole chromosome DNA FISH. In agreement with previous analysis of male hybrids, Chr 2 showed the lowest incidence of asynapsis. The occurrence of univalents of small autosomes 16, 17, 18 and 19 varied between 18% and 49% in asynaptic pachytene oocytes. Strikingly, the highest frequency of asynapsis, 64%, was displayed by Chr X (Figure 9.3 E and F). The asynapsis of conspecific Chr $17^{PWD/PWD}$ dropped to zero in PD17F1 oocytes, although the total frequency of pachynemas with asynapsis was the same as in PB6F1 hybrids. In DX.1sPF1 oocytes, proximal 69.9 Mb of Chr X was conspecifc for PWD sequence, while the remaining 101.4 Mb was PWD/B6 heterospecific. Nevertheless, the partial conspecificity was sufficient to reduce the Chr X asynapsis from 64% down to 5.6% of pachytene oocytes (Figure 9.3F). Thus asynapsis in intersubspecific female and male hybrids follows the same rule, depending on unspecified sequence incompatibility between individual homologs of *Mmm* and *Mmd* origin.

9.6 *Hstx2* introgression enables the testing of dominance theory of Haldane´s rule in mice

To explain Haldane's rule of hybrid sterility, the dominance theory postulates that the recessive nature of X-linked variants that disrupt gametogenesis in hemizygous (XY) but not in homozygous (XX) sex (Muller, 1940; Turelli and Orr, 1995) and Figure 9.4). In its simplest interpretation the F1 hybrid females should become sterile in the same way as their hemizygous male siblings if their genotype could be made homozygous for incompatible Chr X variant (Figure 9.4). We were able to construct such genotype by crossing consomic females B6.PWD-Chr.X.1s and PWD males. The resulting female hybrids were PWD/B6 heterospecific for the whole autosomal genome but conspecific for proximal 69.9 Mb of Chr X^{PWD}, including the *Hstx1/2* hybrid sterility locus. Contradicting the simple interpretation of Muller's dominace hypothesis DX.1sPF1 hybrid females were fully fertile, as were all parental controls (Table 9.1). The DX.1sPF1 hybrid females carry two recessive alleles of *Hstx2* i.e $Hstx2^{PWD/PWD}$, compared to the controls with $Hstx2^{PWD/B6}$ in PB6F1 and B6PF1 hybrid females on otherwise similar hybrid background. As explained in chapter 7, the DX.1sPF1 hybrid males carrying H$stx2^{PWD}$ are sterile due to meiotic arrest. Breeding experiments of F1 hybrid females carrying $Hstx2^{PWD/PWD}$ against PWD males did not detect any significant difference in breeding performance compared to control F1 hybrid females carrying $Hstx2^{PWD/B6}$ up to 8 months of age (Table 9.1). These findings challenge the dominance theory explaining the dimorphism in phenotypes between male and female hybrid.

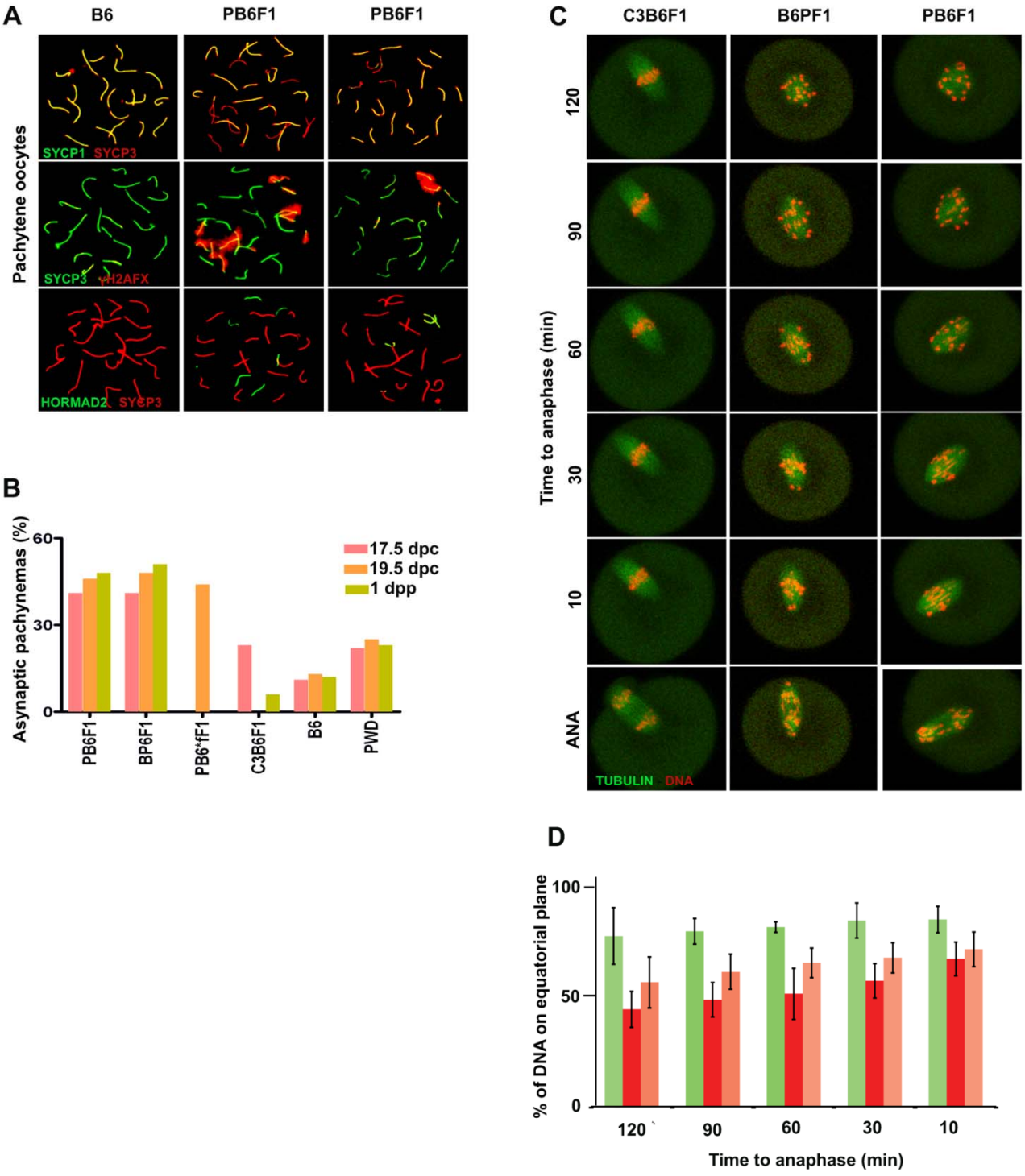
A
B6
PB6F1
PB6F1
Pachytene oocytes
SYCP1 SYCP3
SYCP3 γH2AFX
HORMAD2 SYCP3
B
Asynaptic pachynemas (%)
60
30
0
17.5 dpc
19.5 dpc
1 dpp
PB6F1
BP6F1
PB6ᵗfF1
C3B6F1
B6
PWD
C
C3B6F1
B6PF1
PB6F1
Time to anaphase (min)
120
90
60
30
10
ANA
TUBULIN DNA
D
% of DNA on equatorial plane
100
50
0
120
90
60
30
10
Time to anaphase (min)

Figure 9.1: Asynapsis at prophase I of oocytes of reciprocal hybrids and B6 controls. (A) Almost half of pachynemas of hybrid females show one or more pairs of asynaptic autosomes detected by SYCP3/SYCP1 or HORMAD2/SYCP3 immunostaining. The unsynapsed chromosomes embedded in clouds of histone γH2AFX show a tendency to clustering. (B) The high frequency of asynapsis in intersubspecific hybrids does not depend on the fertility status of their male counterparts. PB6*fF1 is the hybrid (PWD × B6.Hst1f) carrying the C3H allele of Hst1/Prdm9 gene. The males of this phenotype are fertile (Flachs et al., 2012). Three females per genotype and 40 cells per mouse were analyzed. (C and D) Chromosome alignment in meiosis I by time-lapse analysis. The values represent the amount of DNA located near the equatorial plane in C3B6F1 (green, n = 6), B6PF1 (red, n = 7), and PB6F1 (orange, n = 7) oocytes at indicated time points before anaphase.

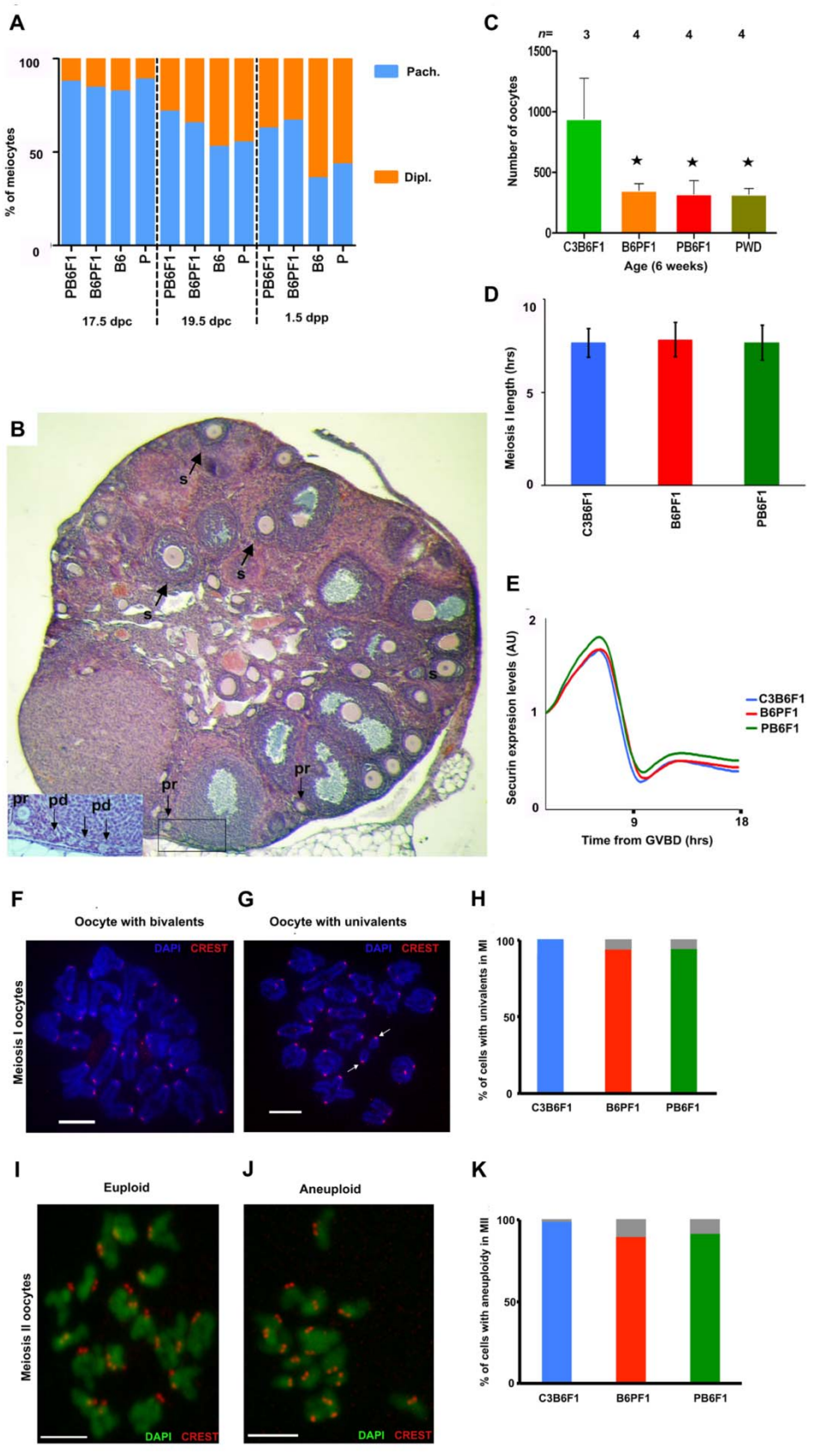
A
100
50
0
% of meiocytes
Pach.
Dipl.
PB6F1
B6PF1
B6
P
17.5 dpc
19.5 dpc
1.5 dpp
C
n=
3
4
4
4
1500
1000
500
0
Number of oocytes
C3B6F1
B6PF1
PB6F1
PWD
Age (6 weeks)
D
10
5
0
Meiosis I length (hrs)
C3B6F1
B6PF1
PB6F1
B
s
pr
pd
E
2
1
0
Securin expresion levels (AU)
C3B6F1
B6PF1
PB6F1
9
18
Time from GVBD (hrs)
F
Oocyte with bivalents
DAPI CREST
Meiosis I oocytes
G
Oocyte with univalents
DAPI CREST
H
100
50
0
% of cells with univalents in MI
C3B6F1
B6PF1
PB6F1
I
Euploid
Meiosis II oocytes
DAPI CREST
J
Aneuploid
DAPI CREST
K
100
50
0
% of cells with aneuploidy in MII
C3B6F1
B6PF1
PB6F1

Figure 9.2: Chromosome defects in meiosis I and II in oocytes of intraspecific and intersubspecific hybrids. (A) The frequency of diplonema (Dipl) oocytes is lower in interspecific hybrids, but the extent of reduction is smaller than in spermatocytes of the same genotype. Pach, pachynema. (B) Representative histological cross-section of ovary from a 6-wk-old C3B6F1 female; H&E staining. Oocytes in primordial (pd), primary (pr), and secondary (s) follicular stages are shown in the section. (C) Sum of oocyte numbers on every 10th section. n, number of biological replicates. (D) The duration of meiosis I don't differ in intra- and intersubspecific oocytes. (E) Securin expression levels do not differ in intra- and intersubspecific oocytes. (F and G) Chromosome configuration in meiosis I analyzed by chromosome spreads. DNA (blue) and kinetochores (red) were detected by DAPI and CREST antiserum, respectively. (Scale bars: 10 μM.) (F) An example of an oocyte with all chromosomes organized in bivalents. (G) An oocyte containing two univalents (arrows). (H) Frequency of univalent chromosomes in meiosis I oocytes: C3B6F1 oocytes (blue, n = 78) contained no univalents, whereas 6% of B6PF1 (red, n = 77) and PB6F1 (green, n = 81) oocytes contained univalent chromosomes. Gray columns indicate cells with univalents. (I and J) Aneuploidy in meiosis II oocytes: chromosomes (green) and kinetochores (red) were detected by DAPI and CREST antiserum, respectively, in oocytes exposed to monastrol. (Scale bars: 5 μM.) (I) Example of an oocyte with 40 kinetochores. (J) An oocyte with 36 kinetochores. (K) Frequency of aneuploidy in meiosis II oocytes: 2% of C3B6F1 oocytes (blue, n = 238); 11% of B6PF1 oocytes (red, n = 129); and 9% of PB6F1 oocytes (green, n = 100) were aneuploid in meiosis II.

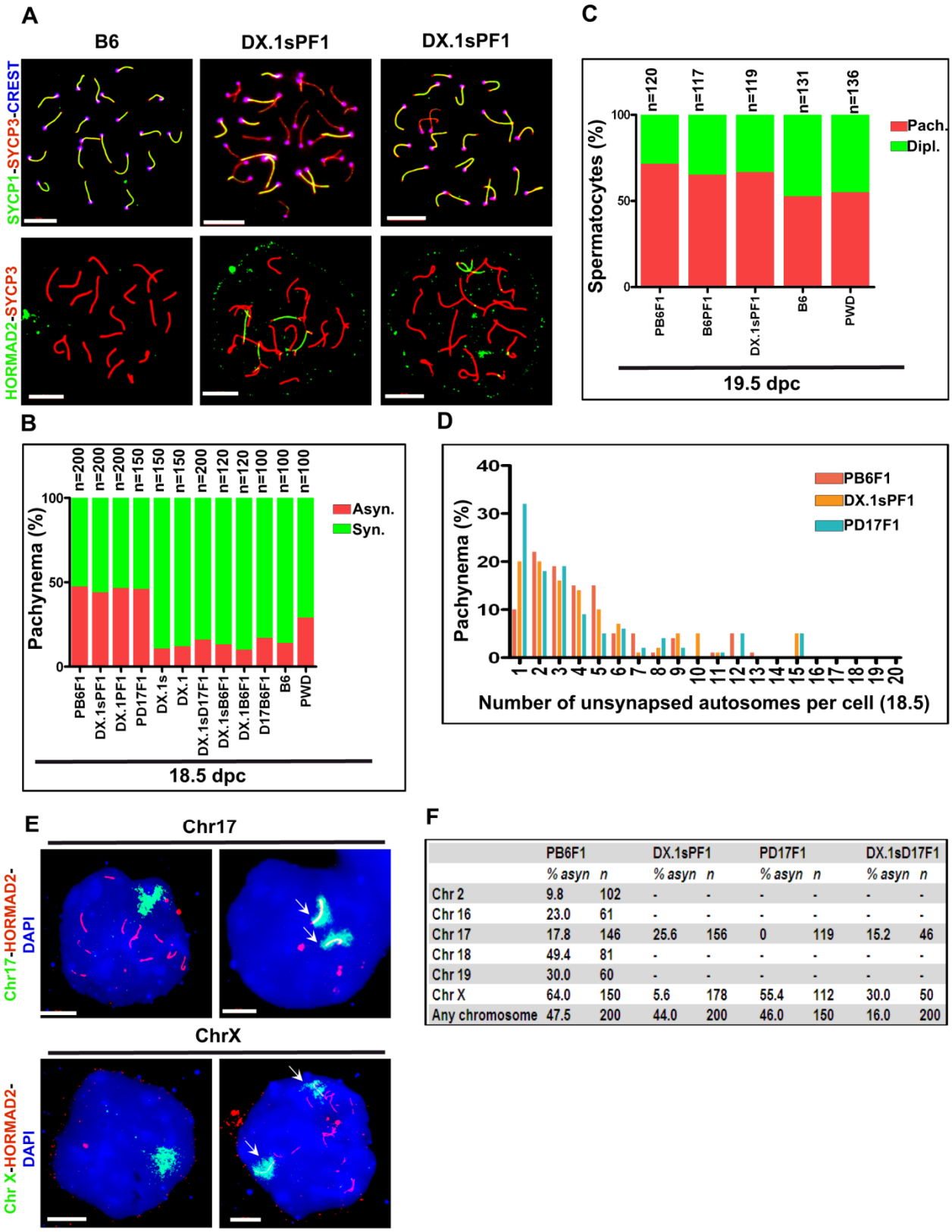

	PB6F1		DX.1sPF1		PD17F1		DX.1sD17F1	
	% asyn	*n*	*% asyn*	*n*	*% asyn*	*n*	*% asyn*	*n*
Chr 2	9.8	102	-	-	-	-	-	-
Chr 16	23.0	61	-	-	-	-	-	-
Chr 17	17.8	146	25.6	156	0	119	15.2	46
Chr 18	49.4	81	-	-	-	-	-	-
Chr 19	30.0	60	-	-	-	-	-	-
Chr X	64.0	150	5.6	178	55.4	112	30.0	50
Any chromosome	47.5	200	44.0	200	46.0	150	16.0	200

Figure 9.3: Asynapsis at prophase I of oocytes of hybrid females and B6 controls. (A) Almost half of pachynemas of hybrid females show one or more pairs of asynaptic autosomes detected by SYCP3/SYCP1 or HORMAD2/SYCP3 immunostaining. (B) The high frequency of asynapsis in DX.1sPF1, PB6F1, DX.1PF1 and PD17F1 hybrids does not depend on the fertility status of their male counterparts. In PD17F1 chromosome 17 is in conspecific condition with *Hst1*/*Prdm9*$^{PWD/PWD}$, whereas in DX.1sPF1 chromosome X is conspecific for proximal 69.9 Mb of Chr X^{PWD} with *Hstx2* $^{PWD/PWD}$ state. (C) The frequency of diplonema (Dipl) oocytes is lower in interspecific hybrids, but the extent of reduction is smaller than in spermatocytes of the same genotype. Pach. Stands for pachynema. (D) Distribution of percentage pachynemas according to the number of asynapsed autosomes estimated by counting the CREST-stained centromeres on SYCP3- labeled synaptonemal complexes. In total 200 aberrant pachynemas with asynapsis were counted for PB6F1, DX.1sPF1 and PD17F1 hybrid females (E) Five autosomes and chromosome X were tested for asynapsis by DNA FISH and HORMAD2 immunolabeling on pachytene spreads from PB6F1 hrbrid females. (E) (Left) A single DNA cloud signals properly aligned autosomes or HORMAD2-positive axes restricted to X chromosome. (Right) Arrows show complete asynapsis of Chr 17 and relaxed chromatin of X chromosome. (F) The frequency of asynapsis of five examined autosomes and X chromosome in PB6F1, DX.1sPF1, PD17F1 and DX.1s D17F1 hybrids. n, total number of cells scored. Scale bar is 10 μm.

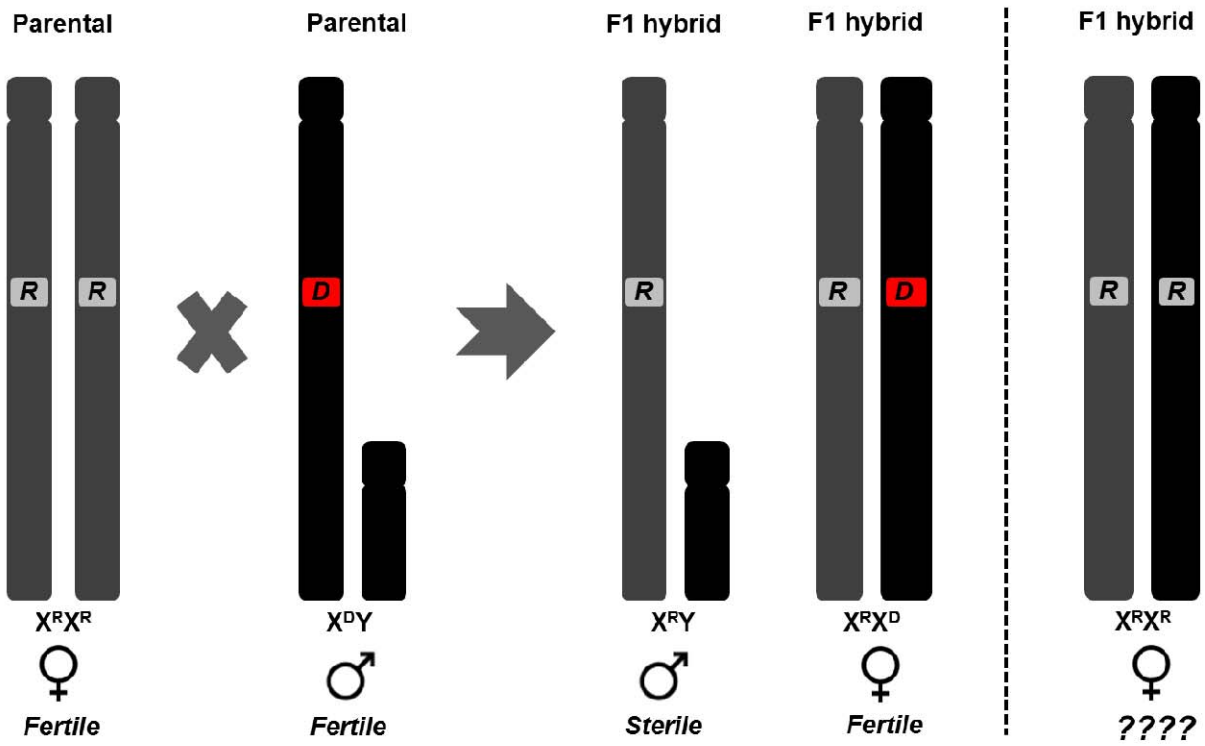

Figure 9.4: Cartoon explaining Muller's dominance theory. The dominance theory posits the recessive nature of X-linked variants that disrupt gametogenesis in hemizygous (XY) but not in homozygous (XX) sex. In its simplest interpretation the F1 hybrid females should become sterile in the same way as their hemizygous male siblings if their genotype could be made homozygous for incompatible Chr X variant. R symbolizes for recessive mutation and D symbolizes for dominant mutation.

Strain or cross	Age (in weeks)	No. of mated females	Autosomal combination in female	*Hstx* status	Litter size per female (mean ± S.D)	No. of litters (in 2 month)
C57BL/6J (B6)	8	8	A^{B6} A^{B6}	$Hstx1^{B6/B6}$	8.2 ± 1.3	12
B6.PWD-Chr X.1	8	6	A^{B6} A^{B6}	$Hstx1^{B6/B6}$	8.5 ± 1.3	12
B6.PWD-Chr X.1s	8	6	A^{B6} A^{B6}	$Hstx1^{PWD/PWD}$	8.2 ± 1.4	12
(PWD x B6)F1	8	6	A^{B6} A^{PWD}	$Hstx2^{PWD/B6}$	7.7 ± 1.0	12
(B6 x PWD)F1	8	6	A^{B6} A^{PWD}	$Hstx2^{B6/PWD}$	8.0 ± 1.3	12
(B6.PWD-ChrX.1 x PWD)F1	8	6	A^{B6} A^{PWD}	$Hstx2^{PWD/B6}$	7.6 ± 1.0	12
(B6.PWD-ChrX.1s x PWD)F1	8	6	A^{B6} A^{PWD}	$Hstx2^{PWD/PWD}$	8.9 ± 1.6	12
(PWD x B6)F1	24	4	A^{B6} A^{PWD}	$Hstx2^{PWD/B6}$	7.2 ± 1.3	6
(B6.PWD-Chr X.1s x PWD)F1	24	4	A^{B6} A^{PWD}	$Hstx2^{PWD/PWD}$	8.3 ± 1.9	6

Table 9.1: Fertility of F1 hybrids females with $Hstx1^{B6/B6}$; $Hstx2^{PWD/B6}$ and $Hstx2^{PWD/PWD}$ in B6 and (PWD x B6)F1 hybrid background. All females were crossed to PWD males for a period of 2 months.

10. Genetics of meiotic recombination.

The PB6F1 hybrid males carrying *Hstx2*^{PWD}allele in hybrid background showed mid-pachytene arrest due to widespread defects in chromosome pairing and meiotic synapsis suggesting the possible problems involving meiotic recombination. Allelic incompatibilities often affect hybrid fitness by hindering meiotic processes as synapsis and recombination. Recently our group has mapped the first mammalian hybrid sterility gene *Prdm9* in the (PWD x B6) F1 hybrid model (Mihola et al., 2009). The same gene was later shown to known to control the recombination hotspots (Parvanov et al., 2010; Baudat et al., 2010). So, we asked whether the different functional variant of *Prdm9* might epistatically interact with different partners of *Hstx2* to recognize and bind distinct DNA sequence motifs important to determine the recombination hotspots. Incompatibilities between functional allelic variant of *Prdm9* and other epistatic locus can possibly create confusion in the determination of recombination hotspots, causing an incomplete or no crossovers which might lead to asynapsis resulting in sterility. Crossovers are marked by the mismatch repair protein MLH1 situated in recombination nodules in mid-to-late pachytene. To test the hypothesis we took a top down approach to look at the global recombination rate in parental strains, B6.PWD-Chr X$^{\#}$ sub-consomics and their sterile and fertile hybrids using the MLH1 immunostaining assay on mid-pachytene spermatocytes (Figure.10.1). Understanding of the influence of epistasic interactions between *Prdm9* subspecies-specific alleles with other hybrid sterility locus on meiotic recombination may shed light on the major issue of chromosomal asynapsis in F1 sterile hybrids.

10.1 *Hstx1/2*^{PWD} locus controls meiotic recombination rate.

The initial experiment was focused on parental B6, PWD and B6.PWD-Chr.X# subconsomic strains. We observed a significant difference in the mean number of MLH1 foci for B6 (24.3±2.1) and PWD (28.6±2.5) (Figure 10.2, Table 10.1 and 10.2 ANOVA-Tukey HSD, $P<10^{-8}$). These results were in agreement with the recently published data on different strain combination (Dumont and Payseur, 2011). So, we conducted MLH1 immuno-staining assays on meiocytes spread of B6.PWD-Chr X$^{\#}$ sub-consomics to dissect the genetic locus controlling the rate of meiotic recombination. The B6.PWD-Chr X$^{\#}$ sub-consomics had the same *Prdm9*$^{B6/B6}$ allele with different pieces of chromosome X^{PWD} with or without *Hstx1/2*^{PWD}locus on B6 genetic background. Analysis of B6.PWD-Chr X.1s and B6.PWD-Chr X.2 spermatocytes showed

significant decrease in the average rate of meiotic crossing over (22.1±1.8 and 22.5±1.9, Table 10.1, ANOVA-TukeyHSD, P<0.01 to B6) compared to B6 control. The average number of MLH1 foci for B6.PWD-Chr X.1 and B6.PWD-Chr X.3 was 23.7± 2.1 and 25.3±2.2 respectively, (Table 10.1, ANOVA-Tukey HSD P= n.s), similar to that of B6. The patterns of the distribution of MLH1 foci maps to the 4.7Mbp X-linked *Hstx1*^{PWD}region between 64,880,641 bp - 69,581,094 bp (GRCm38) influencing the rate of meiotic recombination. Hence, we named the locus as meiotic recombination rate controlling gene 1 or *Mrr1*. This worked was done in collaboration with Maria Dzur-Gejdosova.

10.2 *Hstx1/2*^{PWD} locus controls depression in meiotic recombination rate in *Mmm* x *Mmd* hybrids.

Overlapping of *Hstx1* with *Mrr1* directed us to look at the influence of *Mrr1* on meiotic recombination rate on hybrid background. Previously, the reciprocal F1 hybrids between PWD and B6 have already shown a Chr X^{PWD} linked depression in meiotic recombination rate. It was shown that the mean MLH1 foci for PB6F1 sterile hybrids were 23.2± 2.7 compared to that of 26.8±2.4 for B6PF1 fertile hybrid. However analysis of other genotypes including fertile (PWD × B6.*Hst1*^{f}) F1, (PWD × B6.PWD-chr17) F1 and (PWD × B6.PWD-chr19) F1 hybrids showed similar MLH1 frequency (on average 24.5 foci; Figure 8.2C) to PB6F1 sterile hybrids pointing to an X-linked polymorphism controlling the meiotic recombination rate, rather than the meiotic arrest (Figure 8.2C). So we examined the number of meiotic crossing over events using MLH1 assay on pachytene spreads of (B6.PWD-Chr X.1x PWD)F1 and (B6.PWD-Chr X.1s x PWD)F1 hybrid males. These two F1 hybrids will have similar F1 hybrid background but different alleles of *Mrr1* locus coinciding with *Hstx2* locus. The mean MLH1 count per cell for (B6.PWD-Chr X.1 x PWD)F1 fertile hybrids was 27.1± 2.5 and 23.9± 2.3 for (B6.PWD-Chr X.1s x PWD)F1 sterile hybrid (Figure 10.3, Table 10.2; ANOVA-Tukey HSD, P<10^{-7}). The depression in MLH1 was linked to *Hstx2/Mrr1*^{PWD} locus between the two hybrids. Further comparison between sterile (B6.PWD-Chr X.1s x PWD)F1, (B6 X PWD)F1 and (B6.PWD-Chr X.1 x PWD)F1 hybrids with each other confirms a significant depression in meiotic recombination linking to *Mrr1*^{PWD} locus (Figure 10.3, Table 10.2). The coincidence of *Hstx1, Hstx2* and *Mrr1* locus governing hybrid sterility and meiotic recombination shows similarity in behavior to that of *Prdm9* performing a similar dual role. But it is impossible to conclude that all the three phenotypes are under the

influence of a single gene. Further genetic dissection of the region is required to make any conclusive remark.

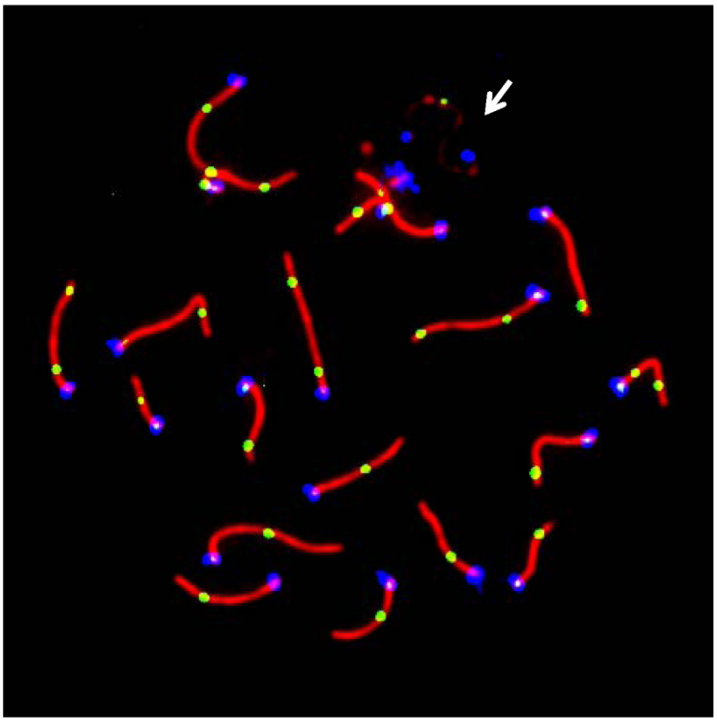

Figure 10.1: Pachytene spermatoctye from an inbreed B6.PWD-Chr.X.1 subconsomic male. SYCP1, a component of the central elements of the synaptonemal complex, is stained in red. Sites of recombination along the synaptonemal complex are denoted by green MLH1 foci. Centromeric proteins targeted by human auto-immuno anti- centromere antibodies are in blue. The white arrow points to the heterogametic sex chromosomes lightly stained by SYCP1. Only MLH1 foci on autosomal bivalents were scored.

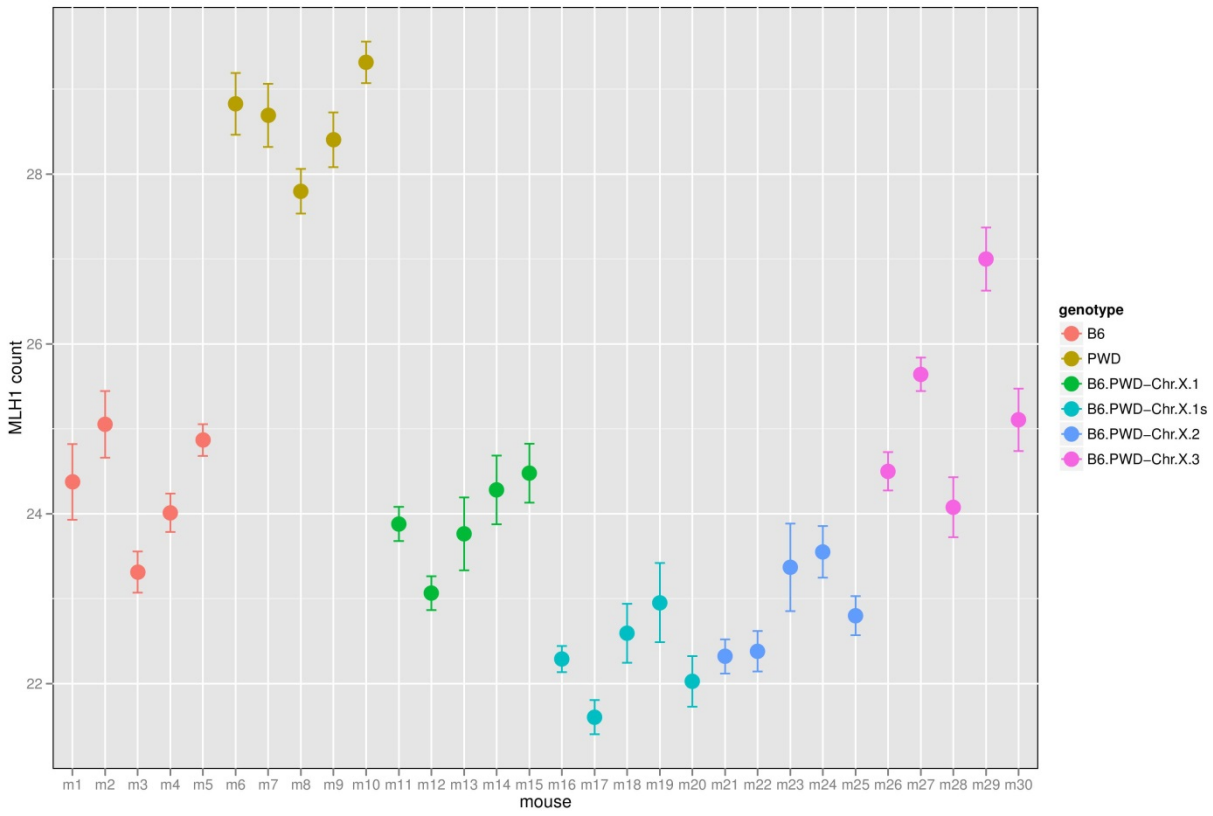

Figure 10.2: Variation in number of MLH1 foci among B6, PWD, and B6.PWD-Chr.X# subconsomic strains. Mean MLH1 counts (± standard errors) were obtained from five males for each genotype. For each mouse at least 30 mid-pachytene cells were analyzed.

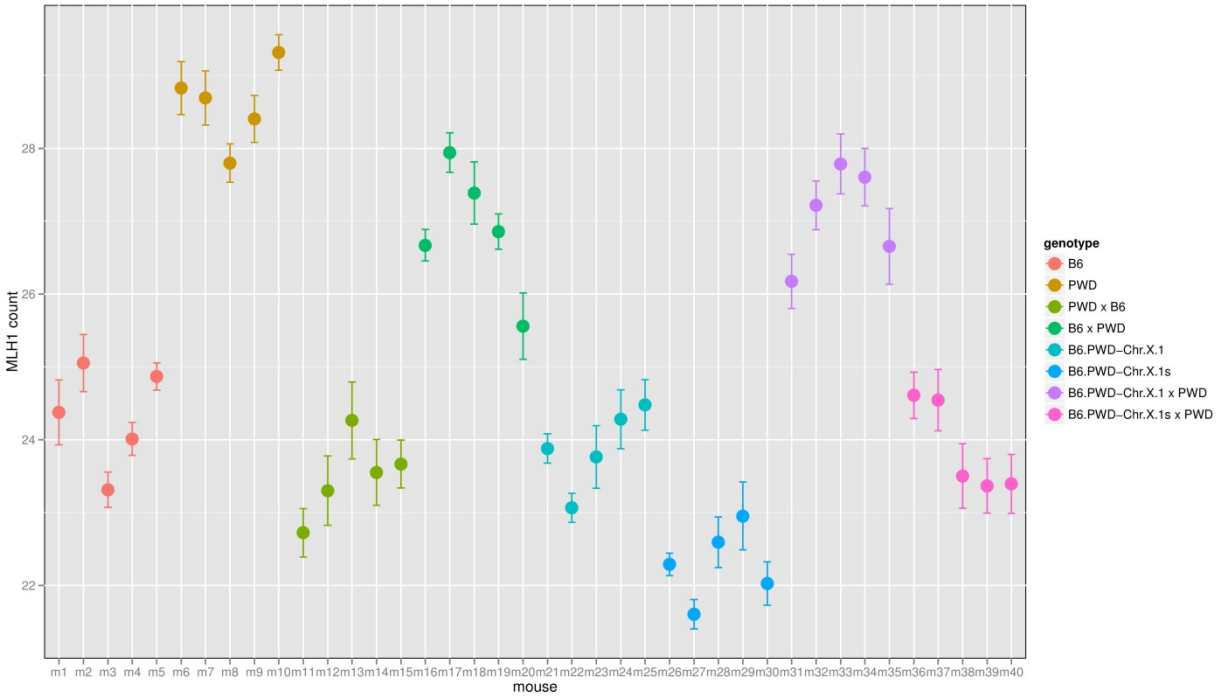

Figure 10.3: Variation in number of MLH1 foci among B6, PWD, and B6.PWD-Chr.X# subconsomic strains and their F_1 hybrids.Parental strains were used as a control. Mean MLH1 counts (± standard errors) were obtained from five males for each genotype. For each mouse at least 30 mid-pachytene cells were analyzed.

p-value / average difference	B6	PWD	B6.PWD-Chr.X.1	B6.PWD-Chr.X.1s	B6.PWD-Chr.X.2	B6.PWD-Chr.X.3
B6		**-4.3**	0.4	**2.0**	**1.4**	-0.9
PWD	**0.00**		**4.7**	**6.3**	**5.7**	**3.3**
B6.PWD-Chr.X.1	0.92	**0.00**		**1.6**	1.0	-1.4
B6.PWD-Chr.X.1s	**0.00**	**0.00**	**0.02**		-0.6	**-3.0**
B6.PWD-Chr.X.2	**0.04**	**0.00**	0.25	0.77		**-2.4**
B6.PWD-Chr.X.3	0.31	**0.00**	0.05	**0.00**	**0.00**	

Table 10.1: Differences in meiotic recombination rate comparing PWD and B6.PWD-Chr.X# subconsomic strains with B6. Upper: Difference between average MLH1 count (row - column).Lower: TukeyHSD-adjusted p-values for pairwise comparison of means. Numbers highlighted in red are statistically significant.

p-value / average difference	B6	PWD	PWD x B6	B6 x PWD	B6.PWD-Chr.X.1	B6.PWD-Chr.X.1s	B6.PWD-Chr.X.1 x PWD	B6.PWD-Chr.X.1s x PWD
B6		**-4.3**	0.8	**-2.6**	0.4	**2.0**	**-2.8**	0.4
PWD	**0.00**		**5.1**	**1.7**	**4.7**	**6.3**	**1.5**	**4.7**
PWD x B6	0.49	**0.00**		**-3.4**	-0.4	1.2	**-3.6**	-0.4
B6 x PWD	**0.00**	**0.00**	**0.00**		3.0	**4.6**	-0.2	**3.0**
B6.PWD-Chr.X.1	0.96	**0.00**	0.98	**0.00**		**1.6**	**-3.2**	0.0
B6.PWD-Chr.X.1s	**0.00**	**0.00**	0.09	**0.00**	**0.01**		**-4.8**	**-1.6**
B6.PWD-Chr.X.1 x PWD	**0.00**	**0.02**	**0.00**	1.00	**0.00**	**0.00**		**3.2**
B6.PWD-Chr.X.1s x PWD	0.96	**0.00**	0.98	**0.00**	1.00	**0.01**	**0.00**	

Table 10.2: Differences in meiotic recombination rate comparing PWD and B6.PWD-Chr.X# subconsomic strains and F_1 hybrids with B6. Upper: Difference between average MLH1 count (row - column).Lower: TukeyHSD-adjusted p-values for pairwise comparison of means. Numbers highlighted in red are statistically significant.

Discussion

Hybrid sterility is a universal phenomenon associated with speciation from *Drosophila* to plants. The genetic dissection of the reproductive barriers is a powerful approach for studying reproductive isolation. In recent history, genetics of post-zygotic reproductive isolation has been overwhelmingly studied in *Drosophila* (Sawamura, 1996; Sawamura et al., 1993a; Sawamura et al., 1993b; Ting et al., 1998; Barbash and Ashburner, 2003; Presgraves et al., 2003; Sun et al., 2004b; Brideau et al., 2006; Bayes and Malik, 2009; Ferree and Barbash, 2009; Phadnis and Orr, 2009; Tang and Presgraves, 2009). House mice as a mammalian model provided a powerful system for studying genetics of reproductive isolation. Two major approaches were widely used. The first was focused on well-defined hybrid zone between *Mmm* and *Mmd* stretching across central Europe. It was aimed to understand the genetics of hybrid sterility in natural populations (Boursot et al., 1993; Richard et al., 1993; Dod et al., 1993; Macholan et al., 2007; Payseur et al., 2004; Macholan et al., 2011). The other approach involved, laboratory crosses of *M. m. musculus* , *M. m. molossinus* , *M. m. castaneus* and *M. m. domesticus* inbred strains (Forejt and Ivanyi, 1974; Oka et al., 2004; Storchova et al., 2004; Britton-Davidian et al., 2005; Vyskocilova et al., 2009; Mihola et al., 2009; White et al., 2011; White et al., 2012; Campbell et al., 2012; Dzur-Gejdosova et al., 2012; Good et al., 2008a; Good et al., 2008b). The genetic dissection experiments showed Dobzhansky-Muller (D-M) incompatibilities (Muller and Pontecorvo, 1942; Dobzhansky, 1936) involving multiple genetic loci as the primary cause of postzygotic isolation (Mihola et al., 2009; White et al., 2011; White et al., 2012; Campbell et al., 2012; Dzur-Gejdosova et al., 2012). Strong hybrid sterility loci were observed on Chr X in the above mentioned models. The first hybrid sterility gene identified in mammals, *Prdm9* (Mihola et al., 2009), shows D-M interaction with Chr X and other autosomal loci (Dzur-Gejdosova et al., 2012) in the (PWD x B6)F1 hybrid model. In this study, we present a high resolution map of genes affecting hybrid sterility on Chr X and its possible mechanistic contribution to meiotic chromosome asynapsis and spermatogenic failure.

11.1 Dissecting the genetic architecture of F1 hybrid sterility.

To study the genetic architecture of hybrid sterility, we used inbred strains PWD and B6 representing *M. m. musculus* and *M. m. domesticus* subspecies (see Materials and Methods) and B6.PWD-Chr# chromosome substitution (consomic) strains carrying individual *M. m. musculus*

chromosomes introgressed in the genome of *M. m. domesticus* (Gregorova et al., 2008; Gregorova and Forejt, 2000). By using the results from F1 hybrids between B6.PWD-Chr# consomic strains and PWD mice we estimated the nature of asymmetry of F1 hybrids, the number of hybrid sterility genes, their location in the genome, and their mode of interaction. The role of mitochondrial genome, autosomal imprinted genes, and Chr Y was also evaluated.

The asymmetry of hybrid sterility in (PWD x B6) model could result from D-M incompatibilities involving uniparental inheritance, such as sex chromosomes, imprinted genes, or mitochondrion (Orr et al., 2004; Coyne et al., 2004; Turelli and Moyle, 2007). The analysis of male hybrids between PWD and B6.PWD-Chr # consomics provided direct evidence that asymmetry in male infertility is controlled from the central region of Chr X^{PWD}, excluding the role of the Chr Y, mitochondrial genome, or imprinted autosomal genes. The rescue of intrameiotic arrest by PWD homozygosity of Chr 19 can be interpreted by the presence of a B6 recessive hybrid sterility gene or it can be the effect of a recessive B6 rescue gene, which overcomes meiotic checkpoint but has no active role in the F1 hybrid sterility. The presence of two copies of Chr 17^{PWD} in (PWD × B6.PWD-Chr17)F1 males resulted in full fertility rescue. The effect of PWD/PWD homosomy of individual autosomes on F1 hybrid genetic background revealed underdominance of the Chr 17 hybrid sterility locus. The action of hybrid sterility gene at Chr 17, most probably *Hst1/Prdm9*, was clearly underdominant because both its homozygous forms i.e. PWD/PWD and B6/B6, rescued hybrid sterility associated meiotic arrest when situated on F1 hybrid background or as shown in N2 hybrid males (Dzur-Gejdosova et al., 2012).The Chr 17 and Chr X showed significant association with TW and fertility in a QTL analysis of the backcross (B6 × *M. macedonicus*) F1 ×B10 (Elliott et al., 2004). While the QTL interval on Chr X seems to overlap *Hstx1*, the peak on Chr 17 is distal to *Hst1/Prdm9*. Another QTL analysis of the backcross (PWD x B6)F1 x B6 showed strong interval on Chr X and Chr 17 overlaping *Hstx1* and *Hst1/Prdm9,* respectively (Dzur-Gejdosova et al., 2012).

11.2 Major hybrid sterility locus on the X chromosome.

Involvement of an X-linked *M.m.musculus* allele(s) in hybrid sterility has been described repeatedly in different hybrid sterility models (Storchova et al., 2004; White et al., 2011; Dzur-Gejdosova et al., 2012; Good et al., 2008b). In our present study we found a 4.7 Mb interval by

high resolution mapping X^{PWD} chromosome, which controls two hybrid sterility phenotypes, i.e. abnormality of post-meiotic cells (Storchova et al., 2004) and F1 meiotic block (Mihola et al., 2009). In the experiment using B6.PWD-Chr.X# consomic strains we found that a 4.7 Mb *Hstx1*^{PWD} region on X chromosome manifested the reduced TW and abnormal sperm head morphology phenotype on B6 genetic background. Similar postmeiotic phenotypes were observed in mouse models carrying introgressions of *M. m. musculus*^{PWK} X chromosome on *M. m. domesticus*^{LEWES} background, *M. m. molossinus*^{MSM} X chromosome on *M. m. domesticus*^{B6} background, and *M. m. musculus*^{PWD} X chromosome on *M. m. domesticus*^{B6} background (Oka et al., 2004; Storchova et al., 2004; Good et al., 2008a). All three studies identified multiple QTLs along the X chromosome influencing abnormal sperm head morphology.

The phenotype of F1 hybrid sterility was mostly represented by postmeiotic block (White et al., 2011; White et al., 2012; Good et al., 2008b), which differed from the intrameiotic arrest seen in (PWD × B6)F1 males (Mihola et al., 2009; Dzur-Gejdosova et al., 2012). The F1 male of PWD and B6 showed asymmetry in sterility phenotype that is manifested as meiotic arrest. In the present study, QTL analysis of hybrids resulting from a heterozygous consomic female, B6-$X^{PWD}X^{B6}$, and PWD male revealed an X-linked 4.7 Mb *Hstx2*^{PWD} region controlling the asymmetry in meiotic arrest phenotype. This finding was later confirmed in F1 hybrids of B6.PWD-Chr.X# females and PWD males. We also found that the same 4.7 Mb *Hstx2*^{PWD} region coincides with *Hstx1*^{PWD} location. Recently, Payseur and co-workers (White et al., 2011) analyzed the genetic architecture of hybrid sterility of *M. m. musculus* × *M. m. domesticus* hybrids using F2 crosses of PWD and WSB inbred strains. They found several QTLs on autosomes and X chromosome. Interestingly, another mouse species, *M. spretus*, carries a hybrid sterility gene in the same overlapping region of Chr X as observed in *M. m. musculus* (PWD) and *M. macedonicus* hybrids (Elliott et al., 2001). A mechanistically similar model of F1 hybrid sterility has been described between *Drosophila* species of *D. pseudoobscura* Bogota and *D. pseudoobscura* USA (Prakash, 1972; Orr and Irving, 2001; Phadnis, 2011; Phadnis and Orr, 2009). As in the *M. musculus* subspecies, both *D. pseudoobscura* subspecies diverged quite recently and their reproductive isolation is incomplete. Hybrid sterility is asymmetric, as the male progeny of Bogota females and USA males are sterile, while reciprocal hybrids are fertile in both sexes. QTL analysis distinguished seven hybrid sterility loci with three strong on the Chr X and four autosomal with a weaker effect. The absence of any effect of the Chr Y (Phadnis, 2011;

Phadnis and Orr, 2009) is an additional feature common between our mouse and the *Drosophila* model. The disproportionate effect of Chr X linked genes on hybrid sterility is known as large X-effect from *Drosophila* studies (Orr et al., 2004; Coyne et al., 2004).

11.3 Dobzhansky-Muller (D-M) incompatibilities associated with *Hstx1* and *Hstx2*.

The genetic basis of D-M incompatibilities lies with an epistatic interactions between different loci with alternative alleles. In a hybrid between two populations, this genetic incompatibility between alternative alleles of multiple genes causes a failure to form a functional unit having adverse effects on hybrids. The co-occurrence of two hybrid sterility loci on Chr X promped us to ask whether these two phenotypes could be two manifestations of a single gene based on D-M interaction with other autosomal locus in different genetic backgrounds. The (B6.PWD-Chr X.1s x B6.PWD-Chr 17)F1 hybrids the males do not show pachytene block phenotype but they are sterile due to abnormal sperm suggesting contribution of weak epistasis between different genetic loci in the manifestation of meiotic arrest phenotype. On the other hand the (PWD x WSB)F1 hybrids have partial meiotic block, carry limited number of sperm cells (White et al., 2011), although they carry $Hstx2^{PWD}$. Similarly, (PWD x C3H)F1 males carrying $Hstx2^{PWD}$ partially escape the meiotic arrest phenotype (Flachs et al., 2012). The spermatogenetic abnormality of (PWD x WSB)F1 males were similar to (PWD x C3H)F1 males. C3H and WSB strains are mostly of *Mmd* origin (like B6), but they have different *Prdm9* alleles from that of B6 (Mihola et al., 2009; Parvanov et al., 2010). These experiments showed that the manifestation of meiotic block phenotype is strongly dependent on D-M interactions between $Hstx2^{PWD}$, *Prdm9* and the genetic background. The correlation between genetic heterozygosity of the genetic background with *Prdm9* – Chr X epistatic incompatibility also suggested additional loci of weaker effect as a requirement for the manifestation of F1 hybrid sterility phenotype (Dzur-Gejdosova et al., 2012; Flachs et al., 2012). In *Drosophila*, such D-M interactions were observed in F1 hybrid sterility between *Drosophila pseudoobscura* Bogota and *Drosophila pseudoobscura* USA. The D-M incompatibility could be changed by the replacement of a "sterility" allele by a compatible "fertile" allele at a single gene resulting in the restoration of fertility (Prakash, 1972; Orr and Irving, 2001; Phadnis, 2011; Phadnis and Orr, 2009). Though the discussion concentrated on single locus - single gene approach, the presence of multiple genetic interactions inside the locus or independent genetic control to the two different phenotypes cannot be ruled out. The

postzygotic reproductive isolation between *Mmm* and *Mmd* is more complex, as it includes interactions of underdominant or recessive hybrid sterility genes. We propose that the D-M incompatibility involved in F1 hybrid sterility is like a "jigsaw puzzle" where *Prdm9* and *Hstx1/2* plays the central characters, whereas other complex interactions involving recessive genes and epigenetic modifications control the variable manifestations in phenotypes. Rescue experiments involving bacterial artificial chromosome (BAC) containing fertile alleles will give a clear answer to these questions.

11.4 The role of meiotic chromosome pairing and synapsis in F1 hybrid sterility.

Asynapsis at pachytene stage was the earliest detectable phenotype that we identified in sterile (PWDx B6)F1 males. The involvement of individual autosomes was not random because out of five chromosomes tested, Chr 19 was the most often affected. Moreover we report, for the first time, that heterospecific autosomal pairs in sterile hybrids are more prone to asynapsis than the homospecific pairs where both homologs come from the same species. We also show that this phenotype is strongly linked to 4.7 Mb $Hstx2^{PWD}$ locus on Chr X. Based on these findings we suggest that the failure of pairing and/or synapsis of heterospecific homologs, probably caused by their fast evolving nongenic DNA divergence, may represent the primary target of the meiotic surveillance mechanism that recurrently breaks down in meiosis of various interspecific hybrids. In this scenario the hybrid sterility genes *Prdm9* and the gene(s) on *Hstx2* locus can act, directly or indirectly either to promote or to suppress the less stable pairing of heterospecific homologs. Asynapsis of multiple chromosomes is a fairly common meiotic aberration reported in carriers of various genic and chromosomal mutations. Whenever it occurrs it almost invariably triggers the pachytene checkpoint and meiotic breakdown (Bolcun-Filas and Schimenti, 2012). Unpaired homologs undergo transcriptional silencing of genes within unsynapsed chromatin (MSUC) (Turner et al., 2005) and their occurrence is the sign of death on pachynemas that carry them. The establishment of MSUC was supported by the heterochromatinization of unsynapsed chromosome observed in the present study.

A few studies have focused on pairing of meiotic chromosomes in interspecific hybrids. In sterile F1 hybrids of *Mus spretus* and *Mus m. domesticus* Eicher and coworkers (Hale et al., 1993) observed 70% of pachytene nuclei with autosomal univalency. Crosses of three taxa of caviomorph rodents *Trychomys* resulted in male sterility in all the three F1 hybrid combinations,

two of them showing extensive failure of chromosome pairing at the pachytene stage (Borodin PM, 2006). Massive asynapsis was also observed in sterile males of a hybrid stock arisen from two chromosome taxa of house musk shrew (*Suncus murinus*). The authors concluded that the hybrid sterility is genic rather than of chromosomal type (Borodin et al., 1998). An alternative explanation is that the sterility could be chromosomal, caused by the heterospecific pairing incompatibilities and the reported variation in pairing failure is under genic control. In sterile F1 hybrids between cattle and yak (*Bos taurus x Bos grunniens*) a reduction of spermatogonia signaled premeiotic genic incompatibility nevertheless, synaptic anomalies and pachytene arrest were seen at the meiotic prophase. The female hybrids were fertile (Tumennasan et al., 1997). Finally, hybrids between domestic pig and *Babyrousa babyrussa* were sterile with meiotic pairing failure and pachytene arrest. Both sexes were affected (Thomsen et al., 2011). We are not aware of any report on meiotic pairing in interspecific *Drosophila* hybrids, but several pieces of indirect evidence are in favor of D-M incompatibilities based on nongenic sequence divergence. Naveira and Maside (Maside et al., 1998) reviewed the polygenic character of hybrid sterility in crosses of *Drosophila koepferae* and *D. buzzatti*. They found a correlation between the length of interspecific substitution in backcross male hybrids and sterility; longer segments produced sterility while shorter segments did not (Maside et al., 1998). More recently Moehring (Moehring, 2011) compiled a dataset from ten interspecific backcrosses/F2 intercrosses of various species concluding that the greater the level of chromosome heterospecificity regardless of the marker location, the greater the level of sterility with the allowance for a stronger effect of Chr X (Moehring, 2011). Our recent analysis of the genetic architecture of hybrid sterility in *Mus m. musculus* and *Mus m. domesticus* backcross identified two strong hybrid sterility loci interacting with a set of weak and interchangeable loci, which may represent non-coding sequence incompatibilities (Dzur-Gejdosova et al., 2012). Direct evidence of the role of sequence diversity in hybrid sterility was provided in crosses between two related species of *Saccharomyces*, where hybrid sterility was partially alleviated by deleting mismatch repair proteins (Hunter et al., 1996). We conclude that our current results and the majority of available experimental data from inter-(sub) specific hybrids are compatible with the idea that genetically modulated meiotic asynapsis of heterospecific chromosomes represents a predetermined pathway leading to sterility of the F1 hybrids.

11.5 Meiotic Sex Chromosome Inactivation (MSCI) in intersubspecific hybrids.

Cytological observations of abnormalities of sex body formation in pachytene spermatocytes of mouse intersubspecific hybrids led us to consider the role of sex chromosome inactivation in hybrid sterility (Forejt, 1996; Forejt et al., 2012). Here we show the absence of the classical sex body in the majority of early pachynemas and the entrapment of unsynapsed autosomes in the sex bodies of the surviving mid–late pachynemas. Four Chr X genes and *Zfy2* on Chr Y tested by RNA FISH were not silenced at the pachytene stage, in accord with the genome-wide expression profiling showing the misregulation of the X-linked genes. A similar conclusion was reported in a study of (PWK/PhJ × LEWES/EiJ)F1 hybrids representing *Mus m. musculus* × *Mus m. domesticus* sterility with meiotic arrest after pachytene stage (Good et al., 2010). Alternative evidence for MSCI failure came from our observation of undercondensation and euchromatinization of X-linked chromatin in pachytene cells of sterile hybrids. The mechanism behind the synapsis checkpoint in the case of extensive asynapsis is still unclear (Bolcun-Filas and Schimenti, 2012). The sequestration of ATR kinase and γH2AFX on unsynapsed autosomal chromatin is the cause proposed for the failure of MSCI (Mahadevaiah et al., 2008), but the possibility that the apoptosis of early pachynemas is induced by the activation of the recombination checkpoint by unrepaired DSBs cannot be ruled out. The observed elimination of pachytene spermatocytes of PB6F1 sterile males in two steps of the first meiotic prophase could indicate that more than one checkpoint is activated.

11.6 Oocytes of hybrid females share the aberrant meiotic phenotype with spermatocytes of the sterile male hybrids.

The infertility of hybrids between the members of the *Mus musculus* group and *Mus spretus* follows Haldane's rule, being restricted to the male sex. However, meiosis of female hybrids is far from normal, as first shown in the B6 × *Mus spretus* cross (Hale et al., 1993). Approximately half of the pachytene oocytes from the crosses between PWD and B6 inbred strains displayed multiple asynapsed chromosomes, most of which disappeared before MI. In contrast to the hybrid males of the same genotype, the incidence of oocytes with asynapsis was not changed by the *Prdm9* or *Hstx2* genotype. To conclude, our results show that, although hybrid females obey Haldane's rule, being fertile, they displayed abnormalities of oogenesis that were similar to,

although less extensive than the abnormalities of spermatogenesis in their male siblings. We also report, for the first time, that heterospecific autosomal pairs in female hybrids are more prone to asynapsis than the homospecific pairs where both homologs come from the same species similar to their male counterpart.

Almost half of the pachytene oocytes carried asynaptic chromosomes and disappeared before MI, probably by ATR-directed MSUC checkpoint (Schimenti, 2005). The surviving oocytes still showed some defects, which contributed to the increased frequency of aneuploidy at MII in both types of reciprocal intersubspecific hybrids. Even the oocytes that proceeded through MI were marked by disorganization of chromosomes at the MI plate and low but significant frequency of aneuploidy in MII. The abnormalities seen at the pachytene stage in male and female mouse intersubspecific hybrids thus appear to be the same, their incidence in females being half of that in males. The lower frequency of oocytes with asynapsis and the absence of MSCI offer a plausible explanation of Haldane's rule in this particular hybrid sterility model.

11.7 *Hstx2*^{PWD} homozygous hybrid females defy Muller's dominance theory.

The Haldane's rule states that, in hybrids between two species, if only one of the sexes are inviable or sterile, the affected sex is more likely to be heterogametic (i.e. XY or ZW) than homogametic (Haldane, 1922). Muller's dominance theory offers an explanation for the Haldane's ruleby assuming that majority of alleles affecting hybrid fitness are recessive. In hemizygous sex, the expression of the recessive alleles creates the sterility. However, in homogametic sex the presence of a dominant allele neutralizes the effect of a recessive one. Thus, the homogametic sex with homozygous recessive allele should become sterile as the hemizygous sex. Thus it can explain the large effect of X chromosome observed in genetic analysis of hybrid sterility. We present the first experimental test of the dominance theory in mammals. Constructing *Hstx2*^{PWD} homozygous F1 hybrid females, we showed that the recessive X-linked hybrid sterility locus, which creates sterility in an F1 hybrid male, fails to do so in homozygous condition in hybrid females. The Muller's theory was previously challenged using "unbalanced" hybrid females, expressing the same X-linked recessive alleles as those of the males in two independent hybridization experiments using *Drosophila simulans* - *D. mauritiana* and *D. simulans* - *D. sechellia* (Orr, 1987; 1989; Orr and Coyne, 1989). Hybrid females carrying two *D. simulans* X chromosomes in hybrid genetic background remained fertile. Later, the "unbalanced"

female results were confirmed in at least six independent *Drosophila* hybridization experiments (Orr, 1987; 1989; Orr and Coyne, 1989; Turelli and Orr, 1995). Although the fertility of "unbalanced" hybrid females in *Drosophila* and mouse questions the dominancy theory for hybrid sterility, it does not rule out the explanation of Haldane's rule for inviability as pointed out earlier (Johnson and Wu, 1992; Wu and Davis, 1993). Two *Drosophila* hybridization experiment, between *D. simulans* - *D. tessieri* and *D. melanogaster*- *D. simulans*, revealed that the females homozygous for a recessive X-linked locus in otherwise hybrid background are not viable like hybrid males (Orr, 1993). An alternative explanation for the mouse is that the X–linked recessive genes causing male sterility in hybrids were testes-specific. If so, incompatibility involving these genes could be sensitive to different meiotic check points involving both genetic and epigenetic processes. In summary, our data showed a limitation of the dominance theory explaining mouse hybrid sterility, although further investigation using alternative models is required to reveal its universality.

11.8 Meiotic recombination and F1 hybrid sterility.

Homologous recombination is an important mechanism for creating genetic variation. There is a considerable difference in the rate of meiotic recombination between species (Broman et al., 1998; Sun et al., 2004a; Coop et al., 2008; Koehler et al., 2002; Dumont and Payseur, 2011; Thomsen et al., 2001; Borodin et al., 2008; Ptak et al., 2005; Winckler et al., 2005). It plays an important role in speciation by shuffling the allelic variation of novel genes. Understanding the genetics of meiotic recombination has been a long term desire. Recently, our laboratory identified the first mammalian speciation-associated gene *Prdm9/Hst1* in the (PWD x B6)F1 hybrid model (Mihola et al., 2009). *Prdm9* gene was also shown to determine the preferred recombination sites or hotspots through sequence-specific binding of its highly polymorphic multi-Zn-finger domain in mouse and humans (Parvanov et al., 2010; Baudat et al., 2010; Myers et al., 2010; Cheung et al., 2010; Berg et al., 2010; Grey et al., 2011). Though genes significantly influencing the rate of genome wide recombinations in humans were identified (Kong et al., 2008; Stefansson et al., 2005; Chowdhury et al., 2009), many questions linked to genetic control of the process remain unanswered.

In this thesis we have demonstrated that (PWD x B6)F1 sterile hybrids shows severe depression in meiotic recombination frequency compared to (B6 x PWD) F1 fertile hybrids, concluding the

role of X chromosome on the number of meiotic crossovers. Using the B6.PWD-Chr.X.# sub-consomic strains and F1 hybrids we showed that a genome wide depression in the meiotic crossover was linked with *Hstx1/ Hstx2*^{PWD} locus. The coincidence of two hybrid sterility loci *Prdm9/Hst1* and *Hstx1/ Hstx2* performing dual role in hybrid sterility and meiotic recombination indicates a possible new role of meiotic recombination in speciation. Meanwhile, multiple loci were mapped using CAST/EiJ (*M. m. castaneus*) and PWD (*M. m. musculus*) F2 population contributing to genome- wide recombination rate. A strong QTL was observed on X chromosome controlling the meiotic recombination rate between CAST and PWD (Dumont and Payseur, 2011). The mapped X-linked locus overlaps *Hstx1/Hstx2* locus. A X-linked depression was also observed between (PWD x CAST)F1 hybrids but the authors observed no overt defects in chromosome pairing or synapsis in any hybrid animals (Dumont and Payseur, 2011). These results indicate a clear role of X chromosome in meiotic recombination but its contribution to hybrid sterility may be far more complicated. The rate of recombination is a complex trait dependent on multiple genes (Chinnici, 1971; Kidwell, 1972; Charlesworth and Charlesworth, 1985; Brooks and Marks, 1986). The (PWD x B6)F1 and (PWD x CAST) F1 hybrids show a convergence in depression in the meiotic recombination rate but diverge in sterility phenotype. This ambiguity may be due to different *Prdm9* allele between B6 and CAST, which binds to distinct DNA sequences (Baudat et al., 2010) based on altered zinc finger DNA-binding domains (Persikov et al., 2009) choosing different hotspots.

The *Prdm9* encodes meiotic histone H3 methyltransferase (Hayashi et al., 2005) marking the recombination hotspots (Baudat et al., 2010; Parvanov et al., 2010). Most of the recombination in *Prdm9*$^{-/-}$ is initiated at promoters with H3K4 trimethylation mark (Brick et al., 2012). Like *Prdm9*$^{-/-}$ mice, repair of meiotic double strand breaks (DSBs) in (PWD x B6) F1 males does not proceeds normally in almost 95% of the spermatocytes showing possible random asynapsis and the formation of univalents suggesting a possible failure of meiotic recombination process. Meanwhile, we cannot rule out that the allelic incompatibilities involved are only limited to meiotic recombination rate without causing sterility. The analysis of other genotypes including fertile (PWD × B6.*Hst1*^{f}) F1; (PWD × B6.PWD-chr17) F1 and (PWD × B6.PWD-chr19) F1 hybrids showed similar meiotic crossover frequency to that of (PWD x B6) F1 sterile hybrids pointing to an *Hstx2*^{PWD} linked polymorphism controlling the meiotic recombination rate, rather

than the meiotic arrest. Further analysis of meiotic hotspot using ChIP-seq approach on different mouse strains and their hybrid strains can resolve these issues.

Conclusions

A. The postzygotic reproductive isolation between *Mmm* and *Mmd* is complex, as it includes interactions of underdominant or recessive hybrid sterility genes. Here we mapped *Hstx2* locus to 4.7 Mbp region on Chr.X. The *4933436I01Rik*,'and *Fmr1nb* protein coding genes and *mmu-miR-743a* and *mmu-miR-465* microRNA cluster are likely candidates for *Hstx2*. We propose that the D-M incompatibility involved in F1 hybrid sterility is like a "jigsaw puzzle" where *Prdm9* and *Hstx2* play the central characters, whereas heterozygous (heterospecific) genetic background and epigenetic modifications modulate the manifestations of the phenotypes.

B. Based on our findings, we suggest that meiotic asynapsis of heterospecific homologous chromosomes is the primary mechanistic basis of hybrid sterility manifested by pachytene arrest. According to our hypothesis, the nongenic sequences, as the fastest diverging component of the mammalian genome, may represent the suitable candidate for a recurrent D–M incompatibility leading to asynapsis. The predisposition to asynapsis occurs in both male and female meiosis of intersubspecific hybrids. In spermatogenesis, but not in oogenesis, certain hybrid sterility genes directly or indirectly modulate the sensitivity of synapsis to the sequence divergence between heterospecific chromosomes, either enhancing or suppressing it. MSCI plays a decisive role in eliminating the asynapsed primary spermatocytes and underlies most of the features of the Haldane's rule. However, because hybrid sterility is a consequence of independent genomic evolution in related taxa, other D–M incompatibilities that do not interfere with chromosome synapsis may act together with it or independently of it.

C. Using female F1 hybrids homozygous for $Hstx2^{PWD}$ we showed defyance of a simple interpretation of dominance theory for Haldane's rule. We also demonstrated that contrary to male meiosis, Chr 17 and *Hstx2* do not control frequency of asynaptic pachynemas in female meiosis of intersubspecific hybrids. The proposed explanation for these differences is that the X–linked recessive genes causing male sterility in hybrids were testes-specific.

D. We found a meiotic recombination rate-controlling locus in the same 4.7Mb interval as the *Hstx2* hybrid sterility gene. The coincidence of the loci governing meiotic recombination and hybrid sterility on Chr 17 and Chr X may indicate a new role of meiotic recombination in speciation.

Relevant publication

1. **Bhattacharyya T**, Reifova R, Gregorova S, Simecek P, Mistrik M, Pialek J, Forejt J. "Insight into the Mechanism of Hybrid Sterility and Haldane's Rule in House Mouse."; 2013 **(in communication)**.
2. **Bhattacharyya T**[#], Flachs P[#], Mihola O, Forejt J, Trachtulec Z. "Prdm9 incompatibility causes oligospermia and delayed fertility but no selfish transmission in mouse intersubspecific (PWK x B6)F1 hybrids" 2013 **(**# equal contribution ; **in communication)**.
3. **Bhattacharyya T** , Gregorova S, Mihola O, Anger M, Sebestova J, Denny P, Simecek P, Forejt J. "Mechanistic Basis of infertility of mouse Inter-Subspecific Hybrids", **Proc Natl Acad Sci U S A**. 2013 Feb 5;110 (6):E468-77 **(IF 9.681).**
4. Dzur-Gejdosova M, Simecek P, Gregorova S, **Bhattacharyya T** , Forejt J. "Dissecting the genetic architecture of F1 hybrid sterility in house mice", **Evolution.** 2012 Nov 66: 3321–3335 **(IF 5.146)**

Other publication

1. Shah AM, Tamang R, Moorjani P, Rani DS, Govindaraj P, Kulkarni G, **Bhattacharya T**, Mustak MS, Bhaskar LV, Reddy AG, Gadhvi D, Gai PB, Chaubey G, Patterson N, Reich D, Tyler-Smith C, Singh L, Thangaraj K. "Indian siddis: african descendants with Indian admixture.", **Am J Hum Genet. 2011** Jul 15; 89 (1):154-61**(IF 10.603)**.

Abbreviations

B6.PWD-Chr.# - Chromosome substitution strain (consmics) with introgressed PWD chromosomes on B6 background.

PB6F1- F1 hybrids from cross between PWD female x B6 male.

B6PF1- F1 hybrids from cross between B6 female x PWD male.

PB6-*Hst1*^{f}F1- F1 hybrids from cross between PB6F1 with *Prdm9* fertile allele.

PD17F1- F1 hybrids from cross between PWD female x B6.PWD-Chr.17 male.

PD19F1- F1 hybrids from cross between PWD female x B6.PWD-Chr.19 male.

DX.1sD17F1-F1 hybrids from cross between B6.PWD-Chr.1s female x B6.PWD-Chr.19 male.

C3B6F1- F1 hybrids from cross between C3H female x B6 male.

DX.1sPF1- F1 hybrids from cross between B6.PWD-Chr.1s female x PWD male.

Hstx1- X-linked hybrid sterility gene 1

Hstx2- X-linked hybrid sterility gene 2

Prdm9- PR domain zinc finger protein 9

Hst1^{f}- Hybrid sterility gene 1 fertile allele.

Mb- Megabase pairs.

TUNEL- Terminal deoxynucleotidyl transferase dUTP nick end labeling

SYCP1- Synaptonemal complex protein 1

SYCP3- Synaptonemal complex protein 3

HORMAD2- HORMA domain protein containing 2

γH2AFX- phosphorylated form of H2AFX histone

ATR- ataxia-telangiectasia- and Rad3-related protein

RAD51- RAD51 homolog of S. cerevisiae

DMC1- DMC1 dosage suppressor of mck1 homolog, meiosis-specific homologous recombination

FISH- Fluorescent in-situ hybridization

MSCI- Meiotic sex chromosome inactivation

MLH1- Mismatch repair protein of the MutL family.

References

Alsheimer, M. (2009) The dance floor of meiosis: evolutionary conservation of nuclear envelope attachment and dynamics of meiotic telomeres. Genome Dyn 5:81-93.

Anderson, E.L., Baltus, A.E., Roepers-Gajadien, H.L., Hassold, T.J., de Rooij, D.G., van Pelt, A.M., and Page, D.C. (2008) Stra8 and its inducer, retinoic acid, regulate meiotic initiation in both spermatogenesis and oogenesis in mice. Proc Natl Acad Sci U S A 105:14976-14980.

Anderson, L.K., Reeves, A., Webb, L.M., and Ashley, T. (1999) Distribution of crossing over on mouse synaptonemal complexes using immunofluorescent localization of MLH1 protein. Genetics 151:1569-1579.

Barbash, D.A., and Ashburner, M. (2003) A novel system of fertility rescue in Drosophila hybrids reveals a link between hybrid lethality and female sterility. Genetics 163:217-226.

Barbash, D.A., Roote, J., Johnson, G., and Ashburner, M. (2004) A new hybrid rescue allele in Drosophila melanogaster. Genetica 120:261-266.

Barbash, D.A., Siino, D.F., Tarone, A.M., and Roote, J. (2003) A rapidly evolving MYB-related protein causes species isolation in Drosophila. Proc Natl Acad Sci U S A 100:5302-5307.

Bastos, H., Lassalle, B., Chicheportiche, A., Riou, L., Testart, J., Allemand, I., and Fouchet, P. (2005) Flow cytometric characterization of viable meiotic and postmeiotic cells by Hoechst 33342 in mouse spermatogenesis. Cytometry A 65:40-49.

Baudat, F., Buard, J., Grey, C., Fledel-Alon, A., Ober, C., Przeworski, M., Coop, G., and de Massy, B. (2010) PRDM9 is a major determinant of meiotic recombination hotspots in humans and mice. Science 327:836-840.

Baudat, F., Manova, K., Yuen, J.P., Jasin, M., and Keeney, S. (2000) Chromosome synapsis defects and sexually dimorphic meiotic progression in mice lacking Spo11. Mol Cell 6:989-998.

Bayes, J.J., and Malik, H.S. (2009) Altered heterochromatin binding by a hybrid sterility protein in Drosophila sibling species. Science 326:1538-1541.

Bellani, M.A., Romanienko, P.J., Cairatti, D.A., and Camerini-Otero, R.D. (2005) SPO11 is required for sex-body formation, and Spo11 heterozygosity rescues the prophase arrest of Atm-/- spermatocytes. J Cell Sci 118:3233-3245.

Berg, I.L., Neumann, R., Lam, K.W., Sarbajna, S., Odenthal-Hesse, L., May, C.A., and Jeffreys, A.J. (2010) PRDM9 variation strongly influences recombination hot-spot activity and meiotic instability in humans. Nat Genet 42:859-863.

Besansky, N.J., Krzywinski, J., Lehmann, T., Simard, F., Kern, M., Mukabayire, O., Fontenille, D., Toure, Y., and Sagnon, N. (2003) Semipermeable species boundaries between Anopheles gambiae and Anopheles arabiensis: evidence from multilocus DNA sequence variation. Proc Natl Acad Sci U S A 100:10818-10823.

Bhattacharyya, T., Gregorova, S., Mihola, O., Anger, M., Sebestova, J., Denny, P., Simecek, P., and Forejt, J. (2012) Mechanistic basis of infertility of mouse intersubspecific hybrids. Proc Natl Acad Sci U S A 110:E468-477.

Bhattacharyya, T., Gregorova, S., Mihola, O., Anger, M., Sebestova, J., Denny, P., Simecek, P., and Forejt, J. (2013) Mechanistic basis of infertility of mouse intersubspecific hybrids. Proceedings of the National Academy of Sciences of the United States of America 110:E468-477.

Bishop, J.B., Dellarco, V.L., Hassold, T., Ferguson, L.R., Wyrobek, A.J., and Friedman, J.M. (1996) Aneuploidy in germ cells: etiologies and risk factors. Environ Mol Mutagen 28:159-166.

Bolcun-Filas, E., Costa, Y., Speed, R., Taggart, M., Benavente, R., De Rooij, D.G., and Cooke, H.J. (2007) SYCE2 is required for synaptonemal complex assembly, double strand break repair, and homologous recombination. J Cell Biol 176:741-747.

Bolcun-Filas, E., Hall, E., Speed, R., Taggart, M., Grey, C., de Massy, B., Benavente, R., and Cooke, H.J. (2009) Mutation of the mouse Syce1 gene disrupts synapsis and suggests a link between synaptonemal complex structural components and DNA repair. PLoS Genet 5:e1000393.

Bolcun-Filas, E., and Schimenti, J.C. (2012) Genetics of meiosis and recombination in mice. Int Rev Cell Mol Biol 298:179-227.

Bono, H., Yagi, K., Kasukawa, T., Nikaido, I., Tominaga, N., Miki, R., Mizuno, Y., Tomaru, Y., Goto, H., Nitanda, H., Shimizu, D., Makino, H., Morita, T., Fujiyama, J., Sakai, T., Shimoji, T., Hume, D.A., Hayashizaki, Y., and Okazaki, Y. (2003) Systematic expression profiling of the mouse transcriptome using RIKEN cDNA microarrays. Genome Res 13:1318-1323.

Borodin PM, B.-G.S., Zhelezova AI, Bonvicino CR, D'Andrea PS. (2006) Reproductive isolation due to the genetic incompatibilities between Thrichomys pachyurus and two subspecies of Thrichomys apereoides (Rodentia, Echimyidae).

. Genome. 49(2):159-167.

Borodin, P.M., Karamysheva, T.V., Belonogova, N.M., Torgasheva, A.A., Rubtsov, N.B., and Searle, J.B. (2008) Recombination map of the common shrew, Sorex araneus (Eulipotyphla, Mammalia). Genetics 178:621-632.

Borodin, P.M., Rogatcheva, M.B., Zhelezova, A.I., and Oda, S. (1998) Chromosome pairing in inter-racial hybrids of the house musk shrew (Suncus murinus, Insectivora, Soricidae). Genome 41:79-90.

Boursot, P., Auffray, J.C., Brittondavidian, J., and Bonhomme, F. (1993) The Evolution of House Mice. . Annual Review of Ecology and Systematics 24:119-152.

Boursot, P., Din, W., Anand, R., Darviche, D., Dod, B., VonDeimling, F., Talwar, G.P., and Bonhomme, F. (1996) Origin and radiation of the house mouse: Mitochondrial DNA phylogeny. Journal of Evolutionary Biology 9:391-415.

Bowles, J., Knight, D., Smith, C., Wilhelm, D., Richman, J., Mamiya, S., Yashiro, K., Chawengsaksophak, K., Wilson, M.J., Rossant, J., Hamada, H., and Koopman, P. (2006) Retinoid signaling determines germ cell fate in mice. Science 312:596-600.

Bowles, J., and Koopman, P. (2007) Retinoic acid, meiosis and germ cell fate in mammals. Development 134:3401-3411.

Brick, K., Smagulova, F., Khil, P., Camerini-Otero, R.D., and Petukhova, G.V. (2012) Genetic recombination is directed away from functional genomic elements in mice. Nature 485:642-645.

Brideau, N.J., Flores, H.A., Wang, J., Maheshwari, S., Wang, X., and Barbash, D.A. (2006) Two Dobzhansky-Muller genes interact to cause hybrid lethality in Drosophila. Science 314:1292-1295.

Britton-Davidian, J., Catalan, J., da Graca Ramalhinho, M., Auffray, J.C., Claudia Nunes, A., Gazave, E., Searle, J.B., and da Luz Mathias, M. (2005) Chromosomal phylogeny of Robertsonian races of the house mouse on the island of Madeira: testing between alternative mutational processes. Genet Res 86:171-183.

Broman, K.W. (2003) Mapping quantitative trait loci in the case of a spike in the phenotype distribution. Genetics 163:1169-1175.
Broman, K.W., Murray, J.C., Sheffield, V.C., White, R.L., and Weber, J.L. (1998) Comprehensive human genetic maps: individual and sex-specific variation in recombination. Am J Hum Genet 63:861-869.
Brooks, L.D., and Marks, R.W. (1986) The organization of genetic variation for recombination in Drosophila melanogaster. Genetics 114:525-547.
Bult, C.J., Eppig, J.T., Kadin, J.A., Richardson, J.E., and Blake, J.A. (2008) The Mouse Genome Database (MGD): mouse biology and model systems. Nucleic Acids Res 36:D724-728.
Burgoyne, P.S., Mahadevaiah, S.K., and Turner, J.M. (2009) The consequences of asynapsis for mammalian meiosis. Nature reviews 10:207-216.
Campbell, P., Good, J.M., Dean, M.D., Tucker, P.K., and Nachman, M.W. (2012) The contribution of the Y chromosome to hybrid male sterility in house mice. Genetics 191:1271-1281.
Coop, G., Wen, X., Ober, C., Pritchard, J.K., and Przeworski, M. (2008) High-resolution mapping of crossovers reveals extensive variation in fine-scale recombination patterns among humans. Science 319:1395-1398.
Costa, Y., and Cooke, H.J. (2007) Dissecting the mammalian synaptonemal complex using targeted mutations. Chromosome Res 15:579-589.
Coyne, J.A. (1989) Genetics of sexual isolation between two sibling species, Drosophila simulans and Drosophila mauritiana. Proc Natl Acad Sci U S A 86:5464-5468.
Coyne, J.A. (1992) Genetics of sexual isolation in females of the Drosophila simulans species complex. Genet Res 60:25-31.
Coyne, J.A., Elwyn, S., Kim, S.Y., and Llopart, A. (2004) Genetic studies of two sister species in the Drosophila melanogaster subgroup, D. yakuba and D. santomea. Genet Res 84:11-26.
Coyne, J.A., Kim, S.Y., Chang, A.S., Lachaise, D., and Elwyn, S. (2002) Sexual isolation between two sibling species with overlapping ranges: Drosophila santomea and Drosophila yakuba. Evolution 56:2424-2434.
Coyne, J.A., and Orr, H.A. (2004) Speciation. Sinauer Associates, Inc., Sunderland, Massachusetts U.S.A.
Dallerac, R., Labeur, C., Jallon, J.M., Knipple, D.C., Roelofs, W.L., and Wicker-Thomas, C. (2000) A delta 9 desaturase gene with a different substrate specificity is responsible for the cuticular diene hydrocarbon polymorphism in Drosophila melanogaster. Proc Natl Acad Sci U S A 97:9449-9454.
de Vries, F.A., de Boer, E., van den Bosch, M., Baarends, W.M., Ooms, M., Yuan, L., Liu, J.G., van Zeeland, A.A., Heyting, C., and Pastink, A. (2005) Mouse Sycp1 functions in synaptonemal complex assembly, meiotic recombination, and XY body formation. Genes Dev 19:1376-1389.
Dietrich, A.J., and Mulder, R.J. (1983) A light- and electron microscopic analysis of meiotic prophase in female mice. Chromosoma 88:377-385.
Dietrich, W.F., Miller, J., Steen, R., Merchant, M.A., Damron-Boles, D., Husain, Z., Dredge, R., Daly, M.J., Ingalls, K.A., and O'Connor, T.J. (1996) A comprehensive genetic map of the mouse genome. Nature 380:149-152.
Ding, X., Xu, R., Yu, J., Xu, T., Zhuang, Y., and Han, M. (2007) SUN1 is required for telomere attachment to nuclear envelope and gametogenesis in mice. Dev Cell 12:863-872.
Dobzhansky, T. (1936) Studies on Hybrid Sterility. II. Localization of Sterility Factors in Drosophila Pseudoobscura Hybrids. Genetics 21:113-135.

Dobzhansky, T. (1937) Further Data on the Variation of the Y Chromosome in Drosophila Pseudoobscura. Genetics 22:340-346.
Dobzhansky, T. (1951) Experiments on Sexual Isolation in Drosophila: X. Reproductive Isolation Between Drosophila Pseudoobscura and Drosophila Persimilis Under Natural and Under Laboratory Conditions. Proc Natl Acad Sci U S A 37:792-796.
Dod, B., Jermiin, L.S., Boursot, P., Chapman, V.H., Nielsen, J.T., and Bonhomme, F. (1993) Counterselection on Sex-Chromosomes in the Mus-Musculus European Hybrid Zone. Journal of Evolutionary Biology 6:529-546.
Dumont, B.L., and Payseur, B.A. (2011) Genetic analysis of genome-scale recombination rate evolution in house mice. PLoS Genet 7:e1002116.
Dzur-Gejdosova, M., Simecek, P., Gregorova, S., Bhattacharyya, T., and Forejt, J. (2012) Dissecting the genetic architecture of F1 hybrid sterility in house mice. Evolution 66:3321-3335.
Edelmann, W., Cohen, P.E., Kane, M., Lau, K., Morrow, B., Bennett, S., Umar, A., Kunkel, T., Cattoretti, G., Chaganti, R., Pollard, J.W., Kolodner, R.D., and Kucherlapati, R. (1996) Meiotic pachytene arrest in MLH1-deficient mice. Cell 85:1125-1134.
Eijpe, M., Offenberg, H., Jessberger, R., Revenkova, E., and Heyting, C. (2003) Meiotic cohesin REC8 marks the axial elements of rat synaptonemal complexes before cohesins SMC1beta and SMC3. J Cell Biol 160:657-670.
Elliott, R.W., Miller, D.R., Pearsall, R.S., Hohman, C., Zhang, Y., Poslinski, D., Tabaczynski, D.A., and Chapman, V.M. (2001) Genetic analysis of testis weight and fertility in an interspecies hybrid congenic strain for Chromosome X. Mamm Genome 12:45-51.
Elliott, R.W., Poslinski, D., Tabaczynski, D., Hohman, C., and Pazik, J. (2004) Loci affecting male fertility in hybrids between Mus macedonicus and C57BL/6. Mamm Genome 15:704-710.
Ferree, P.M., and Barbash, D.A. (2009) Species-specific heterochromatin prevents mitotic chromosome segregation to cause hybrid lethality in Drosophila. PLoS Biol 7:e1000234.
Flachs, P., Mihola, O., Simecek, P., Gregorova, S., Schimenti, J.C., Matsui, Y., Baudat, F., de Massy, B., Pialek, J., Forejt, J., and Trachtulec, Z. (2012) Interallelic and intergenic incompatibilities of the Prdm9 (Hst1) gene in mouse hybrid sterility. PLoS Genet 8:e1003044.
Forejt, J. (1984) X-inactivation and its role in male sterility. In: Bennett, M., Gropp, A., and Wolf, U. (eds) Chromosomes Today. Geroge Allen and Unwin, London, pp. 117-127.
Forejt, J. (1985) Chromosomal and genic sterility of hybrid type in mice and men. Exp Clin Immunogenet 2:106-119.
Forejt, J. (1996) Hybrid sterility in the mouse. Trends Genet 12:412-417.
Forejt, J., Gregorova, S., and Goetz, P. (1981) XY pair associates with the synaptonemal complex of autosomal male-sterile translocations in pachytene spermatocytes of the mouse (Mus musculus). Chromosoma 82:41-53.
Forejt, J., and Ivanyi, P. (1974) Genetic studies on male sterility of hybrids between laboratory and wild mice (Mus musculus L.). Genet Res 24:189-206.
Forejt, J., Pialek, J., and Trachtulec, Z. (2012) Hybrid male sterility genes in the mouse subspecific crosses.
. In: Macholan M, B.S., Muclinger P, Pialek J (ed) Evolution of the House Mouse
Cambridge Univ Press, Cambridge, UK.

Forejt, J., Vincek, V., Klein, J., Lehrach, H., and Loudova-Mickova, M. (1991) Genetic mapping of the t-complex region on mouse chromosome 17 including the Hybrid sterility-1 gene. Mamm Genome 1:84-91.

Fukuda, T., Daniel, K., Wojtasz, L., Toth, A., and Hoog, C. (2010) A novel mammalian HORMA domain-containing protein, HORMAD1, preferentially associates with unsynapsed meiotic chromosomes. Exp Cell Res 316:158-171.

Gentleman, R.C., Carey, V.J., Bates, D.M., Bolstad, B., Dettling, M., Dudoit, S., Ellis, B., Gautier, L., Ge, Y., Gentry, J., Hornik, K., Hothorn, T., Huber, W., Iacus, S., Irizarry, R., Leisch, F., Li, C., Maechler, M., Rossini, A.J., Sawitzki, G., Smith, C., Smyth, G., Tierney, L., Yang, J.Y., and Zhang, J. (2004) Bioconductor: open software development for computational biology and bioinformatics. Genome biology 5:R80.

Geraldes, A., Basset, P., Gibson, B., Smith, K.L., Harr, B., Yu, H.T., Bulatova, N., Ziv, Y., and Nachman, M.W. (2008) Inferring the history of speciation in house mice from autosomal, X-linked, Y-linked and mitochondrial genes. Mol Ecol 17:5349-5363.

Good, J.M., Dean, M.D., and Nachman, M.W. (2008a) A complex genetic basis to X-linked hybrid male sterility between two species of house mice. Genetics 179:2213-2228.

Good, J.M., Giger, T., Dean, M.D., and Nachman, M.W. (2010) Widespread over-expression of the X chromosome in sterile F(1)hybrid mice. PLoS Genet 6.

Good, J.M., Handel, M.A., and Nachman, M.W. (2008b) Asymmetry and polymorphism of hybrid male sterility during the early stages of speciation in house mice. Evolution 62:50-65.

Gregorova, S., Divina, P., Storchova, R., Trachtulec, Z., Fotopulosova, V., Svenson, K.L., Donahue, L.R., Paigen, B., and Forejt, J. (2008) Mouse consomic strains: exploiting genetic divergence between Mus m. musculus and Mus m. domesticus subspecies. Genome Res 18:509-515.

Gregorova, S., and Forejt, J. (2000) PWD/Ph and PWK/Ph inbred mouse strains of Mus m. musculus subspecies--a valuable resource of phenotypic variations and genomic polymorphisms. Folia Biol (Praha) 46:31-41.

Gregorova, S., Mnukova-Fajdelova, M., Trachtulec, Z., Capkova, J., Loudova, M., Hoglund, M., Hamvas, R., Lehrach, H., Vincek, V., Klein, J., and Forejt, J. (1996) Sub-milliMorgan map of the proximal part of mouse Chromosome 17 including the hybrid sterility 1 gene. Mamm Genome 7:107-113.

Grey, C., Barthes, P., Chauveau-Le Friec, G., Langa, F., Baudat, F., and de Massy, B. (2011) Mouse PRDM9 DNA-binding specificity determines sites of histone H3 lysine 4 trimethylation for initiation of meiotic recombination. PLoS Biol 9:e1001176.

Haldane, J.B.S. (1922) Sex ratio and unisexual sterility in animal hybrids. . Journal of Genetics 12:101-109.

Hale, D.W., Washburn, L.L., and Eicher, E.M. (1993) Meiotic abnormalities in hybrid mice of the C57BL/6J x Mus spretus cross suggest a cytogenetic basis for Haldane's rule of hybrid sterility. Cytogenet Cell Genet 63:221-234.

Hamer, G., Gell, K., Kouznetsova, A., Novak, I., Benavente, R., and Hoog, C. (2006) Characterization of a novel meiosis-specific protein within the central element of the synaptonemal complex. J Cell Sci 119:4025-4032.

Hamer, G., Wang, H., Bolcun-Filas, E., Cooke, H.J., Benavente, R., and Hoog, C. (2008) Progression of meiotic recombination requires structural maturation of the central element of the synaptonemal complex. J Cell Sci 121:2445-2451.

Handel, M.A., and Schimenti, J.C. (2010) Genetics of mammalian meiosis: regulation, dynamics and impact on fertility. Nat Rev Genet 11:124-136.
Harrison, R.G. (1990) Hybrid zones - windows on evolutionary process. Oxf. Surv. Evol. Biol 7, pp. 69-128.
Hayashi, K., Yoshida, K., and Matsui, Y. (2005) A histone H3 methyltransferase controls epigenetic events required for meiotic prophase. Nature 438:374-378.
Hochwagen, A., and Amon, A. (2006) Checking your breaks: surveillance mechanisms of meiotic recombination. Curr Biol 16:R217-228.
Holloway, J.K., Booth, J., Edelmann, W., McGowan, C.H., and Cohen, P.E. (2008) MUS81 generates a subset of MLH1-MLH3-independent crossovers in mammalian meiosis. PLoS Genet 4:e1000186.
Homolka, D., Ivanek, R., Capkova, J., Jansa, P., and Forejt, J. (2007) Chromosomal rearrangement interferes with meiotic X chromosome inactivation. Genome Res 17:1431-1437.
Homolka, D., Jansa, P., and Forejt, J. (2011) Genetically enhanced asynapsis of autosomal chromatin promotes transcriptional dysregulation and meiotic failure. Chromosoma 121:91-104.
Hunter, N., Chambers, S.R., Louis, E.J., and Borts, R.H. (1996) The mismatch repair system contributes to meiotic sterility in an interspecific yeast hybrid. EMBO J 15:1726-1733.
Chalmel, F., Rolland, A.D., Niederhauser-Wiederkehr, C., Chung, S.S., Demougin, P., Gattiker, A., Moore, J., Patard, J.J., Wolgemuth, D.J., Jegou, B., and Primig, M. (2007) The conserved transcriptome in human and rodent male gametogenesis. Proceedings of the National Academy of Sciences of the United States of America 104:8346-8351.
Charlesworth, B., and Charlesworth, D. (1985) Genetic variation in recombination in Drosophila. I. Responses to selection and preliminary genetic analysis. Heredity 54:71–83.
Charlesworth, D., Schemske, D.W., and Sork, V.L. (1987) The evolution of plant reproductive characters; sexual versus natural selection. Experientia Suppl 55:317-335.
Cheung, V.G., Sherman, S.L., and Feingold, E. (2010) Genetics. Genetic control of hotspots. Science 327:791-792.
Chi, Y.H., Cheng, L.I., Myers, T., Ward, J.M., Williams, E., Su, Q., Faucette, L., Wang, J.Y., and Jeang, K.T. (2009) Requirement for Sun1 in the expression of meiotic reproductive genes and piRNA. Development 136:965-973.
Chinnici, J.P. (1971) Modification of recombination frequency in Drosophila. II. The polygenic control of crossing over. Genetics 69:85-96.
Chowdhury, R., Bois, P.R., Feingold, E., Sherman, S.L., and Cheung, V.G. (2009) Genetic analysis of variation in human meiotic recombination. PLoS Genet 5:e1000648.
Inselman, A., Eaker, S., and Handel, M.A. (2003) Temporal expression of cell cycle-related proteins during spermatogenesis: establishing a timeline for onset of the meiotic divisions. Cytogenet Genome Res 103:277-284.
Ivanyi, P., Demant, P., Vojtiskova, M., and Ivanyi, D. (1969) Histocompatibility antigens in wild mice (Mus musculus). Transplant Proc 1:365-367.
Jansa, P., Divina, P., and Forejt, J. (2005) Construction and characterization of a genomic BAC library for the Mus m. musculus mouse subspecies (PWD/Ph inbred strain). BMC Genomics 6:161.
Johnson, N.A., and Wu, C.I. (1992) An empirical test of the meiotic drive models of hybrid sterility: sex-ratio data from hybrids between Drosophila simulans and Drosophila sechellia. Genetics 130:507-511.

Kassir, Y., Adir, N., Boger-Nadjar, E., Raviv, N.G., Rubin-Bejerano, I., Sagee, S., and Shenhar, G. (2003) Transcriptional regulation of meiosis in budding yeast. Int Rev Cytol 224:111-171.

Kassir, Y., Granot, D., and Simchen, G. (1988) IME1, a positive regulator gene of meiosis in S. cerevisiae. Cell 52:853-862.

Kauppi, L., Barchi, M., Baudat, F., Romanienko, P.J., Keeney, S., and Jasin, M. (2011) Distinct properties of the XY pseudoautosomal region crucial for male meiosis. Science 331:916-920.

Keane, T.M., Goodstadt, L., Danecek, P., White, M.A., Wong, K., Yalcin, B., Heger, A., Agam, A., Slater, G., Goodson, M., Furlotte, N.A., Eskin, E., Nellaker, C., Whitley, H., Cleak, J., Janowitz, D., Hernandez-Pliego, P., Edwards, A., Belgard, T.G., Oliver, P.L., McIntyre, R.E., Bhomra, A., Nicod, J., Gan, X., Yuan, W., van der Weyden, L., Steward, C.A., Bala, S., Stalker, J., Mott, R., Durbin, R., Jackson, I.J., Czechanski, A., Guerra-Assuncao, J.A., Donahue, L.R., Reinholdt, L.G., Payseur, B.A., Ponting, C.P., Birney, E., Flint, J., and Adams, D.J. (2011) Mouse genomic variation and its effect on phenotypes and gene regulation. Nature 477:289-294.

Kidwell, M.G. (1972) Genetic change of recombination value in Drosophila melanogaster. I. Artificial selection for high and low recombination and some properties of recombination-modifying genes. Genetics 70:419-432.

Koehler, K.E., Cherry, J.P., Lynn, A., Hunt, P.A., and Hassold, T.J. (2002) Genetic control of mammalian meiotic recombination. I. Variation in exchange frequencies among males from inbred mouse strains. Genetics 162:297-306.

Kogo, H., Tsutsumi, M., Inagaki, H., Ohye, T., Kiyonari, H., and Kurahashi, H. (2012) HORMAD2 is essential for synapsis surveillance during meiotic prophase via the recruitment of ATR activity. Genes Cells 17:897-912.

Kolas, N.K., Yuan, L., Hoog, C., Heng, H.H., Marcon, E., and Moens, P.B. (2004) Male mouse meiotic chromosome cores deficient in structural proteins SYCP3 and SYCP2 align by homology but fail to synapse and have possible impaired specificity of chromatin loop attachment. Cytogenet Genome Res 105:182-188.

Kong, A., Thorleifsson, G., Stefansson, H., Masson, G., Helgason, A., Gudbjartsson, D.F., Jonsdottir, G.M., Gudjonsson, S.A., Sverrisson, S., Thorlacius, T., Jonasdottir, A., Hardarson, G.A., Palsson, S.T., Frigge, M.L., Gulcher, J.R., Thorsteinsdottir, U., and Stefansson, K. (2008) Sequence variants in the RNF212 gene associate with genome-wide recombination rate. Science 319:1398-1401.

Koubova, J., Menke, D.B., Zhou, Q., Capel, B., Griswold, M.D., and Page, D.C. (2006) Retinoic acid regulates sex-specific timing of meiotic initiation in mice. Proc Natl Acad Sci U S A 103:2474-2479.

Kouznetsova, A., Lister, L., Nordenskjold, M., Herbert, M., and Hoog, C. (2007) Bi-orientation of achiasmatic chromosomes in meiosis I oocytes contributes to aneuploidy in mice. Nature genetics 39:966-968.

Kouznetsova, A., Wang, H., Bellani, M., Camerini-Otero, R.D., Jessberger, R., and Hoog, C. (2009) BRCA1-mediated chromatin silencing is limited to oocytes with a small number of asynapsed chromosomes. J Cell Sci 122:2446-2452.

Kurahashi, H., Tsutsumi, M., Nishiyama, S., Kogo, H., Inagaki, H., and Ohye, T. (2012) Molecular basis of maternal age-related increase in oocyte aneuploidy. Congenit Anom (Kyoto) 52:8-15.

Libby, B.J., De La Fuente, R., O'Brien, M.J., Wigglesworth, K., Cobb, J., Inselman, A., Eaker, S., Handel, M.A., Eppig, J.J., and Schimenti, J.C. (2002) The mouse meiotic mutation mei1 disrupts chromosome synapsis with sexually dimorphic consequences for meiotic progression. Dev Biol 242:174-187.

Lin, Y., Gill, M.E., Koubova, J., and Page, D.C. (2008) Germ cell-intrinsic and -extrinsic factors govern meiotic initiation in mouse embryos. Science 322:1685-1687.

Liu, L., Franco, S., Spyropoulos, B., Moens, P.B., Blasco, M.A., and Keefe, D.L. (2004) Irregular telomeres impair meiotic synapsis and recombination in mice. Proc Natl Acad Sci U S A 101:6496-6501.

Lu, X., Shapiro, J.A., Ting, C.T., Li, Y., Li, C., Xu, J., Huang, H., Cheng, Y.J., Greenberg, A.J., Li, S.H., Wu, M.L., Shen, Y., and Wu, C.I. (2010) Genome-wide misexpression of X-linked versus autosomal genes associated with hybrid male sterility. Genome Res 20:1097-1102.

Mahadevaiah, S.K., Bourc'his, D., de Rooij, D.G., Bestor, T.H., Turner, J.M., and Burgoyne, P.S. (2008) Extensive meiotic asynapsis in mice antagonises meiotic silencing of unsynapsed chromatin and consequently disrupts meiotic sex chromosome inactivation. J Cell Biol 182:263-276.

Mahadevaiah, S.K., Costa, Y., and Turner, J.M. (2009) Using RNA FISH to study gene expression during mammalian meiosis. Methods Mol Biol 558:433-444.

Mahadevaiah, S.K., Turner, J.M., Baudat, F., Rogakou, E.P., de Boer, P., Blanco-Rodriguez, J., Jasin, M., Keeney, S., Bonner, W.M., and Burgoyne, P.S. (2001) Recombinational DNA double-strand breaks in mice precede synapsis. Nat Genet 27:271-276.

Maheshwari, S., and Barbash, D.A. (2011) The genetics of hybrid incompatibilities. Annu Rev Genet 45:331-355.

Maheshwari, S., Wang, J., and Barbash, D.A. (2008) Recurrent positive selection of the Drosophila hybrid incompatibility gene Hmr. Mol Biol Evol 25:2421-2430.

Macholan, M., Baird, S.J., Dufkova, P., Munclinger, P., Bimova, B.V., and Pialek, J. (2011) Assessing multilocus introgression patterns: a case study on the mouse X chromosome in central Europe. Evolution 65:1428-1446.

Macholan, M., Baird, S.J., Munclinger, P., Dufkova, P., Bimova, B., and Pialek, J. (2008) Genetic conflict outweighs heterogametic incompatibility in the mouse hybrid zone? BMC Evol Biol 8:271.

Macholan, M., Munclinger, P., Sugerkova, M., Dufkova, P., Bimova, B., Bozikova, E., Zima, J., and Pialek, J. (2007) Genetic analysis of autosomal and X-linked markers across a mouse hybrid zone. Evolution 61:746-771.

Maside, X.R., Barral, J.P., and Naveira, H.F. (1998) Hidden effects of X chromosome introgressions on spermatogenesis in Drosophila simulans x D. mauritiana hybrids unveiled by interactions among minor genetic factors. Genetics 150:745-754.

Masly, J.P., Jones, C.D., Noor, M.A., Locke, J., and Orr, H.A. (2006) Gene transposition as a cause of hybrid sterility in Drosophila. Science 313:1448-1450.

Masly, J.P., and Presgraves, D.C. (2007) High-resolution genome-wide dissection of the two rules of speciation in Drosophila. PLoS Biol 5:e243.

Mayr, E. (1963) Animal Species and Evolution. Harvard University Press, Cambridge.

McKee, B.D., and Handel, M.A. (1993) Sex chromosomes, recombination, and chromatin conformation. Chromosoma 102:71-80.

Mihola, O., Forejt, J., and Trachtulec, Z. (2007) Conserved alternative and antisense transcripts at the programmed cell death 2 locus. BMC Genomics 8:20.

Mihola, O., Trachtulec, Z., Vlcek, C., Schimenti, J.C., and Forejt, J. (2009) A mouse speciation gene encodes a meiotic histone H3 methyltransferase. Science 323:373-375.

Moehring, A.J. (2011) Heterozygosity and its unexpected correlations with hybrid sterility. Evolution 65:2621-2630.

Moehring, A.J., Llopart, A., Elwyn, S., Coyne, J.A., and Mackay, T.F. (2006) The genetic basis of postzygotic reproductive isolation between Drosophila santomea and D. yakuba due to hybrid male sterility. Genetics 173:225-233.

Muller, H., and Pontecorvo, G. (1942) Recessive genes causing interspecific sterility and other disharmonies between Drosophila melanogaster and simulans. Genetics 27(1):157.

Muller, H.J. (1940) Bearing of the Drosophila work on systematics. The New Systematics. Clarendon, Oxford.

Myers, S., Bowden, R., Tumian, A., Bontrop, R.E., Freeman, C., MacFie, T.S., McVean, G., and Donnelly, P. (2010) Drive against hotspot motifs in primates implicates the PRDM9 gene in meiotic recombination. Science 327:876-879.

Nagaoka, S.I., Hodges, C.A., Albertini, D.F., and Hunt, P.A. (2011) Oocyte-specific differences in cell-cycle control create an innate susceptibility to meiotic errors. Curr Biol 21:651-657.

Oka, A., Aoto, T., Totsuka, Y., Takahashi, R., Ueda, M., Mita, A., Sakurai-Yamatani, N., Yamamoto, H., Kuriki, S., Takagi, N., Moriwaki, K., and Shiroishi, T. (2007) Disruption of genetic interaction between two autosomal regions and the X chromosome causes reproductive isolation between mouse strains derived from different subspecies. Genetics 175:185-197.

Oka, A., Mita, A., Sakurai-Yamatani, N., Yamamoto, H., Takagi, N., Takano-Shimizu, T., Toshimori, K., Moriwaki, K., and Shiroishi, T. (2004) Hybrid breakdown caused by substitution of the X chromosome between two mouse subspecies. Genetics 166:913-924.

Oka, A., Mita, A., Takada, Y., Koseki, H., and Shiroishi, T. (2010) Reproductive isolation in hybrid mice due to spermatogenesis defects at three meiotic stages. Genetics 186:339-351.

Orr, H.A. (1987) Genetics of male and female sterility in hybrids of Drosophila pseudoobscura and D. persimilis. Genetics 116:555-563.

Orr, H.A. (1989) Localization of genes causing postzygotic isolation in two hybridizations involving Drosophila pseudoobscura. Heredity (Edinb) 63 (Pt 2):231-237.

Orr, H.A. (1993) Haldane's rule has multiple genetic causes. Nature 361:532-533.

Orr, H.A., and Coyne, J.A. (1989) The genetics of postzygotic isolation in the Drosophila virilis group. Genetics 121:527-537.

Orr, H.A., and Irving, S. (2001) Complex epistasis and the genetic basis of hybrid sterility in the Drosophila pseudoobscura Bogota-USA hybridization. Genetics 158:1089-1100.

Orr, H.A., Masly, J.P., and Presgraves, D.C. (2004) Speciation genes. Curr Opin Genet Dev 14:675-679.

Orr, H.A., and Presgraves, D.C. (2000) Speciation by postzygotic isolation: forces, genes and molecules. Bioessays 22:1085-1094.

Otubanjo, O.A., Mosuro, A.A., and Ladipo, T.F. (2007) An in vivo evaluation of induction of abnormal sperm morphology by ivermectin MSD (Mectizan). Pak J Biol Sci 10:90-95.

Paigen, K., Szatkiewicz, J.P., Sawyer, K., Leahy, N., Parvanov, E.D., Ng, S.H., Graber, J.H., Broman, K.W., and Petkov, P.M. (2008) The recombinational anatomy of a mouse chromosome. PLoS Genet 4:e1000119.

Parvanov, E.D., Petkov, P.M., and Paigen, K. (2010) Prdm9 controls activation of mammalian recombination hotspots. Science 327:835.

Payseur, B.A., Krenz, J.G., and Nachman, M.W. (2004) Differential patterns of introgression across the X chromosome in a hybrid zone between two species of house mice. Evolution 58:2064-2078.

Pelttari, J., Hoja, M.R., Yuan, L., Liu, J.G., Brundell, E., Moens, P., Santucci-Darmanin, S., Jessberger, R., Barbero, J.L., Heyting, C., and Hoog, C. (2001) A meiotic chromosomal core consisting of cohesin complex proteins recruits DNA recombination proteins and promotes synapsis in the absence of an axial element in mammalian meiotic cells. Mol Cell Biol 21:5667-5677.

Persikov, A.V., Osada, R., and Singh, M. (2009) Predicting DNA recognition by Cys2His2 zinc finger proteins. Bioinformatics 25:22-29.

Phadnis, N. (2011) Genetic architecture of male sterility and segregation distortion in Drosophila pseudoobscura Bogota-USA hybrids. Genetics 189:1001-1009.

Phadnis, N., and Orr, H.A. (2009) A single gene causes both male sterility and segregation distortion in Drosophila hybrids. Science 323:376-379.

Pialek, J., Vyskocilova, M., Bimova, B., Havelkova, D., Pialkova, J., Dufkova, P., Bencova, V., Dureje, L., Albrecht, T., Hauffe, H.C., Macholan, M., Munclinger, P., Storchova, R., Zajicova, A., Holan, V., Gregorova, S., and Forejt, J. (2008) Development of unique house mouse resources suitable for evolutionary studies of speciation. The Journal of heredity 99:34-44.

Plug, A.W., Peters, A.H., Keegan, K.S., Hoekstra, M.F., de Boer, P., and Ashley, T. (1998) Changes in protein composition of meiotic nodules during mammalian meiosis. J Cell Sci 111 (Pt 4):413-423.

Prakash, S. (1972) Origin of reproductive isolation in the absence of apparent genic differentiation in a geographic isolate of Drosophila pseudoobscura. Genetics 72:143-155.

Presgraves, D.C. (2008) Sex chromosomes and speciation in Drosophila. Trends Genet 24:336-343.

Presgraves, D.C., Balagopalan, L., Abmayr, S.M., and Orr, H.A. (2003) Adaptive evolution drives divergence of a hybrid inviability gene between two species of Drosophila. Nature 423:715-719.

Presgraves, D.C., and Orr, H.A. (1998) Haldane's rule in taxa lacking a hemizygous X. Science 282:952-954.

Prieto, I., Suja, J.A., Pezzi, N., Kremer, L., Martinez, A.C., Rufas, J.S., and Barbero, J.L. (2001) Mammalian STAG3 is a cohesin specific to sister chromatid arms in meiosis I. Nat Cell Biol 3:761-766.

Ptak, S.E., Hinds, D.A., Koehler, K., Nickel, B., Patil, N., Ballinger, D.G., Przeworski, M., Frazer, K.A., and Paabo, S. (2005) Fine-scale recombination patterns differ between chimpanzees and humans. Nat Genet 37:429-434.

Reed, L.K., LaFlamme, B.A., and Markow, T.A. (2008) Genetic architecture of hybrid male sterility in Drosophila: analysis of intraspecies variation for interspecies isolation. PLoS One 3:e3076.

Revenkova, E., Eijpe, M., Heyting, C., Gross, B., and Jessberger, R. (2001) Novel meiosis-specific isoform of mammalian SMC1. Mol Cell Biol 21:6984-6998.

Revenkova, E., Eijpe, M., Heyting, C., Hodges, C.A., Hunt, P.A., Liebe, B., Scherthan, H., and Jessberger, R. (2004) Cohesin SMC1 beta is required for meiotic chromosome dynamics, sister chromatid cohesion and DNA recombination. Nat Cell Biol 6:555-562.

Richard, D.S., William, R.A., and Ernesto, C. (1993) House Mice as Models in Systematic Biology. Syst Biol 42 (4).

Romanienko, P.J., and Camerini-Otero, R.D. (2000) The mouse Spo11 gene is required for meiotic chromosome synapsis. Mol Cell 6:975-987.

Royo, H., Polikiewicz, G., Mahadevaiah, S.K., Prosser, H., Mitchell, M., Bradley, A., de Rooij, D.G., Burgoyne, P.S., and Turner, J.M. (2010) Evidence that meiotic sex chromosome inactivation is essential for male fertility. Curr Biol 20:2117-2123.

Sawamura, K. (1996) Maternal effect as a cause of exceptions for Haldane's rule. Genetics 143:609-611.

Sawamura, K., Taira, T., and Watanabe, T.K. (1993a) Hybrid lethal systems in the Drosophila melanogaster species complex. I. The maternal hybrid rescue (mhr) gene of Drosophila simulans. Genetics 133:299-305.

Sawamura, K., Yamamoto, M.T., and Watanabe, T.K. (1993b) Hybrid lethal systems in the Drosophila melanogaster species complex. II. The Zygotic hybrid rescue (Zhr) gene of D. melanogaster. Genetics 133:307-313.

Sebestova, J., Danylevska, A., Novakova, L., Kubelka, M., and Anger, M. (2012) Lack of response to unaligned chromosomes in mammalian female gametes. Cell Cycle 11:3011-3018.

Sen, S., Johannes, F., and Broman, K.W. (2009) Selective genotyping and phenotyping strategies in a complex trait context. Genetics 181:1613-1626.

She, S.C., Steahly, L.P., and Moticka, E.J. (1990) A method for performing full-thickness, orthotopic, penetrating keratoplasty in the mouse. Ophthalmic Surg 21:781-785.

Shifman, S., Bell, J.T., Copley, R.R., Taylor, M.S., Williams, R.W., Mott, R., and Flint, J. (2006) A high-resolution single nucleotide polymorphism genetic map of the mouse genome. PLoS Biol 4:e395.

Shin, Y.H., Choi, Y., Erdin, S.U., Yatsenko, S.A., Kloc, M., Yang, F., Wang, P.J., Meistrich, M.L., and Rajkovic, A. (2010) Hormad1 mutation disrupts synaptonemal complex formation, recombination, and chromosome segregation in mammalian meiosis. PLoS Genet 6:e1001190.

Shinkai, Y., Satoh, H., Takeda, N., Fukuda, M., Chiba, E., Kato, T., Kuramochi, T., and Araki, Y. (2002) A testicular germ cell-associated serine-threonine kinase, MAK, is dispensable for sperm formation. Mol Cell Biol 22:3276-3280.

Scherthan, H. (2001) A bouquet makes ends meet. Nat Rev Mol Cell Biol 2:621-627.

Schimenti, J. (2005) Synapsis or silence. Nat Genet 37:11-13.

Schramm, S., Fraune, J., Naumann, R., Hernandez-Hernandez, A., Hoog, C., Cooke, H.J., Alsheimer, M., and Benavente, R. (2011) A novel mouse synaptonemal complex protein is essential for loading of central element proteins, recombination, and fertility. PLoS Genet 7:e1002088.

Skarnes, W.C., Rosen, B., West, A.P., Koutsourakis, M., Bushell, W., Iyer, V., Mujica, A.O., Thomas, M., Harrow, J., Cox, T., Jackson, D., Severin, J., Biggs, P., Fu, J., Nefedov, M., de Jong, P.J., Stewart, A.F., and Bradley, A. (2011) A conditional knockout resource for the genome-wide study of mouse gene function. Nature 474:337-342.

Slotman, M., Della Torre, A., and Powell, J.R. (2004) The genetics of inviability and male sterility in hybrids between Anopheles gambiae and An. arabiensis. Genetics 167:275-287.

Smagulova, F., Gregoretti, I.V., Brick, K., Khil, P., Camerini-Otero, R.D., and Petukhova, G.V. (2011) Genome-wide analysis reveals novel molecular features of mouse recombination hotspots. Nature 472:375-378.

Smyth, G.K. (2004) Linear models and empirical bayes methods for assessing differential expression in microarray experiments. Stat Appl Genet Mol Biol 3:Article3.

Song, R., Ro, S., Michaels, J.D., Park, C., McCarrey, J.R., and Yan, W. (2009) Many X-linked microRNAs escape meiotic sex chromosome inactivation. Nat Genet 41:488-493.

Stefansson, H., Helgason, A., Thorleifsson, G., Steinthorsdottir, V., Masson, G., Barnard, J., Baker, A., Jonasdottir, A., Ingason, A., Gudnadottir, V.G., Desnica, N., Hicks, A., Gylfason, A., Gudbjartsson, D.F., Jonsdottir, G.M., Sainz, J., Agnarsson, K., Birgisdottir, B., Ghosh, S., Olafsdottir, A., Cazier, J.B., Kristjansson, K., Frigge, M.L., Thorgeirsson, T.E., Gulcher, J.R., Kong, A., and Stefansson, K. (2005) A common inversion under selection in Europeans. Nat Genet 37:129-137.

Storchova, R., Gregorova, S., Buckiova, D., Kyselova, V., Divina, P., and Forejt, J. (2004) Genetic analysis of X-linked hybrid sterility in the house mouse. Mamm Genome 15:515-524.

Su, A.I., Wiltshire, T., Batalov, S., Lapp, H., Ching, K.A., Block, D., Zhang, J., Soden, R., Hayakawa, M., Kreiman, G., Cooke, M.P., Walker, J.R., and Hogenesch, J.B. (2004) A gene atlas of the mouse and human protein-encoding transcriptomes. Proc Natl Acad Sci U S A 101:6062-6067.

Subramanian, A., Tamayo, P., Mootha, V.K., Mukherjee, S., Ebert, B.L., Gillette, M.A., Paulovich, A., Pomeroy, S.L., Golub, T.R., Lander, E.S., and Mesirov, J.P. (2005) Gene set enrichment analysis: a knowledge-based approach for interpreting genome-wide expression profiles. Proceedings of the National Academy of Sciences of the United States of America 102:15545-15550.

Sun, F., Oliver-Bonet, M., Liehr, T., Starke, H., Ko, E., Rademaker, A., Navarro, J., Benet, J., and Martin, R.H. (2004a) Human male recombination maps for individual chromosomes. Am J Hum Genet 74:521-531.

Sun, S., Ting, C.T., and Wu, C.I. (2004b) The normal function of a speciation gene, Odysseus, and its hybrid sterility effect. Science 305:81-83.

Suzuki, A., and Saga, Y. (2008) Nanos2 suppresses meiosis and promotes male germ cell differentiation. Genes Dev 22:430-435.

Takahashi, A., Tsaur, S.C., Coyne, J.A., and Wu, C.I. (2001) The nucleotide changes governing cuticular hydrocarbon variation and their evolution in Drosophila melanogaster. Proc. Natl Acad. Sci. USA 98, 3920–3925.

Tang, S., and Presgraves, D.C. (2009) Evolution of the Drosophila nuclear pore complex results in multiple hybrid incompatibilities. Science 323:779-782.

Thomsen, H., Reinsch, N., Xu, N., Bennewitz, J., Looft, C., Grupe, S., Kuhn, C., Brockmann, G.A., Schwerin, M., Leyhe-Horn, B., Hiendleder, S., Erhardt, G., Medjugorac, I., Russ, I., Forster, M., Brenig, B., Reinhardt, F., Reents, R., Blumel, J., Averdunk, G., and Kalm, E. (2001) A whole genome scan for differences in recombination rates among three Bos taurus breeds. Mamm Genome 12:724-728.

Thomsen, P.D., Schauser, K., Bertelsen, M.F., Vejlsted, M., Grondahl, C., and Christensen, K. (2011) Meiotic studies in infertile domestic pig-babirusa hybrids. Cytogenet Genome Res 132:124-128.

Ting, C.T., Tsaur, S.C., Wu, M.L., and Wu, C.I. (1998) A rapidly evolving homeobox at the site of a hybrid sterility gene. Science 282:1501-1504.

Trachtulec, Z., Vlcek, C., Mihola, O., Gregorova, S., Fotopulosova, V., and Forejt, J. (2008) Fine haplotype structure of a chromosome 17 region in the laboratory and wild mouse. Genetics 178:1777-1784.

Truett, G.E., Heeger, P., Mynatt, R.L., Truett, A.A., Walker, J.A., and Warman, M.L. (2000) Preparation of PCR-quality mouse genomic DNA with hot sodium hydroxide and tris (HotSHOT). Biotechniques 29:52-+.

Tucker, P.K., Sage, R.D., Warner, J., Wilson, A.C., and Eicher, E.M. (1992) Abrupt cline for sex chromosomes in a hybrid zone between two species of mice. Evolution. 46:1146–1163.

Tumennasan, K., Tuya, T., Hotta, Y., Takase, H., Speed, R.M., and Chandley, A.C. (1997) Fertility investigations in the F1 hybrid and backcross progeny of cattle (Bos taurus) and yak (B. grunniens) in Mongolia. Cytogenet Cell Genet 78:69-73.

Turelli, M., and Moyle, L.C. (2007) Asymmetric postmating isolation: Darwin's corollary to Haldane's rule. Genetics 176:1059-1088.

Turelli, M., and Orr, H.A. (1995) The dominance theory of Haldane's rule. Genetics 140:389-402.

Turelli, M., and Orr, H.A. (2000) Dominance, epistasis and the genetics of postzygotic isolation. Genetics 154:1663-1679.

Turner, J.M. (2007) Meiotic sex chromosome inactivation. Development 134:1823-1831.

Turner, J.M., Mahadevaiah, S.K., Ellis, P.J., Mitchell, M.J., and Burgoyne, P.S. (2006) Pachytene asynapsis drives meiotic sex chromosome inactivation and leads to substantial postmeiotic repression in spermatids. Dev Cell 10:521-529.

Turner, J.M., Mahadevaiah, S.K., Fernandez-Capetillo, O., Nussenzweig, A., Xu, X., Deng, C.X., and Burgoyne, P.S. (2005) Silencing of unsynapsed meiotic chromosomes in the mouse. Nat Genet 37:41-47.

Vernet, N., Mahadevaiah, S.K., Ojarikre, O.A., Longepied, G., Prosser, H.M., Bradley, A., Mitchell, M.J., and Burgoyne, P.S. (2011) The Y-encoded gene zfy2 acts to remove cells with unpaired chromosomes at the first meiotic metaphase in male mice. Curr Biol 21:787-793.

Vyskocilova, M., Prazanova, G., and Pialek, J. (2009) Polymorphism in hybrid male sterility in wild-derived Mus musculus musculus strains on proximal chromosome 17. Mamm Genome 20:83-91.

Vyskocilova, M., Trachtulec, Z., Forejt, J., and Pialek, J. (2005) Does geography matter in hybrid sterility in house mice? Biological Journal of the Linnean Society 84:663–674.

Waterston, R.H., Lindblad-Toh, K., Birney, E., Rogers, J., Abril, J.F., Agarwal, P., Agarwala, R., Ainscough, R., Alexandersson, M., An, P., Antonarakis, S.E., Attwood, J., Baertsch, R., Bailey, J., Barlow, K., Beck, S., Berry, E., Birren, B., Bloom, T., Bork, P., Botcherby, M., Bray, N., Brent, M.R., Brown, D.G., Brown, S.D., Bult, C., Burton, J., Butler, J., Campbell, R.D., Carninci, P., Cawley, S., Chiaromonte, F., Chinwalla, A.T., Church, D.M., Clamp, M., Clee, C., Collins, F.S., Cook, L.L., Copley, R.R., Coulson, A., Couronne, O., Cuff, J., Curwen, V., Cutts, T., Daly, M., David, R., Davies, J., Delehaunty, K.D., Deri, J., Dermitzakis, E.T., Dewey, C., Dickens, N.J., Diekhans, M., Dodge, S., Dubchak, I., Dunn, D.M., Eddy, S.R., Elnitski, L., Emes, R.D., Eswara, P., Eyras, E., Felsenfeld, A., Fewell, G.A., Flicek, P., Foley, K., Frankel, W.N., Fulton, L.A., Fulton, R.S., Furey, T.S., Gage, D., Gibbs, R.A., Glusman, G., Gnerre, S., Goldman, N., Goodstadt, L., Grafham, D., Graves, T.A., Green, E.D., Gregory, S., Guigo, R., Guyer, M., Hardison, R.C., Haussler, D., Hayashizaki, Y., Hillier, L.W., Hinrichs, A., Hlavina, W., Holzer, T., Hsu, F., Hua, A., Hubbard, T., Hunt, A., Jackson, I., Jaffe, D.B., Johnson,

L.S., Jones, M., Jones, T.A., Joy, A., Kamal, M., Karlsson, E.K., Karolchik, D., Kasprzyk, A., Kawai, J., Keibler, E., Kells, C., Kent, W.J., Kirby, A., Kolbe, D.L., Korf, I., Kucherlapati, R.S., Kulbokas, E.J., Kulp, D., Landers, T., Leger, J.P., Leonard, S., Letunic, I., Levine, R., Li, J., Li, M., Lloyd, C., Lucas, S., Ma, B., Maglott, D.R., Mardis, E.R., Matthews, L., Mauceli, E., Mayer, J.H., McCarthy, M., McCombie, W.R., McLaren, S., McLay, K., McPherson, J.D., Meldrim, J., Meredith, B., Mesirov, J.P., Miller, W., Miner, T.L., Mongin, E., Montgomery, K.T., Morgan, M., Mott, R., Mullikin, J.C., Muzny, D.M., Nash, W.E., Nelson, J.O., Nhan, M.N., Nicol, R., Ning, Z., Nusbaum, C., O'Connor, M.J., Okazaki, Y., Oliver, K., Overton-Larty, E., Pachter, L., Parra, G., Pepin, K.H., Peterson, J., Pevzner, P., Plumb, R., Pohl, C.S., Poliakov, A., Ponce, T.C., Ponting, C.P., Potter, S., Quail, M., Reymond, A., Roe, B.A., Roskin, K.M., Rubin, E.M., Rust, A.G., Santos, R., Sapojnikov, V., Schultz, B., Schultz, J., Schwartz, M.S., Schwartz, S., Scott, C., Seaman, S., Searle, S., Sharpe, T., Sheridan, A., Shownkeen, R., Sims, S., Singer, J.B., Slater, G., Smit, A., Smith, D.R., Spencer, B., Stabenau, A., Stange-Thomann, N., Sugnet, C., Suyama, M., Tesler, G., Thompson, J., Torrents, D., Trevaskis, E., Tromp, J., Ucla, C., Ureta-Vidal, A., Vinson, J.P., Von Niederhausern, A.C., Wade, C.M., Wall, M., Weber, R.J., Weiss, R.B., Wendl, M.C., West, A.P., Wetterstrand, K., Wheeler, R., Whelan, S., Wierzbowski, J., Willey, D., Williams, S., Wilson, R.K., Winter, E., Worley, K.C., Wyman, D., Yang, S., Yang, S.P., Zdobnov, E.M., Zody, M.C., and Lander, E.S. (2002) Initial sequencing and comparative analysis of the mouse genome. Nature 420:520-562.

White, M.A., Steffy, B., Wiltshire, T., and Payseur, B.A. (2011) Genetic dissection of a key reproductive barrier between nascent species of house mice. Genetics 189:289-304.

White, M.A., Stubbings, M., Dumont, B.L., and Payseur, B.A. (2012) Genetics and evolution of hybrid male sterility in house mice. Genetics 191:917-934.

Winckler, W., Myers, S.R., Richter, D.J., Onofrio, R.C., McDonald, G.J., Bontrop, R.E., McVean, G.A., Gabriel, S.B., Reich, D., Donnelly, P., and Altshuler, D. (2005) Comparison of fine-scale recombination rates in humans and chimpanzees. Science 308:107-111.

Wittbrodt, J., Adam, D., Malitschek, B., Maueler, W., Raulf, F., Telling, A., Robertson, S.M., and Schartl, M. (1989) Novel putative receptor tyrosine kinase encoded by the melanoma-inducing Tu locus in Xiphophorus. Nature 341:415-421.

Wojtasz, L., Cloutier, J.M., Baumann, M., Daniel, K., Varga, J., Fu, J., Anastassiadis, K., Stewart, A.F., Remenyi, A., Turner, J.M., and Toth, A. (2012) Meiotic DNA double-strand breaks and chromosome asynapsis in mice are monitored by distinct HORMAD2-independent and -dependent mechanisms. Genes Dev 26:958-973.

Wojtasz, L., Daniel, K., Roig, I., Bolcun-Filas, E., Xu, H., Boonsanay, V., Eckmann, C.R., Cooke, H.J., Jasin, M., Keeney, S., McKay, M.J., and Toth, A. (2009) Mouse HORMAD1 and HORMAD2, two conserved meiotic chromosomal proteins, are depleted from synapsed chromosome axes with the help of TRIP13 AAA-ATPase. PLoS Genet 5:e1000702.

Wu, C.I., and Davis, A.W. (1993) Evolution of postmating reproductive isolation: the composite nature of Haldane's rule and its genetic bases. Am Nat 142:187-212.

Wu, C.I., Johnson, N.A., and Palopoli, M.F. (1996) Haldane's rule and its legacy: Why are there so many sterile males? Trends Ecol Evol 11:281-284.

Wu, C.I., and Ting, C.T. (2004) Genes and speciation. Nat Rev Genet 5:114-122.

Xu, H., Beasley, M.D., Warren, W.D., van der Horst, G.T., and McKay, M.J. (2005) Absence of mouse REC8 cohesin promotes synapsis of sister chromatids in meiosis. Dev Cell 8:949-961.

Yang, F., De La Fuente, R., Leu, N.A., Baumann, C., McLaughlin, K.J., and Wang, P.J. (2006) Mouse SYCP2 is required for synaptonemal complex assembly and chromosomal synapsis during male meiosis. J Cell Biol 173:497-507.

Yanowitz, J. (2010) Meiosis: making a break for it. Curr Opin Cell Biol 22:744-751.

Yuan, L., Liu, J.G., Hoja, M.R., Wilbertz, J., Nordqvist, K., and Hoog, C. (2002) Female germ cell aneuploidy and embryo death in mice lacking the meiosis-specific protein SCP3. Science 296:1115-1118.

Yuan, L., Liu, J.G., Zhao, J., Brundell, E., Daneholt, B., and Hoog, C. (2000) The murine SCP3 gene is required for synaptonemal complex assembly, chromosome synapsis, and male fertility. Mol Cell 5:73-83.

Zeng, L.W., and Singh, R.S. (1993) The genetic basis of Haldane's rule and the nature of asymmetric hybrid male sterility among Drosophila simulans, Drosophila mauritiana and Drosophila sechellia. Genetics 134:251-260.